Geomagnetic Service
of Canada

ANNUAL REPORT 1983-84 - ROCK
MAGNETIC PROPERTIES TASK

Part of the Canadian Nuclear Fuel
Waste Management Program

by

W.A. Morris, P. Lapointe and
B.A. Chomyn, and K.L. Balch

Earth Physics Branch Open
File Number 84-20

Department of Energy, Mines and
Resources Canada
Earth Physics Branch
Divison of Seismology and
Geomagnetism

Price: $22.00
103 pages

Service géomagnétique
du Canada

RAPPORT ANNUEL 1983-84 - PROPRIETÉES
MAGNÉTIQUE DES ROCHES

Faisant partie du programme Canadien
d'evaluation de l'enfouissement des
déchets nucleaire

par

W.A. Morris, P. Lapointe, B.A. Chomyn,
et K.L. Balch

Dossier public de la Direction de la
Physique du Globe no. 84-20

Ministère de l'Énergie, des Mines et des
Ressources du Canada
Direction de la physique du globe
Divison de Séismologie et du
Géomagnetisme

Prix: $22.00
103 pages

1983 - 1984

ANNUAL REPORT

Task: Rock Magnetic Property

Activity: Rock Property

Nuclear Fuel Waste Management Program

E.M.R./E.P.B.

A.E.C.L.

RAPPORT ANNUEL

Tâche: Propiété Magnétique des Roches

Activité: Propriété des Roches

Programme pour la Gestion des Déchets Radioactifs Nucléaires

E.M.R./D.P.G.

E.A.C.L.

P. Lapointe
Task Leader
B.A. Chomyn
Research Associate
K.L. Balch
Research Assistant
Energy, Mines and Resources Canada
Earth Physics Branch
1 Observatory Crescent
Ottawa, Ontario, Canada
K1A 0Y3
1-613-837-3032

W.A. Morris
Contractor
Morris Magnetics
R.R. #2
Lucan, Ontario, Canada
N0M 2J0
1-519-227-1106

TABLE OF CONTENTS

ABSTRACT

Under the Rock Property Activity, the Rock Magnetic Property Task has as its objective the characterization of rock formations and rock samples using their magnetic properties. In 1983/84, work performed included relogging results from URL-6, Manitoba (at 10 cm intervals) and magnetic susceptibility and its anisotropy, magnetic remanence, density and opaque mineralogy of surface and borehole samples for East Bull Lake, Ontario.

The URL-6 closely-spaced logging showed an enhanced relationship between fractures/alterations and low susceptibilities. The East Bull Lake results demonstrate the major importance and effect of magnetic remanence. Contrary to other research areas the remanence is used to pick out the alteration zones on surface and deep samples. The dendritic gabbro unit is readily characterized by high susceptibility values and high remanence both on surface and in borehole samples and hence can be easily mapped.

RÉSUMÉ

A l'intérieur du cadre d'activité du groupe de propriété des roches, la tâche, propriété magnétiques des roches, est responsable de l'étude des variations des propriétés magnétiques des formations rocheuses. Les différents paramètres sont: la susceptibilité magnétique et son anisotropie, la rémanence naturelle, la densité ainsi qu'une description pétrographique des oxides porteurs d'aimantations. Ces études sont faites soit en surface, soit sur les échantillons provenant de trou de forage. Cette année la rapport continent. Les études en surface et en profondeur de la région de East Bull Lake, Ontario ainsi qu'une nouvelle diagraphie pour le trou de forage URL-6, Manitoba cette fois à intervalle de 10 cm.

La diagraphie du trou de forage URL-6 démontre trés précisement la relation fractures/alterations et des basses de susceptibilité. Les résultats de la région de East Bull démontrent l'importance de l'aimantation remanente comparativement à la susceptibilité. L'unité de gabbro dendritique est facilement reconnaissable et cartographiable en surface et en profondeur grâce à une rémanence et une susceptibilité très forte.

1. Introduction to the Rock Magnetic Property Task

The Rock Magnetic Property Task is part of the Rock Property Activity of the Canadian Nuclear Fuel Waste Management Program (NFWMP). As such, it has the mandate to characterize the magnetic properties of rocks in an attempt to estimate quantitatively and qualitatively the degree of homogeneity of a geological formation and to identify the geological processes that might have affected it.

The work involves measurements of both surface and deep borehole magnetic variations. The parameters which are measured are:

- magnetic susceptibility
- anisotropy of magnetic susceptibility
- magnetic remanence (natural remanent magnetization, NRM)
- induced remanent magnetization
- content of opaque minerals.

Over the last four years both surface and deep samples were measured at five different research areas (Fig. 83-1). The measurement of magnetic susceptibility on cores obtained from the deep borehole program has proved to be quite successful and has led to numerous useful applications, especially in the evaluation of fracture/alteration zones (Lapointe et al., 1983; Chomyn et al., 1984; Hillary et al., 1984). As can be seen in Table 1, the population of magnetic susceptibility measurement is large and enables us to proceed from a qualitative estimate of the degree of a rock homogeneity, on a relative scale, to a quantitative estimate.

A total of 13 km of core from 28 different holes were measured. These measurements have enabled us to draw general conclusions:

a) The magnetic susceptibility over a fracture zone will have an enhanced signal. The lowering of the signal has been interpreted to represent the alteration zone associated with a fracture.

b) There is a direct relationship between the stability and the level of the magnetic susceptibility signal and the homogeneity of a rock.

Surface measurement of magnetic properties was not emphasized at the beginning of the program but is now fully entrenched in the program. No general conclusion concerning all research areas can be drawn but current work at East Bull Lake has revealed the true potential of surface methods.

The following report contains preliminary results and interpretations of work done at URL-6, Pinawa, Manitoba and at East Bull Lake, Massey, Ontario (Fig. 83-1)

Please note that all raw data are available from the Gravity Data Centre, Earth Physics Branch, 1 Observatory Crescent, Ottawa, Ontario. All the work reported has been supported by Atomic Energy of Canada Ltd.

2. URL-6 Magnetic Susceptibility Logging of Cores at 10 cm intervals, Pinawa, Manitoba

i) Introduction

Because of the importance of the URL-6 hole as being representative of the Underground Research Laboratory shaft location, it was decided to relog the cores obtained from URL-6 at 10 cm intervals. Previously the URL-6 cores were logged at 2 m intervals but the data base at this interval is insufficient to interpret precisely the nature and extent of the alteration seen in the cores. The data base obtained with a 10 cm sampling interval enables one to clearly map and define the alteration zones (Chomyn et al., 1984). The following are the results and noteworthy features seen in the URL-6 magnetic susceptibility borehole logging. For the URL 1-7 magnetic susceptibility data at 2 m intervals, one may refer to Lapointe et al., 1984.

ii) Results

The results of the re-logging of borecore URL-6 using a 10 cm sampling interval are shown in Fig. 83-2 to Fig. 83-12. As a result of some missing segments of core, 3,978 data points over 400 m length of core were obtained.

Figs. 83-2 and 83-3 show the frequency distribution of the data on normal probability paper, plotting $\log_{10}$ bulk magnetic susceptibility versus cumulative frequency. One can interpret a number of important features from these figures:

a) the data from URL-6 neatly fall into a simple three-fold subdivision, i.e., the data consist of three partially overlapping $\log_{10}$ normal distributions.

b) data previously reported from borecores URL 1-5, and from surface measurements of BMS (bulk magnetic susceptibility) also contain the same three

populations, although the percentage of observations in each group is slightly different. For example, URL-6 contains a higher percentage of low susceptibility values than the URL 1-5 population and the surface survey data. As these low BMS values are usually related to alteration this indicates that statistically the examined section of URL-6 has a higher percentage of fractures per unit length than the URL 1-5 cores. The reduced content of low BMS values in the surface data is probably related to a sampling bias, this distribution being based on only 400 points versus over 4,000 points of the core data. Secondly, taking readings directly over fractures enhances the frequency of homogeneous rock values.

c) over 70% of the rock is represented by BMS values in the range 4 to 20×10^{-3} SI. This range corresponds to the distribution of a low (or zero) alteration level in the granite. The observed variation of BMS values within this group is possibly related to random variation within a given population, and possibly some lithological control of total oxide content. BMS values above approximately 20×10^{-3} SI are almost certainly related to local oxide concentrations possibly caused by mafic clots or xenoliths.

d) in Fig. 83-2 the lower segment appears to be defined by only four points. Fig. 83-3 is a replot of this same segment of the curve using a decade lower interval for the cumulative frequency spectrum (i.e., 1×10^{-4} SI for Fig. 83-3 and 1×10^{-3} SI for Fig. 83-2). This plot (Fig. 83-3) confirms the sharpness of the translation from a well-defined lower segment to the intermediate group of values. Visually fitting lines to these segments gives an intersection between the two populations at 4.3×10^{-3} SI. This value may be taken as the lower boundary of the unaltered granite population.

iii) Plotting Conventions

In previous reports we have used a sampling pattern that required three measurements at 2 m intervals along the core. The observed values were then plotted against depth using the depth of the mid-point value. In this study we report our first example of logging the core at 10 cm intervals. As resolution is directly related to sampling frequency, this marked increase in sampling density permits better resolution of geological phenomena. This new measuring procedure has also given rise to the possibility of applying more sophisticated filtering procedures to the data set. Because the investigation of complex digital filtering procedures is not supported by this program as presently defined, we have chosen at this stage to present a number of simple data treatments.

Figure 83-4	linear - depth plot	no filtering
Figure 83-5	linear - depth plot	5 point boxcar filter
Figure 83-6	linear - depth plot	10 point boxcar filter
Figure 83-7	$\log_{10}$ - depth plot	no filtering
Figure 83-8	$\log_{10}$ - depth plot	5 point boxcar filter
Figure 83-9	$\log_{10}$ - depth plot	10 point boxcar filter
Figure 83-10	$\log_{10}$ - depth plot	20 point boxcar filter
Figure 83-11	$\log_{10}$ - depth plot	10 point boxcar filter followed by stacking of the Ith, I+1, and I+2 points.

Fig. 83-6 compares the 10 point boxcar filter linear/depth plot of this year's study to that obtained from the 2 m spacing used in the previous study (shown in bold). Although the old logging method conforms to the general

form of the new approach it is readily apparent that the 10 cm spacing provides much greater detail of the significant variations of BMS. It is a commonly accepted fact that anomaly resolution is dependent upon the frequency of the sampling interval: i.e., one cannot expect to identify features of less than 2 m extent with a 2 m measuring interval.

Fig. 83-11 provides an important constraint on the reliability of our BMS curve. Because the overlapping of sequential points does not generate a broad swathe of lines, we have good reason to believe that all BMS fluctuations observed in this data set are of real significance and not the result of instrument error.

iv) Correlation between Bulk Magnetic Susceptibility and Fracturing

Previous studies in this series of concept evaluations have indicated the presence of a relationship between fracture density and bulk susceptibility values (see for example the reports by Chomyn et al., 1984 and Hillary et al., 1984). Using the probability distribution as a means of discriminating the number and boundaries of the populations in this data set, we find that Figs. 83-2 and 83-3 clearly indicate the presence of three populations in this data set as discussed above. Support for this concept is found in the regional applicability of these boundary zones. Again as shown in Fig. 83-2, the three populations are equally applicable to the URL-6, the combined URL 1-5 data, and the URL surface data.

If we use the boundary between the two lowest populations as the criterion for separating altered (fractured, permeable) from unaltered (pristine, hydraulically tight) granite, we then have a means of describing the distribution of altered granite zones from our susceptibility log. Fig. 83-12 (a 10 point boxcar log/depth plot) shows the distribution of the alteration

zones in stipple. The fracture density and number of open fractures are indicated for comparison. Clearly there is a correlation between fracturing and the BMS values indicated on the diagram. In detail, however, this correlation may be more complex than is initially apparent.

For the segment of core above 300 m depth there appears to be a one-to-one correlation between enhanced fracture density and reduced susceptibility values. Furthermore, the texture of the bulk susceptibility values gives some indication of the type of fracturing that one may be observing. For example, the narrow peaks at 100 m, 120 m, 230 m, and c.270 m are all associated with zones of very localized high fracture density. The broader BMS anomalies, for example 160-175 m, and 120-140 m are associated with broad zones of uniform low fracture density. The anomaly at 160-175 m shows a broad scale depression of the bulk susceptibility values. Likewise, the anomaly at 120-140 m has a broad depth extent but this susceptibility is dominated by the narrow zone of intense fracturing around 120 m. This initial survey shows that it is visually possible to recognize alteration features of different severity and lateral extent. From this premise one might assume that the application of rigorous filtering techniques may be able to differentiate between zones of localized intense fracturing and zones of more broad-scale, low-level fracturing.

Below 300 m the fracture density log indicates that no fractures are present in this section of the core, yet the bulk susceptibility values define at least four apparently well-defined alteration zones. Also of significance in this segment of core is the presence of a number of distinct xenolith-rich zones - as defined by BMS in excess of 20×10^{-3} SI (the boundary between the uniform granite population and the population of higher BMS values). Each of the top three of these apparent alteration zones at approximately 315 m,

335 m, and 345 m is located on the downhole side of a xenolith enriched zone. (In the fourth case the BMS low is also located next to a high, but the high at this point is below the level of the xenolith rich granite). Rather than representing oxide alteration zones the geometry of these "anomalies" suggests they may represent "shadow zones" of oxide depletion below the overlying xenoliths. A similar situation may be present at 175 m in the upper portion of this core.

v) Conclusions

1) A detailed 10 cm interval survey of the bulk magnetic susceptibility of borecore URL-6 has permitted the statistical recognition of three distinct populations of BMS level;

a) $0 - 4 \times 10^{-3}$ SI is related to "apparent" alteration zones,

b) $4 - 20 \times 10^{-3}$ SI corresponds to unaltered granite,

c) values $> 20 \times 10^{-3}$ SI indicate zones of xenolith, or mafic pod enhanced susceptibility.

2) Log_{10} BMS versus depth plots provide a better discrimination of the significant zones of reduced BMS.

3) By using the population concept and log_{10} plotting, it is possible to recognize the distribution of apparent alteration zones and xenolith rich zones.

4) In the first 300 m of core there is an almost one-to-one correlation between fracture density and the apparent alteration (low BMS) zones.

5) On the basis of their geometrical character two types of fracture pattern can be recognized:

a) a sharp spike of low susceptibility corresponds to a narrow zone of intense fracturing, and

b) a broad depression of the susceptibility level corresponds to wide zones of low fracture density.

6) In the zone 300-400 m four apparent alteration zones are consistently found on the downhole side of significant zones of xenolith enhanced levels of BMS. These are interpreted as "shadow zones" of oxide depletion below the overlying xenoliths. As such, they are lithological effects and hence may not have any significance in terms of water percolation.

3. East Bull Lake Ground Magnetic Properties, Massey, Ontario

i) Introduction

Magnetic minerals in rocks contain sensitive records of many events in the history of a particular rock mass from its initial formation, through its subsequent alteration, deformation and metamorphism. When collected at the present day the physical and chemical characteristics of the magnetic oxides represent a summation of all the processes involved in the rock's history. Previous studies of rock masses for the Canadian Nuclear Waste Management Program have shown that in lithologically uniform granitic terrains (for example, Atikokan) significant reductions in bulk susceptibility values correlate with zones of high fracture density. This technique has provided a rapid means for documenting the distribution, and semi-quantitatively estimating the degree of alteration (and hence the importance in a geotechnical sense) of individual fracture sets. This paper extends this methodology to the study of a Late Archean gabbro-anorthosite pluton.

The East Bull Lake body outcrops approximately 30 km north of Massey, Ontario (Fig. 83-1). Geologically, the pluton contains a number of layered units ranging in composition from gabbro to anorthosite. Cross-cutting the gabbro are at least three separate dyke suites. The youngest one, only found at the northern edge of a zone of stripped outcrop, appears much younger than the northeast and northwest dyke sets both of which, along with the gabbro, have been subjected to a regional greenschist grade metamorphic event. Deformation of the pluton appears to have taken place in two distinctly different forms. Broad-scale plastic deformation of the pluton records the effects of a regional folding event which appears to pre-date the metamorphism (D.T.A. Symons personal communications, 1983) while localized brittle deformation with associated mineral alteration and quartz veining is now

marked in particular by the Folson Lake Fault zone. In the design of any nuclear waste repository it is the extent of alteration, the timing, and the evolution of these fracture sets that are crucial in evaluating the long term stability of a rock pluton.

The rock magnetic properties study at East Bull Lake has now examined samples from over 120 localities within and around the grid area of the East Bull Lake gabbro body (Fig. 83-13). Within the rock magnetic properties task it is possible to identify four separate studies:

a) documentation of the areal variation of the rock magnetic properties, bulk susceptibility, remanence intensity, and remanence direction over the gridded area;

b) analysis of the paleomagnetic record of certain rock structures that contain evidence of specific events in the geological history of the East Bull Lake gabbro;

c) examination of the anisotropic magnetic susceptibility of specimens from the area of the Folson Lake Fault zone;

d) bulk susceptibility logging of the four borecores that have been drilled from the East Bull Lake gabbro.

Instrumentation used in these investigations includes a Schonstedt DSM-1 spinner magnetometer for the measurement of magnetic remanence values, a Schonstedt GSD-5 for sequential alternating field demagnetization, and a Schonstedt TSD-1 for performing stepwise thermal treatments. The field susceptibility measurements and the bulk susceptibility core logging was made using a Bison 3101A unit with, respectively, an 8" diameter circular field coil, and a 3" diameter core logging coil. All anisotropic susceptibility measurements were made using a Sapphire Instruments SA-1 tool.

ii) Results

a) Surface Observations

The rock magnetic properties, bulk susceptibility, remanence intensity and direction and rock density, have now been measured at 120 localities within the East Bull Lake Research Area (Figs. 83-1 and 83-13). Details of the results of this survey are listed in Tables 2 to 7 and presented in Figs. 83-13 to 83-32.

Rock magnetic property studies at other research areas, all located in granitic terrain, have suggested that bulk susceptibility is the magnetic parameter most sensitive to petrological and geochemical variations. In contrast, in the East Bull Lake gabbro-anorthosite body it is magnetic remanence that contains the major record of magnetic variations related to lithology and alteration. An obvious explanation for this feature is the initial oxide grain size distribution in the two bodies. Whereas the granites are typified by accumulations of coarse, multi-grain magnetite crystals, the gabbros more commonly have disseminated, fine grained magnetite. Fig. 83-14, a plot of the site mean Koenigsberger ratio (Q = remanent/induced magnetization) versus bulk susceptibility, is dominated by a trend of data points stretching from low Q(<1) to extremely high Q values (>100). Over this same range the bulk susceptibility varies by only one order of magnitude from around 50 to 190 x 10^{-5} SI units. Within this trend there appears to be a hiatus of Q values between 5 and 10. This separation provides a distinction between more- and less-altered gabbros and, as shown in later figures, it is a boundary that defines the areal extent of alteration around the Folson Lake Fault zone. A second subsidiary trend on the Q versus susceptibility plot records the presence of a number of strongly magnetic sites with Q values ranging from 100 down to 10, and BMS values ranging from 90 to over 5,000 x 10^{-5} SI units. This subsidiary trend appears to be associated with the dendritic gabbro unit.

With one notable exception, all the dykes sampled agree with the trend defined by the majority of gabbro sites. As with the gabbro, we see a major cluster of points with Q values between 6 and 25. Two more altered sites having Q values less than 2 are located in the Folson Lake Fault zone. This implies that the processes responsible for generating the Q value variation in the gabbro also produced the variation in most of the dykes. The one exceptional dyke clearly does not belong to this group. It is characterized by a very strong magnetic signal (Q=6, BMS $\simeq$ 5,000 x 10^{-5} SI). The dyke giving these results is exposed at the northern edge of the stripped outcrop. Geological mapping of this area indicates this dyke does indeed post-date the regional metamorphism of the East Bull Lake gabbro and the major faulting and shearing along the Folson Lake Fault zone.

Fig. 83-15, a plot of Koenigsberger ratio versus density, shows that the same paucity of observations of Q values between 5 and 10 also marks a change in the character of the density observations. Below a Q value of 10 the density values are quite dispersed, and do not appear to define any specific trend. Above Q values of 30, with some minor exceptions, the density appears to be restricted to values of between 2.8 and 2.9 g/cm^3.

The large variations in Q value shown in Figs. 83-14 and 83-15 result from two effects: a) alteration, where the composition of the original oxides has been degraded to more oxygen rich (less magnetic) phases as a result of chemical regeneration by oxygen rich percolating fluids, and b) lithology, where each rock unit has a magnetic signature, defined by its own mixture of oxide composition, oxide grain size, and oxide content. The Folson Lake Fault zone provides an excellent example of the changes in magnetic character that can be produced by alteration (Fig. 83-16). The fault zone is typified by Q values less than 2.5. The northern edge of the alteration zone around the

fault is relatively sharp and is defined by a rapid progression to Q values of approximately 25. The southern margin is poorly constrained, suggesting that most of the gabbro between the northern edge of the fault zone and the southern contact of the gabbro body has been extensively altered. Examples of the lithological control of Q values indicate:

a) the association of the massive gabbro unit with enhanced Q values (remanence » susceptibility),

b) the association of the dendritic gabbro unit with reduced Q values (susceptibility » remanence).

Previous figures have emphasized the importance of magnetic remanence intensity for differentiating lithologic and alteration zones within the East Bull Lake gabbro. Of course, when performing ground or airborne magnetic surveys, one also needs to take into consideration the orientation of the magnetic remanence vector. The observed magnetic anomaly is clearly a vector summation of contributions from both the induced and the remanent magnetic fields. The vertical component of the remanent magnetization for each site was calculated by first performing an algebraic vector addition of all specimen directions from a site. Secondly, the total vector length was divided by the number of specimens at each site. Thirdly, this resultant vector was multiplied by the sine of the mean vector inclination to give a site mean vertical remanence component. Fig. 83-19 presents a contour plot of this parameter. Significant features of this plot are:

a) the northern boundary of the Folson Lake Fault is marked by a sharp increase in magnetic signal.

b) the anomaly associated with this boundary is further enhanced by the presence of the strongly magnetic late stage dyke. On Fig. 83-19 the dyke has a vertical component of 1000×10^{-5} SI/cm^3 in a region where values are generally of the order of 30×10^{-5} SI/cm^3.

c) most of the area south of the fault has a low vertical magnetic signature. A major boundary is found close to the contact with the southern group of metavolcanics. These features closely correspond to the profiles produced by the ground based magnetic gradiometer survey. It is possible that it is the presence of these large changes in remanent magnetic signal that precluded accurate modelling of the observed anomaly across the Folson Lake Fault.

d) the massive gabbro is associated with a large positive magnetic component.

e) the sites sampled above Moon Lake explain another confusing feature of the gradiometer survey. Large amplitude fluctuations from positive to negative magnetic gradient found in this zone do not exhibit any direct correlation to local lithological features. The rock magnetic data across this same section show this area to be characterized by the presence of separate zones of normal and reverse polarity magnetization. The extent and geological significance of these zones is as yet unknown.

Plots of bulk magnetic susceptibility (Fig. 83-17) and log site mean intensity (Fig. 83-20) reinforce the observations defined in Figs. 83-14 and 83-15. That is:

a) the Folson Lake Fault zone is defined by reduced susceptibility and reduced remanence.

b) the area above Moon Lake is marked by locally enhanced values for both susceptibility and remanence.

c) the dyke at the stripped outcrop has anomalously high values of both susceptibility and remanence for its location, indicating that its intrusion post-dates most of the alteration processes associated with the fracturing along the Folson Lake Fault.

b) Magnetic Remanence

Remanence directions are acquired when a particular oxide grain passes through a specific blocking threshold parameter. This threshold may depend on temperature or grain size, depending on the type of remanence acquisition process (thermal, chemical, etc.) that is operative. Remanence directions then, when cleanly isolated, can provide estimates of the time that certain geological remagnetization processes are operative. The directional data obtained thus far from the East Bull Lake gabbro are summarized in Tables 2, 4, and 5, and Figs. 83-21 to 83-27.

No detailed remanence analysis has been performed on the samples from the main gabbro. Hence, it is not possible to derive a complete remanence acquisition history of the gabbro. The NRM data merely give us a broad guide to the directions that one might anticipate upon performing a more complete paleomagnetic analysis. Fig. 83-21 presents an equal area stereonet contoured at a 2.5% interval of all the statistically significant Fisher site mean remanence directions (Table 2). The distribution has a dominant central mode with lobes extending off in the NW and a WSW direction. The dominant direction in this data set is D=302°, I=78°. Removing the sites (33) that contribute to this first mode and re-running the modal analysis gives the location of the second mode as D=250°, I=59°. The genesis and acquisition timing of these magnetizations is unknown. However, it might be noted that these magnetizations are very similar to a metamorphic overprint direction previously reported from adjacent areas of the Southern Province (Morris, 1977). The preferred age of this component is presently set at around 2,150 ma; i.e, post-Nipissing diabase.

Rotating the first modal direction to the centre of the stereonet, along with all the individual site mean remanence directions, permits the

discrimination of sites which do not conform to the expected circular distribution about the mode. As shown in Fig. 83-22, two divergent groups can be recognized. The first group has a moderately inclined westerly direction. The genesis of this component is defined by the presence of the direction from the late dyke at the stripped outcrop. At other sites where the dyke is not exposed magnetic overprinting is detected probably because one is in the thermal aureole of the dyke. The second component is more correctly described as a smear of remanence directions from the modal direction to shallow positive, and even shallow negative, vectors with a SW declination. The form of this distribution suggests genesis by localized thermal overprinting with the true orientation of the vector remaining unknown.

Setting a boundary at 30° around the mode and identifying the location of those sites that fall into a particular divergent group, it is then possible to derive a map of the areal distribution of these aberrant directions (Fig. 83-23). The westerly inclined late dyke direction is consistently found in the Folson Lake Fault zone . This paleomagnetic anomaly only occurs in the SE part of the study area. However, the ground magnetic anomaly is found across the study area. This suggests that in the NW portion of the study area the top of the dyke is deeper than in the SE part such that the baked zone above the dyke is not exposed at the surface. The second most diffuse overprint direction appears to be associated with the massive gabbro.

Selected samples from the late stage dyke were subjected to stepwise alternating field demagnetization. Orthogonal vector plots of demagnetization trajectories from these specimens (Fig. 83-24) exhibit very uniform characteristics. During the first 10 mT of treatment a steeply inclined northerly direction is removed which very closely approximates the present Earth's Field direction. Upon further treatment, a characteristic NW shallow

inclination vector is detected. (Note the directions outlined above in the gabbro effectively describe a positive contact test for this direction). Fig. 83-25 summarizes the remanence directions found in these specimens and Table 4 gives the mean directions and paleopoles of the two components. Comparison of this result with presently available Pre-Cambrian apparent polar wander curves tentatively supports an intrusion age of around 1,250 ma. If this age is valid then a pre-1,250 ma age is suggested for the main fracturing of the East Bull Lake gabbro.

In contrast to the simple clean results from the dykes, the results obtained from hematitic specimens in the fracture zones are very poorly constrained. Fig. 83-26 shows that upon thermal demagnetization the specimens commonly retain the record of a steep positive and steep negative inclined remanence vector. Demagnetization trajectories are always jagged and line fits usually approximate to the minimum acceptance criteria (3 points, MAD 7.5). Plotting the derived remanence directions (Fig. 83-27) shows the presence of two directional populations; the negative vectors are oriented mainly northerly, while the positive vectors are mainly southerly directed. The mean directions are not in themselves exactly anti-polar, but taking into consideration the population distribution the two directions are not statistically distinct. Remanence acquisition spanning at least one field reversal is suggested, this is in good agreement with the proposed chemical remanence acquisition by progressive hematite grain growth. The age of this magnetization is uncertain. It is not of recent origin nor are there any well-defined Phanerozoic pole segments that this result matches. A segment for the period Ordovician/Silurian could contain this pole, but as yet this pole path segment is so poorly-defined that any pole-matching would be pure speculation. Simplistically, it would appear that the best age estimate has to be greater than 1,600 ma, because it is during this time period that the pole path traversed this segment.

c) Anisotropy of Magnetic Susceptibility

A small collection of oriented samples were obtained from a major shear zone which outcrops near the northern edge of the stripped outcrop. The object of this study was to use anisotropic magnetic susceptibility (magnetic fabric) data to estimate the sense and magnitude of motion on this fault plane.

Petrological examination of the specimens reveals two features that reduce the chances of obtaining reliable fabric estimates. Firstly, much of the rock is cross-cut by a later set of quartz veining which may have locally re-oriented magnetic grains. Secondly, the specimens contain a high percentage of hematite. The Sapphire SA-1 measuring system used in this experiment is designed to measure magnetite rich specimens. At the present time there are no high field torquemeters in Canada capable of specifically identifying hematite results.

The results of this study are summarized in Tables 6 and 7 and Figs. 83-28 to 83-32. Most specimens in this collection have a total anisotropy less than 2.5%; the only exception is specimen 526A. Fig. 83-28 shows that the majority of specimens plot close to the no strain line. Minor exceptions are specimens 519A, 519B, and 521A. Specimen 526A is again very divergent, and is located in the area of elongation. Figs. 83-29, 83-30, and 83-31, summarize the orientation of respectively the maximum, intermediate, and minimum susceptibility axes. Of these three plots only the minimum axis plot shows any well defined concentration of data points. The maximum axis plot shows a loose concentration in the NW quadrant, but this is only poorly defined. Along with the intermediate axis plot, the maximum axis plot mainly shows great circle trends of data points.

Fig. 83-32 summarizes the magnetic fabrics defined by this suite of samples from the stripped outcrop. Two foliation planes have been recognized

in the data set; A = dip of 35° towards 010°, and B = dip of 40° towards 160°. The trend of both of these planes is sub-parallel to the orientation of the Folson Lake Fault at the sampling point. However, in the absence of more detailed geological information on the sampling area, further interpretation is deferred to the geologists who have mapped the area.

d) Borehole Logging

Borecore susceptibility logs have been completed for holes EBL 2, 3, and 4. Borecore EBL 1 has only been logged down to 160 m. The logging procedure involved a single measurement of the bulk susceptibility at a 10 cm spacing along the total length of core available. Susceptibility measurements were made using a Bison 3101A instrument with a 3" diameter pass-through coil. Corrections applied to the field data allowed for the difference between the core diameter and the coil opening diameter, and changed the values to S.I. units. No corrections were applied for the presence of variable volumes of core, say in a rubble zone, or at a drilling thinned zone.

The results (Figs. 83-33 to 83-48) were plotted as $\log_{10}$ magnetic susceptibility (S.I. units) versus borecore length (metre). No correction has been applied to obtain true depth. To smooth the data, simple boxcar filters (running means) of 10, 25, and 50 observation length were applied to the data, corresponding to averaging the data over 1, 2.5, and 5 m of core. More sophisticated filtering could probably highlight the separation between an inherent noise (instrument drift, and transient pick up) in the instrument and true signal. This is particularly important for this data set where over 40% of the observations are close to the reliable measurement level of the instrument.

At the time of submission of this report detailed geological logs had only been received for borecore EBL 1. Hence, at this stage, it is only possible to give a description of the major features present in this set. Fig. 83-49 presents a comparison of the logs from the four borecores. A zone of enhanced BMS can be correlated from EBL 3, through EBL 4 to EBL 2. The presently available log of EBL 1 just marks the beginning of this enhanced BMS zone. As these plots have not been corrected to true depth the thickening of this highly magnetic unit in borecore 4 may be more apparent than real. Once the borecore lithology logs become available it will be possible to identify the specific rock unit that correlates to this anomaly. The low susceptibility horizons within the high BMS region mark the presence of localized fracture/ alteration zones. That is, for this magnetic horizon, just as in the granites, alteration is marked by reduced susceptibility values.

In EBL 3 a second zone of high BMS is found between 225 and 300 m. This zone has not been detected in any other borecore. In the absence of a lithological log for this core one can but speculate that this zone represents the highly magnetic dyke that outcrops just to the south of the drill collar. There is also a third boundary at 380 m in core EBL 3 and 450 m in EBL 4. The geological lineament encountered around 550 m in core EBL 2, which consists of silicified and unconsolidated fault breccia is marked by a zone of zero susceptiblity readings. Further details will be presented once further data processing is complete, and when the lithological logs become available.

Fig. 83-50 presents cumulative frequency plots for each of the four EBL borecores. Cores EBL 2, EBL 3, and EBL 4 all show a simple four- or five-fold subdivision of susceptibility populations. In EBL 1 the high BMS group of values is absent. This is explained by the short length (~160 m) of EBL 1 that has been logged; it was noted above that the present logging has just

started into the high susceptibility. Two major populations can be recognized in all cores. A group of data with susceptibility values from 310 to 1,250 x 10^{-5} SI has exactly the same distribution in all cores. It is most prominent in EBL 3 and least developed in EBL 1 (possibly because of limited logging length?). The second common population which extends from 40 to 310 x 10^{-5} SI has identical distribution and magnitude in EBL 3 and 4, and occurs with a slightly different distribution in EBL1 and 2. The latter having a lower percentage of observations at the upper end of this distribution group. The multiple populations of enhanced BMS values are probably related to detailed lithological differences between the individual cores.

e) Peripheral Studies

To develop our understanding of rock magnetic property variations, a number of peripheral studies on material from other research areas have been on-going. It is anticipated that full reports on the details of these experiments will be presented in the upcoming financial year.

BMS derived alteration index:

It is now well recognized that especially in granites the BMS level is directly correlated to locally observed fracture zones. The question we next chose to ask was whether the degree of BMS reduction is equivalent to the degree of fracture-related alteration. To answer this question an incremental weighting scheme was applied to the observed susceptibility data. The first step in this procedure requires one to identify a BMS level that is typical of unaltered granite. All values above this level are ignored. Secondly, for particular BMS levels below this base level, the observed values are accorded a numerical value. The lower the susceptibility the higher the value, increments between specific levels are exponential. Thirdly, the assigned

values are summed for a specific sampling level (this was applied to cores logged by the old 3 x 10 cm at 2 m interval technique), and then divided by the total maximum value. The resulting value gives an approximation of the degree of alteration at each level. At first glance the agreement between observed fracture density and BMS derived alteration in startling.

IRM derived alteration index:

Petrological studies of the granites have shown that alteration is usually marked in oxide minerals by an increase in hematite content at the expense of the magnetite. Magnetically these oxide changes can be described by IRM analysis. Our new results confirm that, especially for the ATK area, by using acquisition coercive force versus BMS/saturation remanence one can document not only the location of zones of major alteration, but also quantitatively measure the degree to which alteration has proceeded.

iii) Conclusions

Rock magnetic property studies at the East Bull Lake research area have yielded a variety of interesting results relating to the pluton:

a) a description of the areal extent of alteration around the Folson Lake Fault zone.

b) an explanation why the northern edge of this fault zone should be so difficult to model. This zone is marked by a rapid change of magnetic properties, and also contains a highly magnetic dyke.

c) an explanation of the complex magnetic anomaly above Moon Lake by the presence of normal and reversed magnetic remanence zones.

d) approximate age estimate limitations for major faulting of the pluton (greater than 1,250 ma; that is, older than the young dyke cross-cutting the fracture zone). This suggests that the hematite in the fracture zone may be quite old.

e) an indication that the major fabrics in the fracture consist of two planes dipping at 35° to 010°, and 40° to 160°.

f) an outline of the presence of both lithologic and alteration related BMS structure in the borecore susceptibility logs.

REFERENCES

Chomyn, B.A., MORRIS, W.A., LAPOINTE, P. and R.L. COLES, 1984. Applications of magnetic susceptibility to the degree of alteration of rock. 17th Annual Information meeting of the Canadian Nuclear Fuel Waste Managment Program symposium Volume, AECL; Pinawa, Manitoba (in press).

FISHER, R.A., 1953. Dispersion on a sphere. Proceedings of the Royal Society of London, 17, pp. 295-305.

HILLARY, E.M., MCEWEN, J.H. and N.A.C. REY, 1984. The evaluation of fracture zones at Atikokan drill site, and their physical response. In Proceeding of the 17th Annual Information meeting of the Canadian Nuclear Fuel Waste Management Program, Ottawa.

HROUDA, F., JAVAK, F., REJIL, L. and J. WEISS, 1971. The use of magnetic susceptibility anisotropy for estimating the ferromagnetic mineral fabric of metamorphic rocks. Geologishe Rundschau, V. 60, No. 3, pp. 1124-1142.

LAPOINTE, J.P., CHOMYN, B.A. and W.A. MORRIS, 1983. Annual Report 1982-83 Rock Magnetic Properties Task, Earth Physics Branch Open File No. 83-4, Energy, Mines and Resources Canada, Ottawa, Ontario, 100 pp.

LAPOINTE, P., MORRIS, W.A., CHOMYN, B.A. and P. FOURNIER, 1984. Compilation of magnetic susceptibility of cores from the Lac du Bonnet Research area, Manitoba, AECL Technical Report (in press).

REFORD, S.W., 1983. A detailed ground magnetic survey of the East Bull Lake Intrusion Research Area RA-7, Algona District, Ontario. Energy, Mines and Resources Open File Report.

VAN ALSTINE, D.R, 1980. Analysis of the modes of directional data with particular reference to paleomagnetism. Geophys. J.R. Astr. Soc., V. 61, pp. 101-114.

TABLE 1

COMPILATION OF MAGNETIC SUSCEPTIBILITY DATA
IN THE DEEP BOREHOLES PROGRAM

RESEARCH AREA	ROCK TYPE	BOREHOLES	TOTAL LENGTH IN METRES	NUMBER OF SUSCEPTIBILITY MEASUREMENTS*
URL	GRANITE	1-7	3,426	5,598
ATK	GRANITE	1-5	3,353	5,406
CR	GRANITE	1-9	2,450	3,708
WN	GRANITE	1,2,4	1,546	2,497
EBL	GABBRO	1-4	2,575	25,000
TOTAL		28	13,350	42,209

*URL, ATK, CR and WN were sampled at 2 m intervals, while EBL was sampled at 10 cm intervals.

TABLE 2

MAGNETIC REMANENCE DATA FROM THE EAST BULL LAKE RESEARCH AREA #7, MASSEY, ONTARIO

1983 EBL SITES

SITE	LOCATION E	LOCATION N	FISHER MEAN D°,I°	(n,k,alpha$_{95}$)	VECTOR MEAN D°,I°	ROTATED MEAN D°,I°
01	271E	215.6N	305,63	(6,194,5)	305,63	316,70
02	271E	214N	297,43	(6,6,32)	287,38	289,56**
03	271E	212N	312,59	(5,9,27)	319,65	335,70
04	269E	212N	283,73	(6,204,5)	289,72	301,79
05	269E	214N	277,44	(6,17,16)	277,34	278,42**
06	267E	213.5N	277,44	(4,37,15)	274,47	278,55**
07	267E	212N	245,33	(5,43,12)	244,33	241,40*
08	265E	213.7N			334,59	347,62
09	265E	212N	333,74	(6,61,9)	337,74	006,75
10	269.3E	214.7N	320,52	(5,172,6)	321,50	329,55
11	271E	217N	290,41	(5,94,8)	290,41	293,49**
12	269E	227N	270,77	(4,20,21)	224,77	187,81
13	269E	226N			249,31	247,38*
14	269E	223N	217,09	(4,8,34)	217,02	217,07*
15	269E	221N	233,46	(3,13,35)	228,42	222,47*
16	269E	216.5N	294,-78	(5,4,43)	308,-76	295,-65
17	269E	216.2N	231,37	(6,44,10)	231,36	227,42*
18	269E	219N	232,28	(6,52,9)	231,25	228,31*
19	269E	220N	019,55	(5,18,18)	030,46	037,42
20	269E	223.9N	260,75	(6,12,20)	240,78	301,83
21	269E	224.8N			009,29	013,28
22	267E	224.2N	306,54	(6,47,10)	306,54	313,60
23	263.2E	216.9N	043,77	(6,17,17)	041,75	058,70
24	263.2E	216.9N	309,86	(5,21,17)	333,88	078,83
25	263.2E	217.2N	293,46	(13,6,19)	287,58	291,66**
26	273E	213N	282,27	(5,141,6)	280,26	281,34**
27	273E	212N	140,78	(4,32,16)	144,79	123,73
28	273E	216N			128,67	120,60
29	269E	220N	254,69	(4,17,23)	237,66	223,72

Fisher Mean = average using Fisher (1953)
Vector Mean = given unit weight to remanence intensities of each specimens
Rotated Mean = orientation of a site mean remanence vector relative to the average mean vector of the entire population
D°,I° = declination, inclination
N = number of cores
k = best precision estimate (Fisher, 1953)
Alpha$_{95}$ = radius of circle of confidence (P = 0.05)

*,** different mean populations

TABLE 2 (Cont'd)

1983 EBL SITES

SITE	LOCATION E	LOCATION N	FISHER MEAN D°,I° (n,k,alpha$_{95}$)		VECTOR MEAN D°,I°	ROTATED MEAN D°,I°
30	263E	221.2N	309,62	(6,180,5)	310,62	322,68
31	263E	223N			246,60	238,67
32	263E	225N	303,82	(6,24,14)	307,81	009,85
33	263E	226N	266,50	(6,141,6)	266,50	265,58
34	263E	227N	247,49	(6,49,10)	246,48	241,55
35	265E	227N	245,38	(3,38,20)	244,37	241,44*
36	265E	224N			174,08	173,07
37	265E	222.1N	352,83	(6,343,4)	349,82	040,80
38	265E	221N	309,73	(6,15,18)	309,73	333,78
39	263E	218N	283,36	(6,71,8)	281,34	282,42**
40	263E	216.5N	284,47	(4,54,13)	288,49	291,57**?
41	263E	214.2N	109,72	(6,17,17)	098,74	096,66
42	261E	219N	327,69	(6,83,7)	323,68	342,72
43	261E	217N	265,71	(6,7,27)	272,60	272,68
44	261E	215N	310,78	(6,629,3)	310,78	350,82
45	261E	213.5N	034,81	(6,99,7)	016,79	047,75
46	259E	212N	024,74	(6,25,14)	022,77	047,73
47	259E	213.1N	302,80	(6,13,19)	279,84	072,88
48	259E	214N	301,69	(6,308,4)	302,69	317,75
49	259E	216N			327,47	335,51
50	259E	218.1N	323,81	(5,126,7)	331,80	020,81
51	259E	219.1N	320,59	(5,45,12)	319,58	330,63
52	273E	223N	333,49	(6,137,6)	331,47	339,51
53	273E	225N	320,54	(4,103,9)	319,52	328,57
54	257E	227N	315,65	(3,11,39)	311,66	326,72
55	257E	226N	270,61	(6,141,6)	271,62	271,70
56	257E	224N			308,24	310,30
57	257E	222.5N	260,84	(4,1764,2)	259,84	124,87
58	257E	221.7N	324,44	(4,197,7)	324,44	330,49
59	255.2E	221.5N	011,75	(6,30,12)	012,75	037,72
60	255E	216.4N	250,41	(6,170,5)	251,42	248,49*
61	257E	219N			008,-1	008,09
62	257E	217N	265,37	(5,37,13)	266,37	265,45*
63	257E	215N	277,82	(5,22,17)	284,81	339,88
64	257E	213.3N	258,80	(5,66,9)	253,82	192,87
65	273E	227N	304,54	(6,236,4)	304,53	311,60
66	OUTCROP		290,78	(12,3,29)	326,66	344,70
66	OUTCROP		342,78	(9,10,17)	352,81	038,79

TABLE 2 (Cont'd)

1982 BS SITES

SITE	LOCATION E	N	FISHER MEAN D°,I° (k,alpha$_{95}$)		VECTOR MEAN D°,I°	ROTATED MEAN D°,I°
05	267E	227N			168,-49	
6A	267E	222N	221,32	(11,39)	211,25	206,29*
6B	267E	222N	215,58	(35,11)	212,63	196,66
07	267E	217N	224,10	(287,4)	224,10	223,15*
08	267E	216N			262,-44	
09	265E	218N	235,23	(41,11)	234,22	232,28*
10	265E	225N	250,30	(47,10)	251,30	249,37*
11	265E	228N			343,04	344,06
12	271E	224N	230,60	(23,14)	232,63	219,68
13	271E	222N	287,74	(26,13)	290,66	298,73
14	271E	218N			052,-26	
15	272.2E	220.2N			176,-06	
16	273E	224.5N	352,76	(521,3)	349,76	021,76
18	266.7E	214.8N	304,51	(44,10)	303,52	310,59
19	270.8E	213.8N	279,39	(101,8)	276,35	276,43**
28	253E	227N	213,-1	(50,9)	213,-1	212,03*
29	253E	224N			240,72	220,78
30	253E	221N	265,62	(11,22)	308,72	330,78
31	253E	218N	260,42	(124,6)	259,42	247,50*
32	253E	215N	227,-20	(15,18)	228,-21	230,-15
33	253E	212N	011,67	(39,11)	008,66	024,64
34	255E	212N			248,63	239,70
35	255E	213N	244,-4	(11,22)	243,-5	243,02*
36	255E	215N	234,64	(10,23)	228,53	219,58
37	255E	218N			248,04	248,11*
38	255E	221N	319,14	(8,25)	329,37	335,41
39	255E	224N	264,78	(103,6)	265,78	252,86
40	255.5E	227N	245,55	(29,13)	249,56	243,63
41	261E	227N	250,58	(63,9)	249,60	242,57
42	261E	224N	249,64	(276,4)	249,65	240,72
43	261E	222N	221,61	(117,6)	215,63	200,66
44	261E	221N	277,68	(53,9)	271,81	263,89
45	261E	219.8N	301,57	(27,13)	301,57	209,64
46	259E	221N			190,77	157,76
47	259E	224N	262,72	(82,8)	266,72	261,80
48	259E	225N	258,66	(45,10)	252,68	242,75
49	259E	227N	244,50	(210,5)	244,50	238,57
50	268E	227N	168,86	(74,7)	165,80	133,76

TABLE 3

ROCK MAGNETIC PARAMETERS FROM THE EAST BULL LAKE RESEARCH AREA #7

EBL SITES 1983

SITE	LOG MEAN INT.* $x10^{-6}$ emu/cm³	SUSCEP. $x10^{-6}$ cgs	Q	REM VERT. COMP. $x10^{-6}$ emu/cm³	DENSITY g/cm³	
01	276.4	172	35.0	263.0	2.92	DYKE
02	51.3	38	28.9	25.9	2.72	DYKE
03	3.7	52	1.5	3.3	2.80	DYKE
04	15.3	68	4.9	18.3	2.86	DYKE
05	3.2	42	1.6	2.0	2.81	DYKE
06	8.1	48	3.6	6.4	2.84	DYKE
07	8.8	52	3.7	4.8	2.84	DYKE
08	1.1	34	0.7	2.2	2.77	DYKE
09	215.4	108	43.3	236.8	2.81	DYKE
10	39.3	54	15.7	35.3	2.87	DYKE
11	42.9	34	27.6	28.5	2.86	DYKE
12	1242.3	454	59.6	1652.8	2.81	DYKE
13	511.9	100	111.3	225.3	2.84	DYKE
14	111.4	42	57.1	5.7	2.84	DYKE
15	101.1	58	37.7	72.6	2.86	DYKE
16	71.0	48	32.3	-58.2	2.84	DYKE
17	116.1	60	41.7	68.8	2.85	DYKE
18	41.3	62	14.3	22.9	2.85	DYKE
19	21.1	76	6.0	22.3	2.97	DYKE
20	101.4	118	18.7	95.4	2.97	DYKE
21	435.6	242	39.2	120.3	2.94	
22	141.6	120	26.0	113.1	2.99	DYKE
23	1.5	48	0.7	1.5	2.79	
24	1.3	54	0.6	1.3	2.84	
25	1190.2	3894	6.7	799.6	2.90	DYKE
26	108.0	132	17.2	54.1	2.92	
27	37.3	96	8.5	40.2	3.00	
28	212.9	96	48.1	173.2	2.83	
29	9.0	56	3.5	15.7	2.90	
30	95.1	86	28.8	83.8	3.00	
31	103.7	78	29.3	72.8	2.99	
32	5.7	90	1.4	5.5	3.03	DYKE
33	77.1	54	31.5	58.6	2.92	
34	41.5	56	16.3	30.6	2.96	
35	211.6	72	63.2	128.1	2.93	

Site mean remanence intensity x 10^{-6} emu/cm³ using logarithm average.
Susceptibility in $x10^{-6}$ cgs
Q = Koenigsberger ratio
Remanence vertical component

TABLE 3 (CONT'D)

EBL SITES 1983

SITE	LOG MEAN INT.* $x10^{-6}$ emu/cm³	SUSCEP. $x10^{-6}$ cgs	Q	REM VERT. COMP. $x10^{-6}$ emu/cm³	DENSITY g/cm³	
36	198.5	266	66.0	11.9	2.97	
37	42.7	136	6.8	43.4	3.05	DYKE
38	107.5	82	28.4	97.3	3.03	
39	6.8	62	2.4	3.9	2.96	
40	13.9	72	4.2	11.7	3.05	
41	3.3	54	1.4	3.1	2.88	DYKE
43	3.4	64	1.2	3.2	2.99	
44	32.1	60	11.5	31.4	3.02	
45	5.6	84	1.5	6.2	2.98	
46	314.0	190	36.1	338.0	2.92	
47	46.5	84	12.1	45.8	2.98	
48	23.6	64	8.1	27.5	3.00	
49	1.4	60	0.5	0.8	2.99	
50	1.5	58	0.5	1.6	2.97	
51	8.6	76	2.5	7.4	2.96	
52	10.4	62	3.6	9.5	2.97	
53	1326.2	2244	12.8	1282.2	2.90	
54	63.9	72	19.1	54.9	3.02	
55	34.6	58	12.8	30.4	2.98	
56	38.4	78	10.8	5.0	2.99	
57	684.0	94	156.8	694.9	3.07	
58	46.2	60	17.0	32.3	2.99	
59	1.7	40	0.9	1.7	2.88	
60	10.0	70	3.1	6.9	3.03	
61	8.3	62	2.9	-1.0	2.99	
62	20.8	58	7.8	12.4	2.96	
63	3.8	78	1.1	3.9	2.96	
64	16.4	70	5.2	18.6	3.05	
65	91.7	158	12.6	73.4	2.92	
66	1.2	38	0.7	2.3	2.99	
67	1.2	26	1.0	1.2	2.84	

TABLE 3 (CONT'D)

BS SITES 1982

SITE	LOG MEAN INT.* $x10^{-6}$ emu/cm³	SUSCEP. $x10^{-6}$ cgs	Q	REM VERT. COMP. $x10^{-6}$ emu/cm³	DENSITY g/cm³	
05	1266.7	316	87.2	-913.3	2.83	
6A	86.0	81	23.1	35.2	2.89	
6B	123.8	149	18.0	117.1	3.00	DYKE
07	154.5	58	57.6	28.2	2.81	
08	52.5	86	13.1	-38.9	2.96	DYKE
09	51.9	69	16.3	19.2	2.89	
10	135.7	65	45.3	66.4	2.84	
11	631.7	109	125.9	79.6	2.91	
12	439.4	471	20.3	412.2	2.84	
13	2666.6	1233	47.0	3693.3	2.86	
14	244.8	70	75.3	-137.4	2.85	
15	2335.3	230	220.3	-103.1	2.86	
16	3457.1	3969	18.9	3581.7	2.92	
18	3.7	49	1.6	2.9	2.84	
19	7.9	87	1.9	4.3	2.93	
28	80.3	49	35.3	-0.1	2.93	
29	106.1	56	41.4	73.4	2.89	
30	174.6	51	74.9	3688.7	2.95	
31	25.4	38	14.6	17.3	2.88	
32	49.5	62	17.4	-17.1	2.98	
33	1924.2	4329	9.7	3307.8	3.17	
34	1229.3	180	148.6	1024.9	2.87	
35	41.1	48	18.6	-3.4	2.91	
36	5.7	55	2.3	5.7	2.94	
37	35.7	44	17.7	2.4	2.87	
38	30.1	53	12.3	759.2	2.95	
39	49.3	53	20.2	48.1	2.92	
40	148.5	89	36.4	126.6	2.93	
41	638.5	75	185.3	576.2	2.89	
42	83.2	68	26.6	81.1	2.94	
43	342.2	63	119.0	374.9	2.90	
44	16.9	79	4.7	17.3	2.89	
45	1.4	62	0.5	1.2	2.89	
46	197.9	61	70.6	223.8	2.91	
47	132.3	143	20.1	130.7	3.01	
48	189.3	59	69.4	189.9	2.94	
49	86.5	47	39.8	66.2	2.89	
50	1770.8	1199	32.1	2726.1	3.09	

TABLE 4

MODAL ANALYSIS OF NRM DIRECTIONS FROM EBL (1983) AND BS (1982) COLLECTIONS FROM DYKES AND GABBRO OF EAST BULL LAKE RESEARCH AREA #7

1ST PASS

A) D = 283°, I = 67°	N = 90	BETA = 5.19	PROB = 59.8	SMOOTH PARAM =	1
B) D = 295°, I = 75°	N = 56	BETA = 3.98	PROB = 26.7	SMOOTH PARAM =	5
C) D = 302°, I = 78°	N = 33	BETA = 3.51	PROB = 16.8	SMOOTH PARAM =	10
D) D = 272°, I = 82°	N = 9	BETA = 2.90	PROB = 5.8	SMOOTH PARAM =	50
E) D = 272°, I = 82°	N = 9	BETA = 2.90	PROB = 4.2	SMOOTH PARAM =	100

2ND PASS

DATA DECK RUN A SECOND TIME AFTER THE 33 POINTS GIVING RESULT C) ABOVE HAVE BEEN DELETED.

A) D = 269°, I = 55°	N = 64	BETA = 8.69	PROB = 38.7	SMOOTH PARAM =	1
B) D = 258°, I = 53°	N = 64		PROB = 16.3	SMOOTH PARAM =	5
C) D = 250°, I = 59°	N = 19	BETA = 5.33	PROB = 10.1	SMOOTH PARAM =	10
D) D = 248°, I = 62°	N = 4	BETA = 2.83	PROB = 4.5	SMOOTH PARAM =	50
E) D = 249°, I = 61°	N = 11	BETA = 4.73	PROB = 3.6	SMOOTH PARAM =	100

REFER TO VAN ALSTINE (1980) FOR COMPLETE EXPLANATION OF THE STATISTICAL ANALYSIS.

TABLE 5

PALEOMAGNETIC RESULTS FROM THE STRIPPED OUTCROP AREA
AT THE EAST BULL LAKE RESEARCH AREA #7

A) LATE STAGE DYKE INTRUSION

CHARACTERISTIC DIRECTION:

D = 292°, I = 23° N = 11 R = 10.941 k = 169 alpha = 3.5°
POLE LONG = 180°E, LAT = 24°N

LOW COERCIVITY OVERPRINT:

D = 010°, I = 77° N = 7 R = 6.754 k = 24 alpha = 12.5°
POLE LONG = 290°E, LAT = 71°N

B) HEMATITIC FRACTURE ZONES

LOW TEMPERATURE:

D = 143°, I = 83° N = 9 R = 8.741 k = 31 alpha = 9.4°
POLE LONG = 286°E, LAT = 34°N

MODERATE TEMPERATURE:

D = 349°, I = -64° N = 8 R = 7.542 k = 15 alpha = 14.6°
POLE LONG = 105°E, LAT = 03°S

D°,I°	→	declination, inclination
N	→	number of cores
R	→	resultant vector
k	→	best precision estimate (Fisher, 1953)
$alpha_{95}$	→	radius of circle of curvature (P = 0.05)
POLE LONG,LAT	→	longitude and latitude of the paleopoles obtained from the remanence direction

TABLE 6

ORIENTATION OF AXES OF ANISOTROPIC SUSCEPTIBILITY ELLIPSES OF SPECIMENS FROM THE FRACTURE ZONE AT THE STRIPPED OUTCROP OF THE EAST BULL LAKE RESEARCH AREA #7

SPEC	MINIMUM			INTERMEDIATE			MAXIMUM		
	D°,	I°,	INT	DI°,	I°,	INT	DI°,	I°,	INT
510A	277,	79,	4.63-5	052,	08,	4.68-5	145,	02,	4.70-5
510B	116,	33,	4.82-5	304,	56,	4.88-5	208,	04,	4.92-5
511A	164,	43,	2.15-5	263,	09,	2.16-5	002,	45,	2.21-5
512A	147,	18,	3.06-5	239,	03,	3.12-5	336,	71,	3.35-5
513A	326,	42,	3.57-5	227,	10,	3.72-5	126,	46,	3.97-5
513B	343,	46,	2.89-5	224,	25,	3.09-5	116,	34,	3.29-5
514A	278,	47,	3.90-5	172,	14,	4.21-5	070,	40,	4.37-5
514B	251,	57,	3.37-5	136,	15,	3.62-5	038,	28,	3.73-5
515A	310,	37,	3.17-5	195,	28,	3.40-5	079,	40,	3.52-5
515B	307,	45,	2.99-5	190,	25,	3.19-5	082,	35,	3.25-5
516A	212,	50,	2.86-5	087,	25,	3.00-5	343,	28,	3.11-5
516B	186,	50,	2.07-5	296,	16,	2.22-5	033,	36,	2.22-5
517A	215,	37,	1.56-5	111,	17,	1.68-5	001,	48,	1.87-5
517B	203,	52,	1.62-5	067,	29,	1.75-5	324,	22,	1.94-5
518A	001,	50,	2.87-5	250,	17,	3.07-5	148,	35,	3.10-5
519A	306,	50,	7.08-6	047,	09,	8.38-6	145,	38,	8.70-6
519B	352,	49,	6.31-6	243,	16,	7.26-6	141,	36,	7.71-6
520A	084,	41,	3.42-5	323,	31,	3.58-5	209,	34,	3.65-5
520B	195,	56,	3.46-5	151,	26,	3.62-5	251,	20,	3.65-5
521A	041,	54,	2.65-5	297,	14,	3.10-5	194,	43,	3.42-5
521B	353,	48,	3.00-5	084,	01,	3.13-5	174,	42,	3.28-5
522A	232,	38,	2.96-5	093,	44,	3.06-5	340,	22,	3.12-5
523A	187,	52,	2.79-5	076,	16,	2.89-5	335,	34,	2.96-5
524A	164,	44,	5.77-5	072,	12,	5.96-5	330,	43,	6.06-5
526A	348,	48,	6.14-6	253,	04,	8.90-6	158,	41,	1.34-5
527A	086,	61,	1.30-5	190,	08,	1.39-5	284,	28,	1.47-5

D°,I° → declination, inclination
INT → intensity of magnetization in 10^{-6} emu/cm^3

<

TABLE 7

STATISTICAL PARAMETERS OF MAGNETIC FABRICS*

SPEC	A/B	C/B	E	LIN	FOLN	% ANIS
510A	.989	1.004	1.007	1.010	1.013	2.023
510B	.988	1.008	1.004	1.014	1.017	2.031
511A	.995	1.023	.982	1.026	1.016	2.042
512A	.981	1.074	.950	1.084	1.057	2.141
513A	.960	1.067	.976	1.089	1.077	2.166
513B	.935	1.065	1.004	1.100	1.104	2.204
514A	.926	1.038	1.040	1.078	1.100	2.178
514B	.931	1.030	1.043	1.067	1.091	2.158
515A	.932	1.035	1.036	1.072	1.092	2.163
515B	.937	1.019	1.047	1.052	1.077	2.129
516A	.953	1.037	1.012	1.061	1.068	2.129
516B	.932	1.000	1.072	1.035	1.072	2.107
517A	.929	1.113	.967	1.154	1.138	2.292
517B	.926	1.109	.974	1.151	1.139	2.290
518A	.935	1.010	1.059	1.044	1.075	2.119
519A	.847	1.041	1.135	1.127	1.205	2.332
519B	.869	1.062	1.083	1.136	1.186	2.323
520A	.955	1.019	1.027	1.043	1.057	2.100
520B	.956	1.008	1.038	1.031	1.051	2.082
521A	.855	1.103	1.060	1.190	1.230	2.420
521B	.958	1.048	.996	1.070	1.068	2.138
522A	.967	1.020	1.014	1.037	1.044	2.081
523A	.965	1.024	1.011	1.042	1.048	2.091
524A	.968	1.017	1.016	1.033	1.042	2.075
526A	.690	1.506	.963	1.782	1.816	3.598
527A	.935	1.058	1.011	1.093	1.100	2.193

A/B, C/B → ratio of anisotropy axes maximum/intermediate and minimum/intermediate

E → shape of susceptibility ellipsoid; prolate (E>1) or oblate (E<1)

LIN, FOLN → magnetic lineation and foliation

% ANIS → percent anisotropy

* → Refer to Hrouda et al., 1971 for complete explanation of the anisotropy parameters.

FIGURES

Figure 83-1. Location map of the different research areas which are studied in the NFWMP. The two areas reported in this year's report are the URL area near Pinawa, Manitoba and the East Bull Lake area near Massey, Ontario.

Figure 83-2. The frequency distribution of susceptibility population measured from URL surface and borecore samples is plotted on normal probability paper. Such a plot is used to readily identify the sub-populations present in the data set and therefore identify susceptibility intervals associated with each sub-population. (Susceptibility = SI units x 10^{-3}.)

Figure 83-3. The frequency distribution of the lower susceptibility population measured from URL-6. This shows the best fit of the third sub-population and the intersection of the intermediate and low value population at 3.58 x 10^{-3} SI. (Susceptibility = SI units x 10^{-4}.)

Figure 83-4. The magnetic susceptibility measured at 10 cm intervals along the cores obtained from URL-6 is plotted against the borehole length (metre). Note that this plot shows all data without any averaging and is plotted on a linear scale.

Figure 83-5. The magnetic susceptibility measured at 10 cm intervals along the cores obtained from URL-6 is plotted against the borehole length (metre). Note that this plot shows the average over an area of 0.5 m and is plotted on a linear scale.

Figure 83-6. The magnetic susceptibility measured at 10 cm intervals along the cores obtained from URL-6 is plotted against the borehole length (metre). Note that this plot shows the average over an area of 1.0 m and is plotted on a linear scale.

Figure 83-7. The magnetic susceptibility measured at 10 cm intervals along the cores obtained from URL-6 is plotted against the borehole length (metre). Note that this plot shows the susceptibility using a semi-log scale and has not been averaged.

Figure 83-8. The magnetic susceptibility measured at 10 cm intervals along the cores obtained from URL-6 is plotted against the borehole length (metre). Note that this plot shows the susceptibility using a semi-log scale average over an area of 0.5 m.

Figure 83-9. The magnetic susceptibility measured at 10 cm intervals along the cores obtained from URL-6 is plotted against the borehole length (metre). Note that this plot shows the susceptibility using a semi-log scale average over 1.0 m.

Figure 83-10. The magnetic susceptibility measured at 10 cm intervals along the cores obtained from URL-6 is plotted against the borehole length (metre). Note that this plot shows the susceptibility using a semi-log scale average over 2.0 m.

Figure 83-11. The magnetic susceptibility measured at 10 cm intervals along the cores obtained from URL-6 is plotted against the borehole length (metre). Note that this plot shows the susceptibility on a semi-log scale using the 10 point boxcar filter followed by stacking of the Ith, I+1 and I+2 points. This curve indicates that all fluctuations of the susceptibility are of real significance and not the result of instrumental error.

Figure 83-12. The comparison between the alteration zones (defined by the susceptibility data), the magnetic susceptibility and the fracture histogram plotted on a semi-log scale against the borehole length. Note the excellent correlation between the alteration zones defined by the magnetic susceptibility sub-population and the fracture histogram.

Figure 83-13. The East Bull Lake Research Area grid lines are shown. The numbers identify the sites where the different rock magnetic properties were sampled and measured. This base map is used throughout the series of following figures. The different symbols refer to the sampling years.

Figure 83-14. The plot of the Koenigsberger ratio (Q = remanent/induced magnetization) against susceptibility for the gabbro and the dyke sites. Some features are noteworthy. Most of the gabbro show a rather well defined trend along a narrow band of susceptibility from a very low Q value (~0.5) to a very high Q value (>100). This trend is interpreted as the signature of the alteration associated with the Folson Lake Fault (from highly altered to a lowered level of alteration respectively). The star symbol represents the site where the youngest dyke cutting the gabbro was sampled. The dyke post-dates the faulting and alteration events and sets an upper age limit for the faulting at 1500 Ma.

Figure 83-15. Plot of the Koenigsberger ratio against density. The sampling of 1983 gabbro confirms the trend defined in the 1982 surveys where a trend from low to high Koenigsberger ratio is associated with the alteration level of the rock from high (low Q) to low (high Q).

Figure 83-16. Cumulative percent frequency distribution plotted against BMS for surface samples at East Bull Lake Research Area using a semi-log scale. Three sub-populations are derived from the data set and are used to define the susceptibility intervals needed to interpret the different levels of alteration.

Figure 83-17. Contour plot of the magnetic susceptibility variation from the surface sampled specimens. The site locations are as in Fig. 83-13 and the site values are listed in Tables 2 and 3. The V symbol indicates the presence of dyke.

Figure 83-18. Contour plot of the Koenigsberger ratio obtained from the surface sampled specimens. The site locations are as in Fig. 83-13. The V symbol indicates the presence of dyke. Note the very rapid increase of the Q ratio away from the Folson Lake Fault. The site mean value were used and are listed in Tables 2 and 3.

Figure 83-19. Contour plots of the calculated vertical remanence component. The site locations are as in Fig. 83-13 and the V symbol indicates the presence of dyke. The site mean values are listed in Tables 2 and 3. The rapid variation seen above the Moon Lake area coincides with the high variations seen in the total field and gradiometer survey. The explanation for this phenomenon is the presence of a high intensity remanence with both normal and reverse polarity. Such a feature has not yet been related to any geological phenomena seen in the area.

Figure 83-20. Contour plots of the site mean averages using log mean intensity of magnetic susceptibility. The site locations are as in Fig. 83-13 and the values are listed in Tables 2 and 3. The V symbol indicates the presence of dyke.

Figure 83-21. Equal angle stereonet contoured at a 2.5% interval of all statistically significant site mean remanence directions. Data obtained using a 1% counting window.

Figure 83-22. Equal angle stereonet plot of all vector site means after rotation to bring first mode of total population to the centre of the stereonet.

Figure 83-23. Areal distribution of aberrant site mean remanence directions. One group aligned along the Folson Lake Fault is clearly associated with intrusion of a late stage dyke. The genesis of the other group is presently unknown.

Figure 83-24. Orthogonal plots of typical alternating field demagnetization results from late stage dyke.

Figure 83-25. Equal angle stereonet showing the distribution of remanence directions obtained from specimens of the late stage dyke.

Figure 83-26. Orthogonal plots of typical thermal treatment results from samples of hematitic gouge from fault zones at stripped outcrop.

Figure 83-27. Equal angle stereonet showing the distribution of the remanence directions obtained from specimens of hematitic fault gouge.

Figure 83-28. Flinn-type deformation diagram applied to parameters of the individual susceptibility ellipsoids.

Figures 83-29, 83-30, 83-31. Equal angle stereonets of, respectively, the maximum, intermediate, and minimum anistropic magnetic susceptibility axes of specimens from the Folson Lake Fault zone.

Figure 83-32. Equal angle stereonet presenting the interpreted fabrics present in the Folson Lake Fault zone.

Figure 83-33. Magnetic susceptibility log from the East Bull Lake Research Area borecore EBL-1, Massey, Ontario, plotted using a semi-log scale against depth in metres. The sampling was done at 10 cm intervals along the length of the borecores. The data are shown without any averaging. The EBL-1 is incomplete and should be completed by June 1985.

Figure 83-34. Magnetic susceptibility log from the East Bull Lake Research Area borecore EBL-1, Massey, Ontario, plotted using a semi-log scale against depth in metres. The sampling was done at 10 cm intervals along the length of the borecores. The data shown is averaged using a 10 point boxcar filter, an average over 1 m.

Figure 83-35. Magnetic susceptibility log from the East Bull Lake Research Area borecore EBL-1, Massey, Ontario, plotted using a semi-log scale against depth in metres. The sampling was done at 10 cm intervals along the length of the borecores. The data shown are averaged using a 25 point boxcar filter, an average over 2.5 m.

Figure 83-36. Magnetic susceptibility log from the East Bull Lake Research Area borecore EBL-1, Massey, Ontario, plotted using a semi-log scale against depth in metres. The sampling was done at 10 cm intervals along the length of the borecores. The data shown are averaged using a 50 point boxcar filter, an average over 5 m.

Figure 83-37. Magnetic susceptibility log from the East Bull Lake Research Area borecore EBL-2, Massey, Ontario, plotted using a semi-log scale against depth in metres. The sampling was done at 10 cm intervals along the length of the borecores. The data are shown without any averaging.

Figure 83-38. Magnetic susceptibility log from the East Bull Lake Research Area borecore EBL-2, Massey, Ontario, plotted using a semi-log scale against depth in metres. The sampling was done at 10 cm intervals along the length of the borecores. The data shown are averaged using a 10 point boxcar filter, an average over 1 m.

Figure 83-39. Magnetic susceptibility log from the East Bull Lake Research Area borecore EBL-2, Massey, Ontario, plotted using a semi-log scale against depth in metres. The sampling was done at 10 cm intervals along the length of the borecores. The data shown are averaged using a 25 point boxcar filter, an average over 2.5 m.

Figure 83-40. Magnetic susceptibility log from the East Bull Lake Research Area borecore EBL-2, Massey, Ontario, plotted using a semi-log scale against depth in metres. The sampling was done at 10 cm

intervals along the length of the borecores. The data shown are averaged using a 50 point boxcar filter, an average over 5 m.

Figure 83-41. Magnetic susceptibility log from the East Bull Lake Research Area borecore EBL-3, Massey, Ontario, plotted using a semi-log scale against depth in metres. The sampling was done at 10 cm intervals along the length of the borecores. The data are shown without any averaging.

Figure 83-42. Magnetic susceptibility log from the East Bull Lake Research Area borecore EBL-3, Massey, Ontario, plotted using a semi-log scale against depth in metres. The sampling was done at 10 cm intervals along the length of the borecores. The data shown are averaged using a 10 point boxcar filter, an average over 1 m.

Figure 83-43. Magnetic susceptibility log from the East Bull Lake Research Area borecore EBL-3, Massey, Ontario, plotted using a semi-log scale against depth in metres. The sampling was done at 10 cm intervals along the length of the borecores. The data shown are averaged using a 25 point boxcar filter, an average over 2.5 m.

Figure 83-44. Magnetic susceptibility log from the East Bull Lake Research Area borecore EBL-3, Massey, Ontario, plotted using a semi-log scale against depth in metres. The sampling was done at 10 cm intervals along the length of the borecores. The data shown are averaged using a 50 point boxcar filter, an average over 5 m.

Figure 83-45. Magnetic susceptibility log from the East Bull Lake Research Area borecore EBL-4, Massey, Ontario, plotted using a semi-log scale against depth in metres. The sampling was done at 10 cm intervals along the length of the borecores. The data are shown without any averaging.

Figure 83-46. Magnetic susceptibility log from the East Bull Lake Research Area borecore EBL-4, Massey, Ontario, plotted using a semi-log scale against depth in metres. The sampling was done at 10 cm intervals along the length of the borecores. The data shown are averaged using a 10 point boxcar filter, an average over 1 m.

Figure 83-47. Magnetic susceptibility log from the East Bull Lake Research Area borecore EBL-4, Massey, Ontario, plotted using a semi-log scale against depth in metres. The sampling was done at 10 cm intervals along the length of the borecores. The data shown are averaged using a 25 point boxcar filter, an average over 2.5 m.

Figure 83-48. Magnetic susceptibility log from the East Bull Lake Research Area borecore EBL-4, Massey, Ontario, plotted using a semi-log scale against depth in metres. The sampling was done at 10 cm intervals along the length of the borecores. The data shown are averaged using a 50 point boxcar filter, an average over 5 m.

Figure 83-4. The magnetic susceptibility logs are plotted against borehole lengths for borecores EBL-1 to -4 from the East Bull Lake Research Area, Massey, Ontario. The 5 m average lot is used to

illustrate the most probable extent of the dendritric gabbro unit from EBL-3, -4, -2 and possibly EBL-1. A second zone, geologically not yet identified, may be seen between EBL-3 and 4 at depths of approximately 375 and 400 m.

Figure 83-50. The plots of magnetic susceptibility against the frequency distribution for the three boreholes EBL-2, -3 and -4 show up to 5 different sub-populations indicating complex susceptibility patterns associated with a highly fractured and a highly variable litholigical unit.

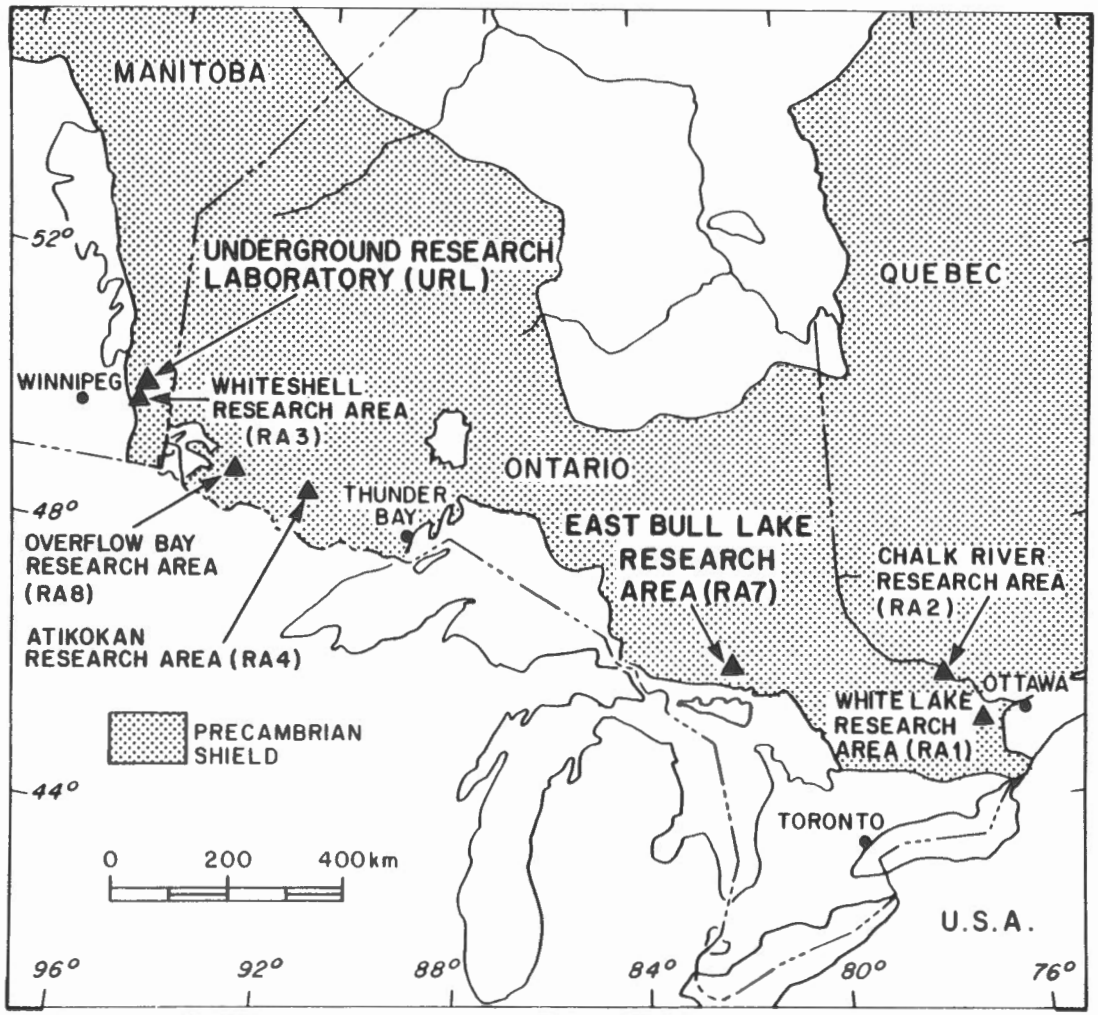
MANITOBA
52°
UNDERGROUND RESEARCH LABORATORY (URL)
QUEBEC
WINNIPEG
WHITESHELL RESEARCH AREA (RA3)
ONTARIO
48°
THUNDER BAY
OVERFLOW BAY RESEARCH AREA (RA8)
EAST BULL LAKE RESEARCH AREA (RA7)
CHALK RIVER RESEARCH AREA (RA2)
ATIKOKAN RESEARCH AREA (RA4)
OTTAWA
WHITE LAKE RESEARCH AREA (RA1)
PRECAMBRIAN SHIELD
44°
TORONTO
0 200 400km
U.S.A.
96°
92°
88°
84°
80°
76°

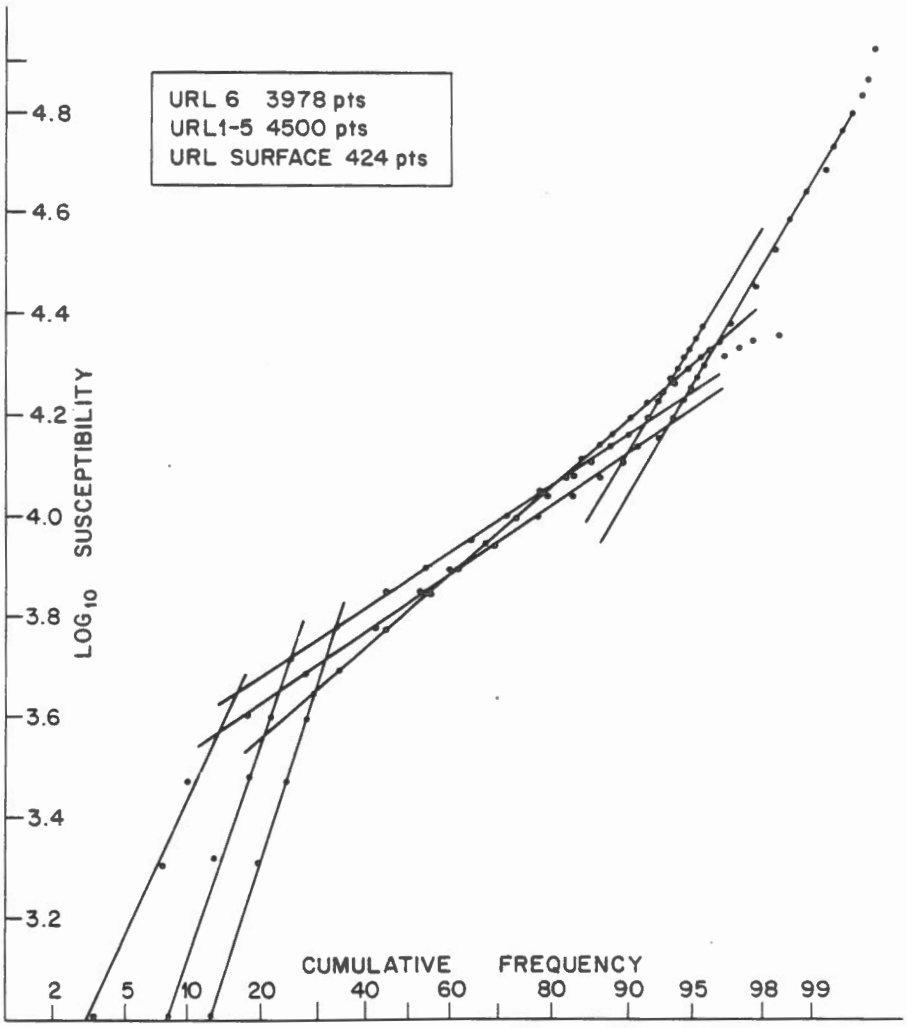
URL 6 3978 pts
URL1-5 4500 pts
URL SURFACE 424 pts
4.8
4.6
4.4
4.2
4.0
3.8
3.6
3.4
3.2
LOG10 SUSCEPTIBILITY
2
5
10
20
40
60
80
90
95
98
99
CUMULATIVE FREQUENCY

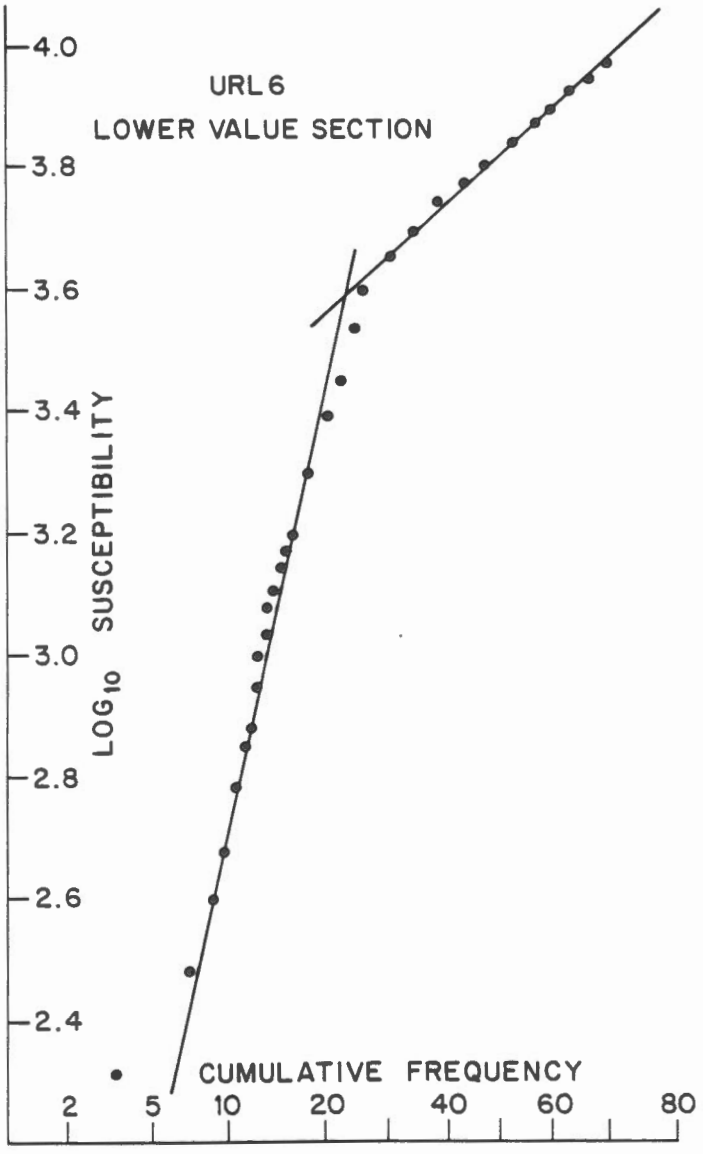
URL 6
LOWER VALUE SECTION
4.0
3.8
3.6
3.4
3.2
3.0
2.8
2.6
2.4
LOG10 SUSCEPTIBILITY
CUMULATIVE FREQUENCY
2
5
10
20
40
60
80

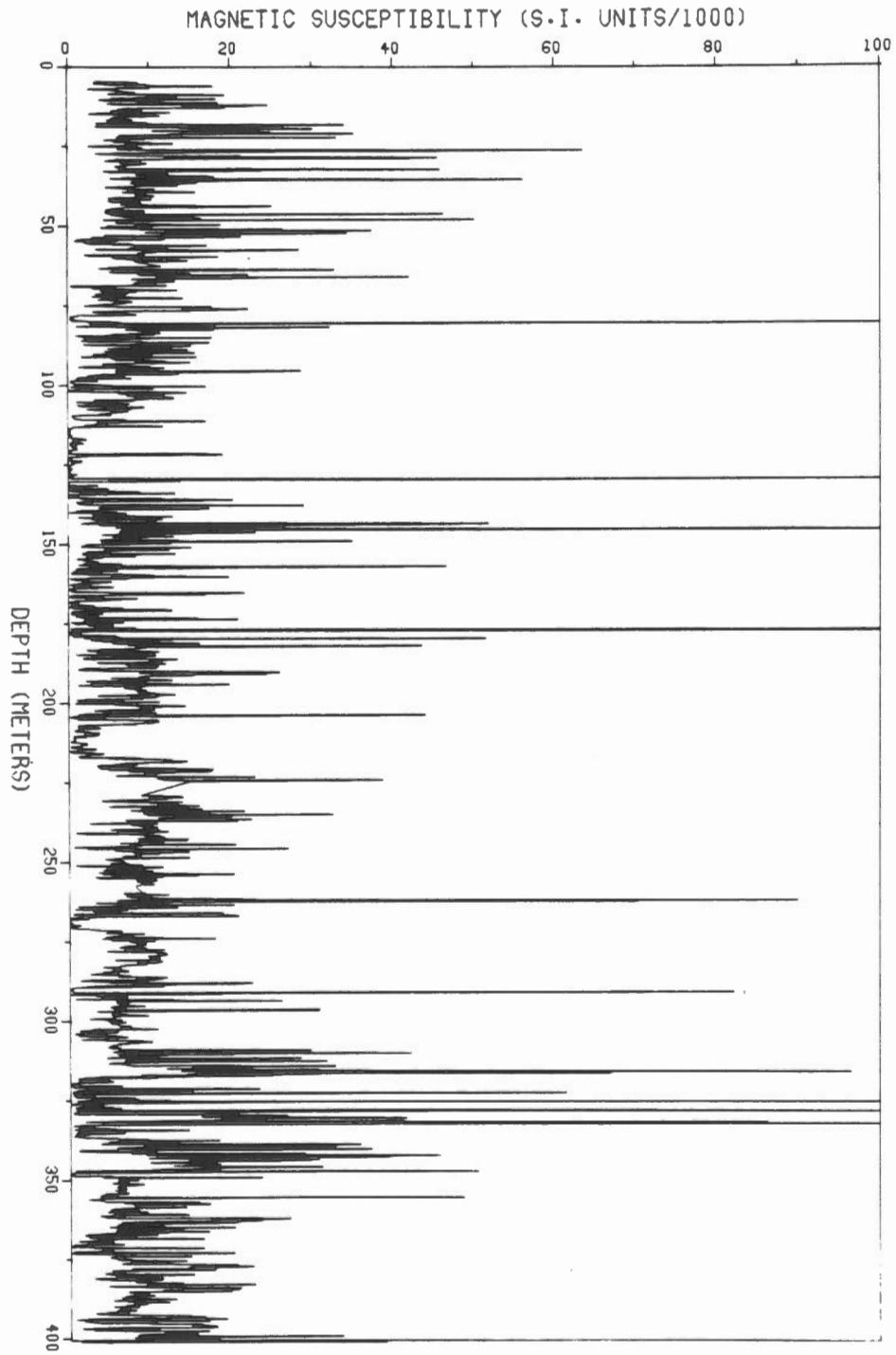
MAGNETIC SUSCEPTIBILITY (S.I. UNITS/1000)
0
20
40
60
80
100
0
50
100
150
200
250
300
350
400
DEPTH (METERS)

URL - 6

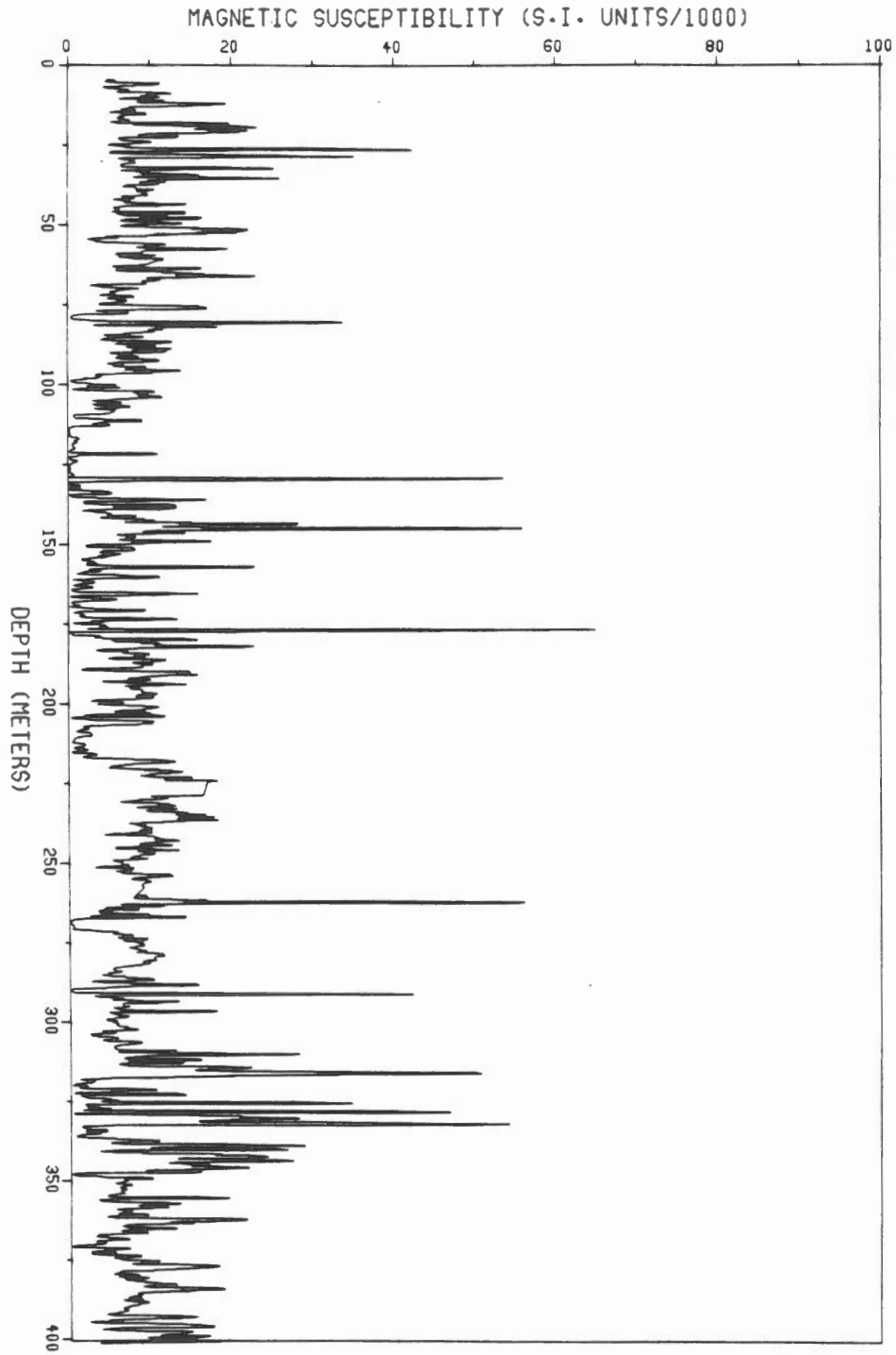

URL - 6

SMOOTHED WITH 5 POINT BOXCAR

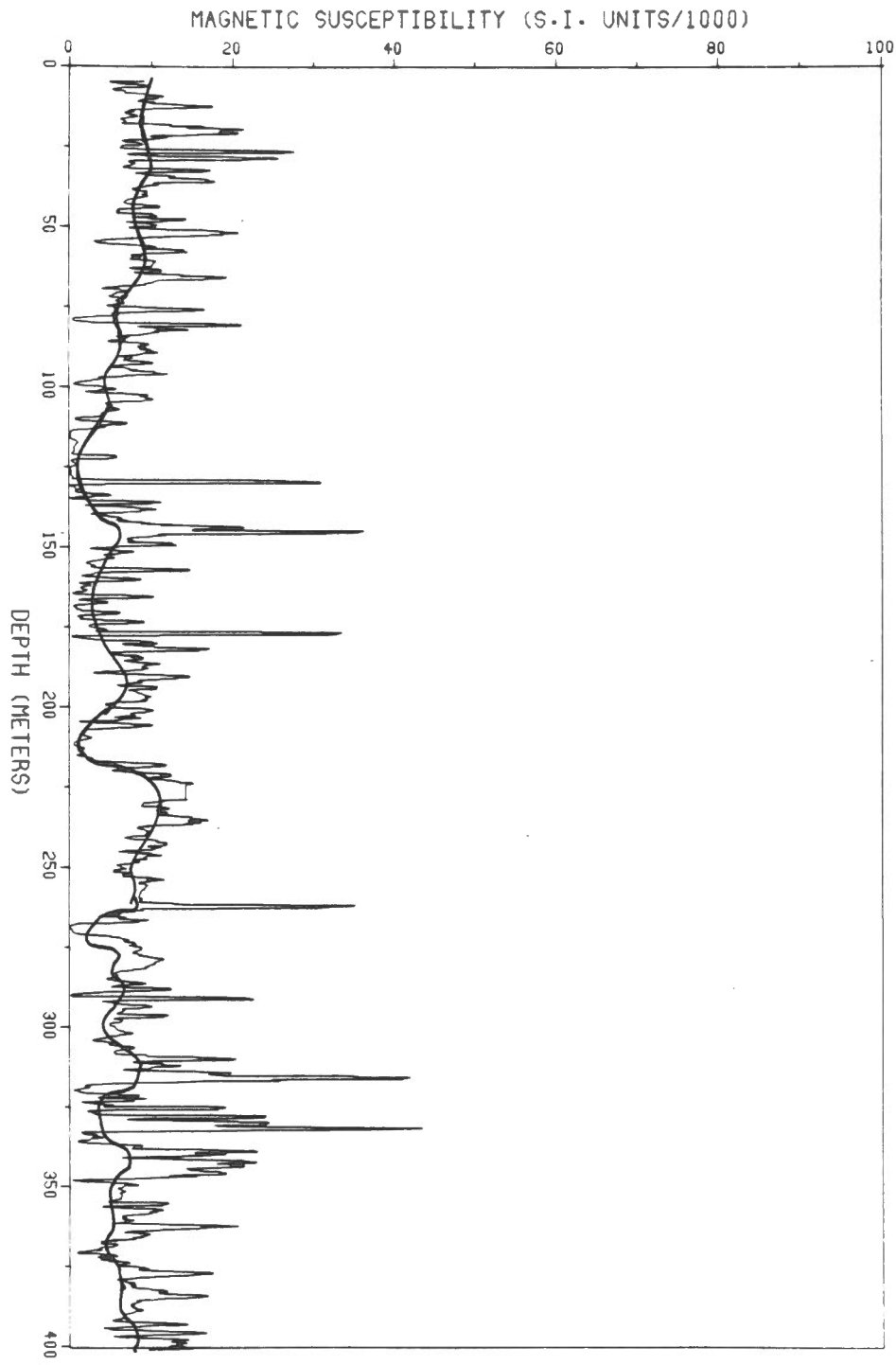

URL - 6

SMOOTHED WITH 10POINT BOXCAR

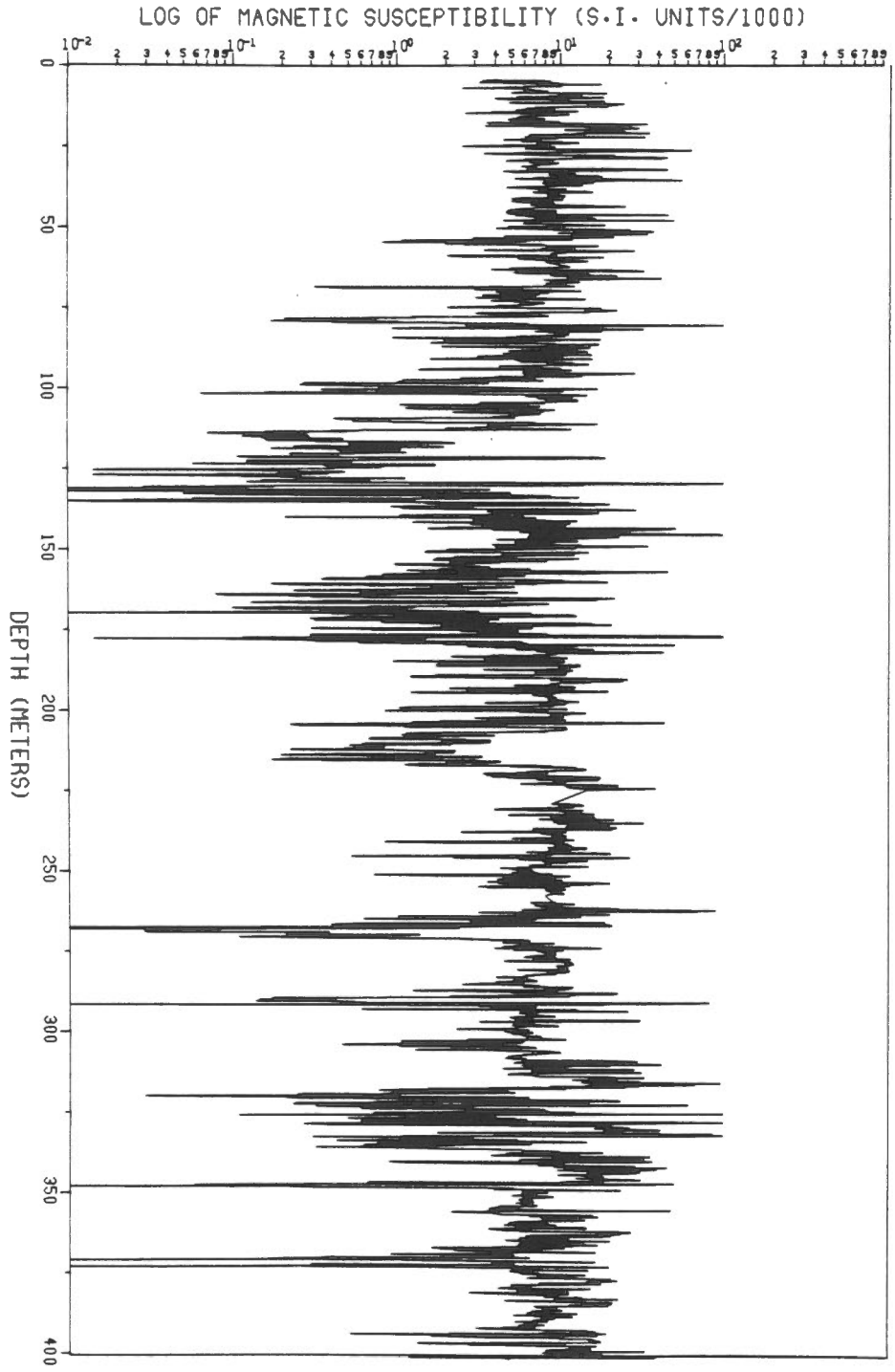
LOG OF MAGNETIC SUSCEPTIBILITY (S.I. UNITS/1000)
10^{-2}
10^{-1}
10^{0}
10^{1}
10^{2}
0
50
100
150
200
250
300
350
400
DEPTH (METERS)

URL - 6

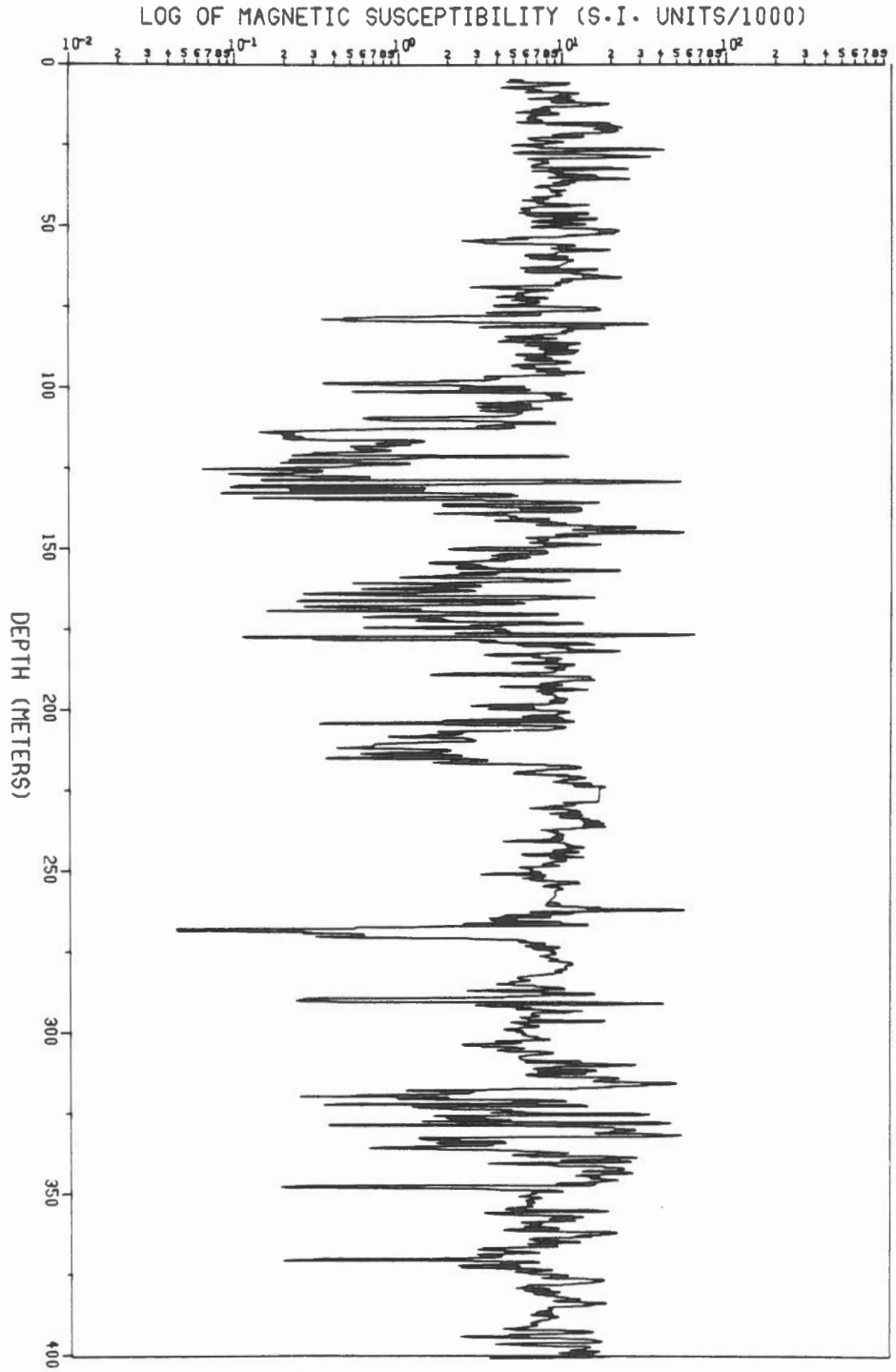

URL - 6

SMOOTHED WITH 5 POINT BOXCAR

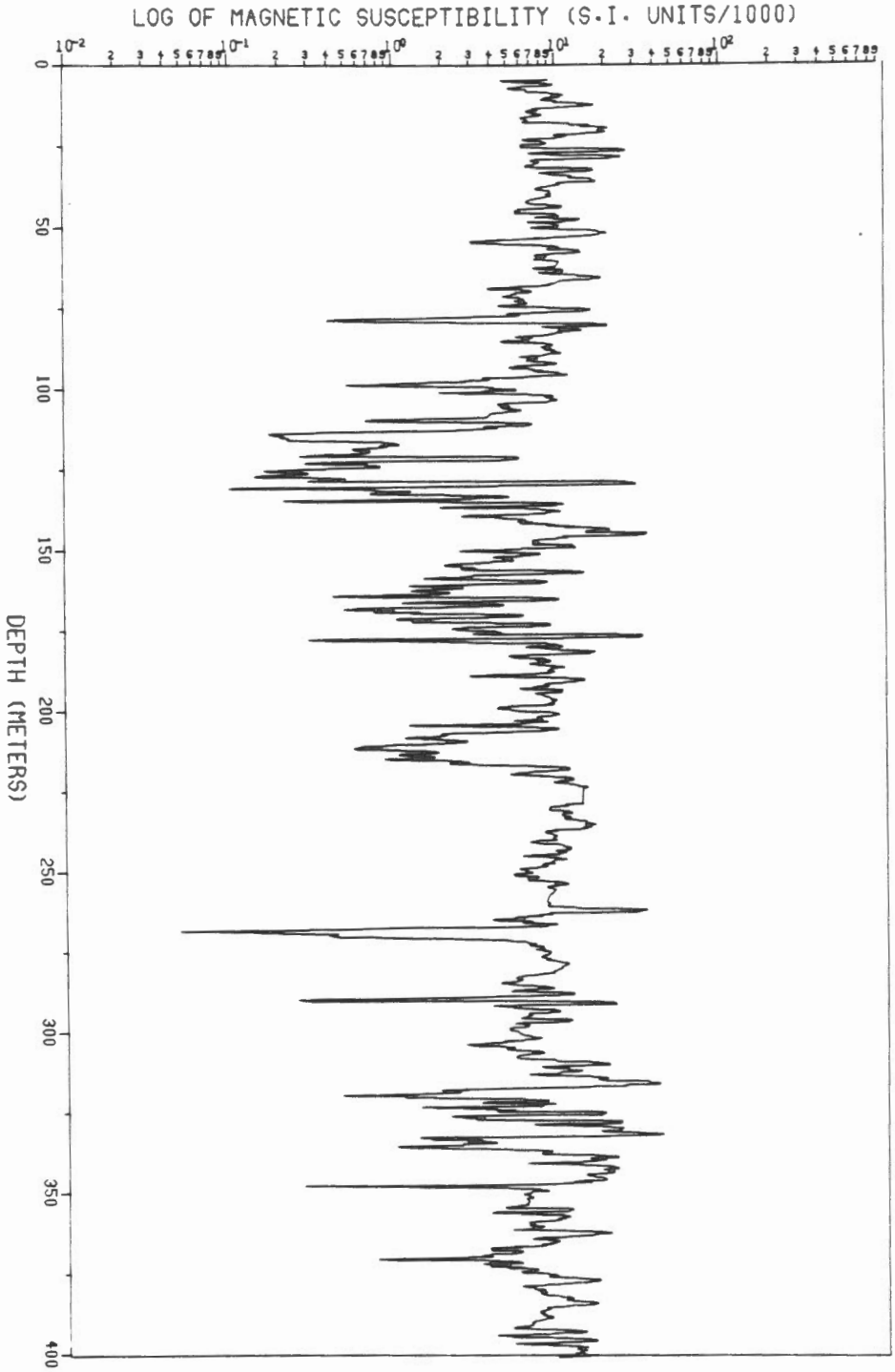

URL - 6

SMOOTHED WITH 10POINT BOXCAR

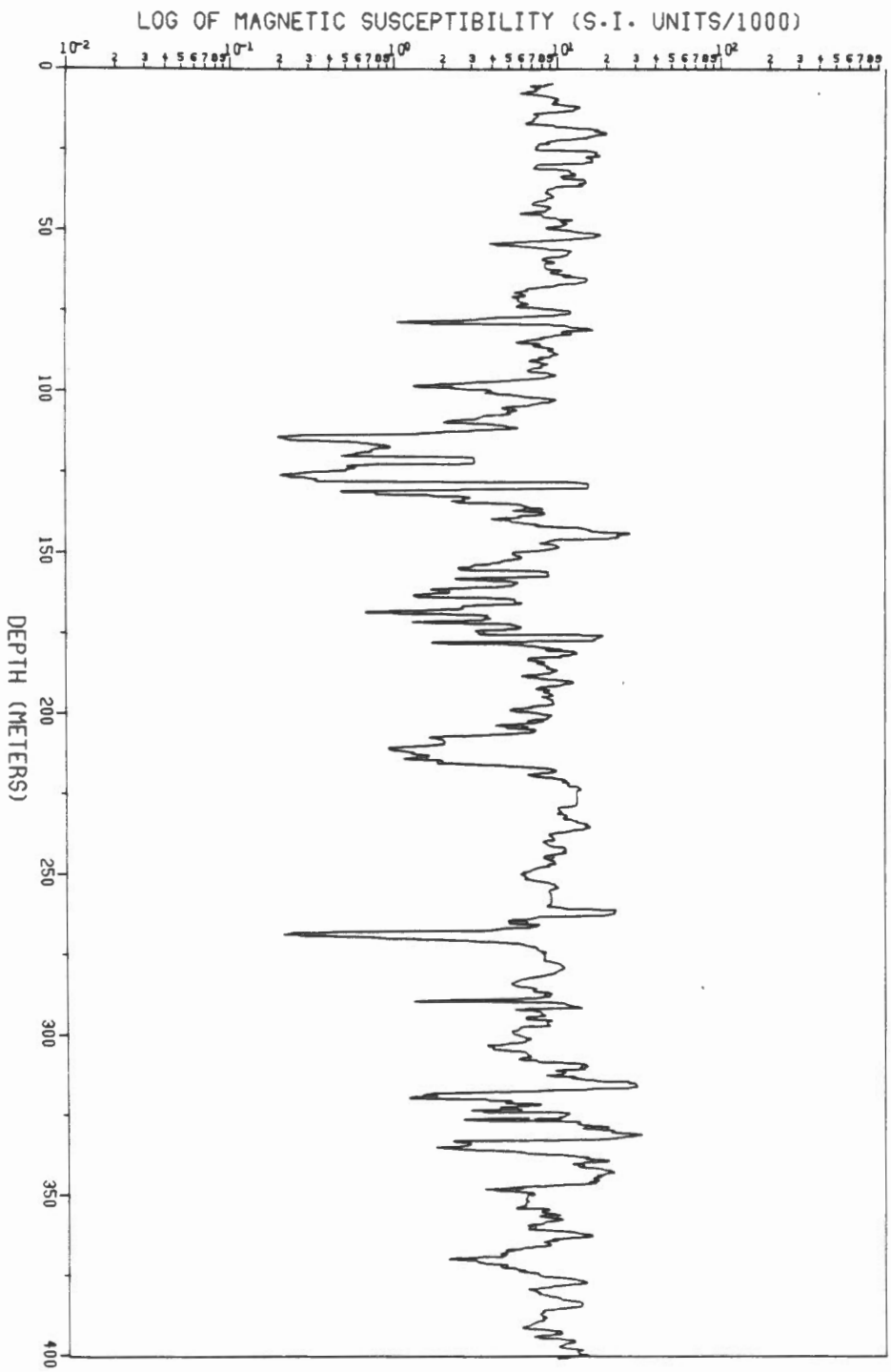

URL - 6

SMOOTHED WITH 20POINT BOXCAR

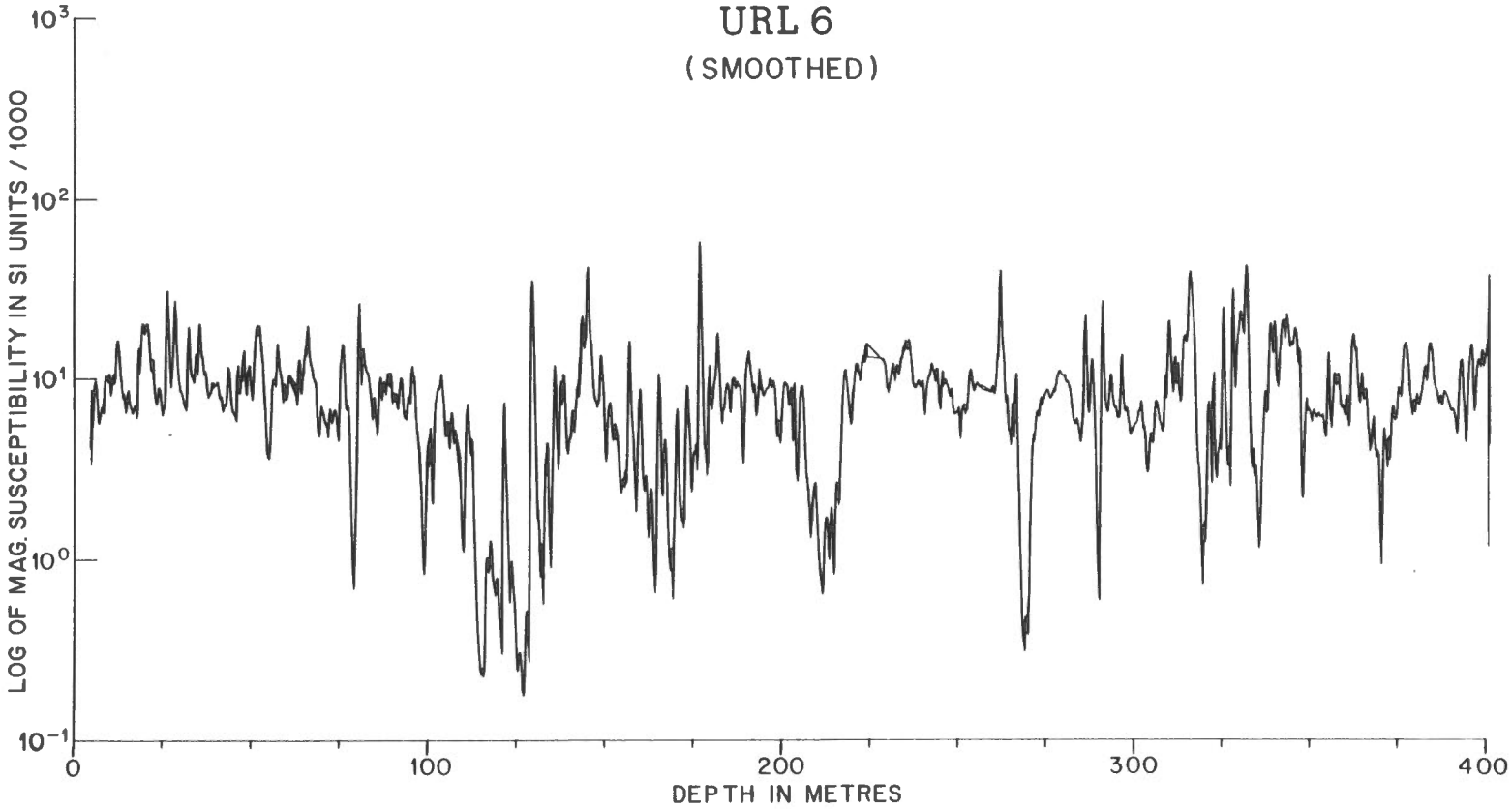
URL 6
(SMOOTHED)
LOG OF MAG. SUSCEPTIBILITY IN SI UNITS / 1000
10^3
10^2
10^1
10^0
10^{-1}
0
100
200
300
400
DEPTH IN METRES

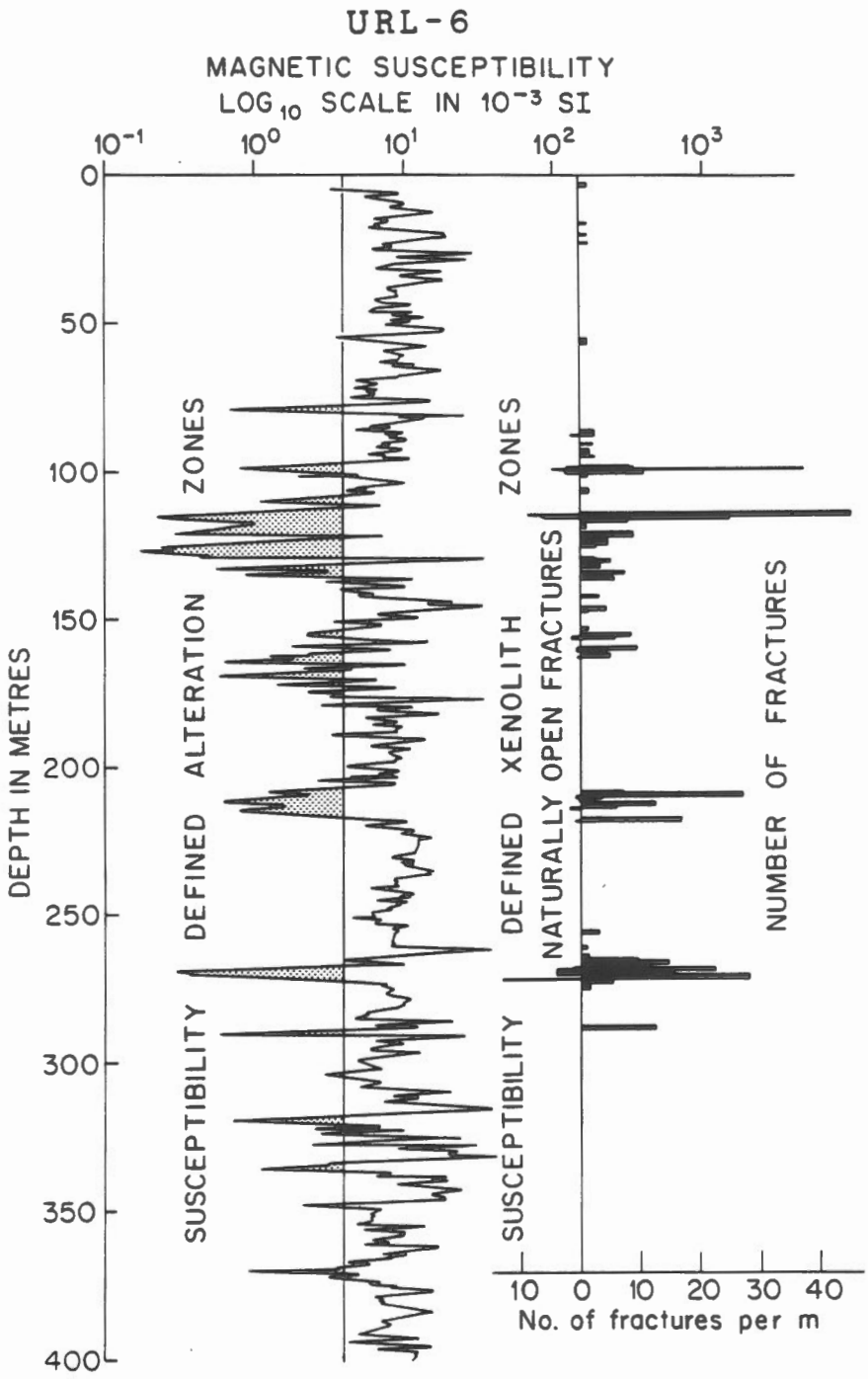
URL-6
MAGNETIC SUSCEPTIBILITY
LOG 10 SCALE IN 10⁻³ SI
10⁻¹
10⁰
10¹
10²
10³
0
50
100
150
200
250
300
350
400
DEPTH IN METRES
SUSCEPTIBILITY DEFINED ALTERATION ZONES
SUSCEPTIBILITY DEFINED XENOLITH NATURALLY OPEN FRACTURES ZONES
NUMBER OF FRACTURES
10 0 10 20 30 40
No. of fractures per m

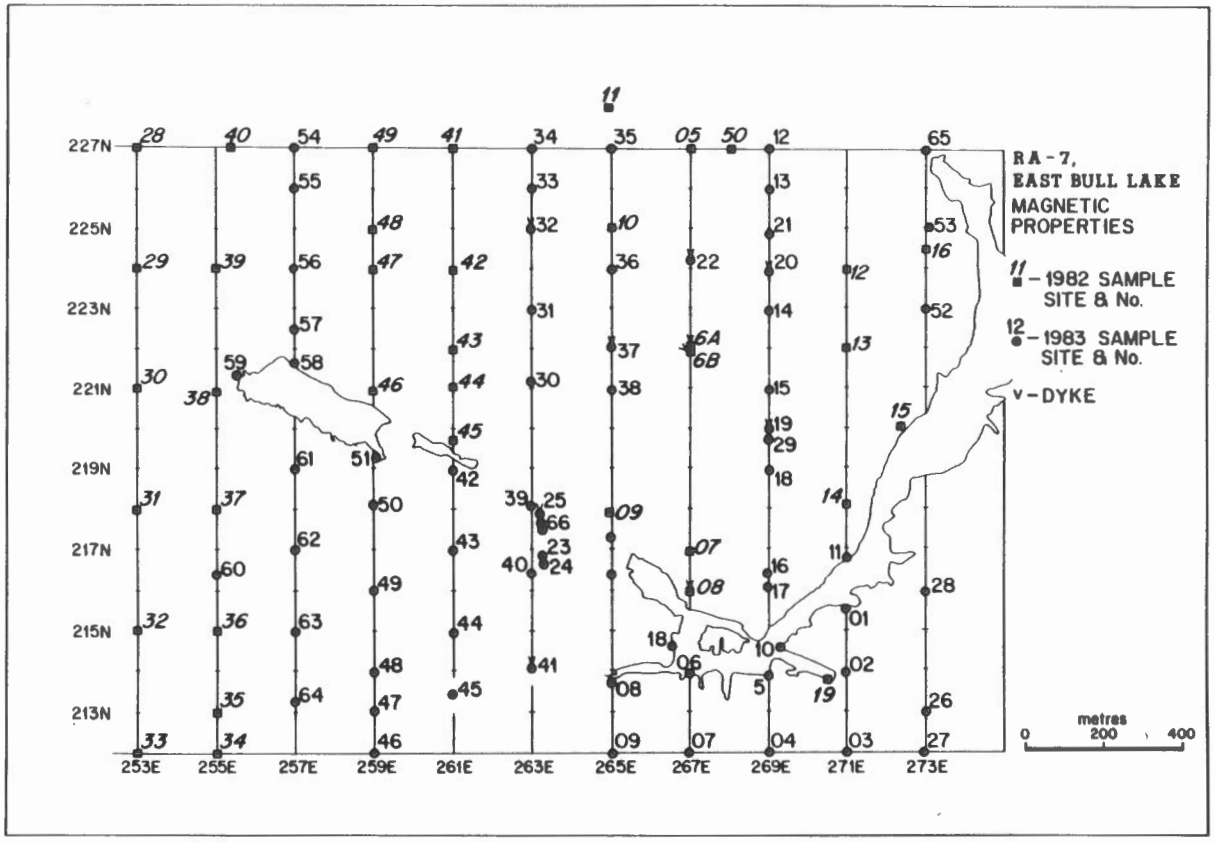
RA-7,
EAST BULL LAKE
MAGNETIC
PROPERTIES
11 – 1982 SAMPLE SITE & No.
12 – 1983 SAMPLE SITE & No.
v – DYKE
metres
0
200
400
227N
225N
223N
221N
219N
217N
215N
213N
253E
255E
257E
259E
261E
263E
265E
267E
269E
271E
273E

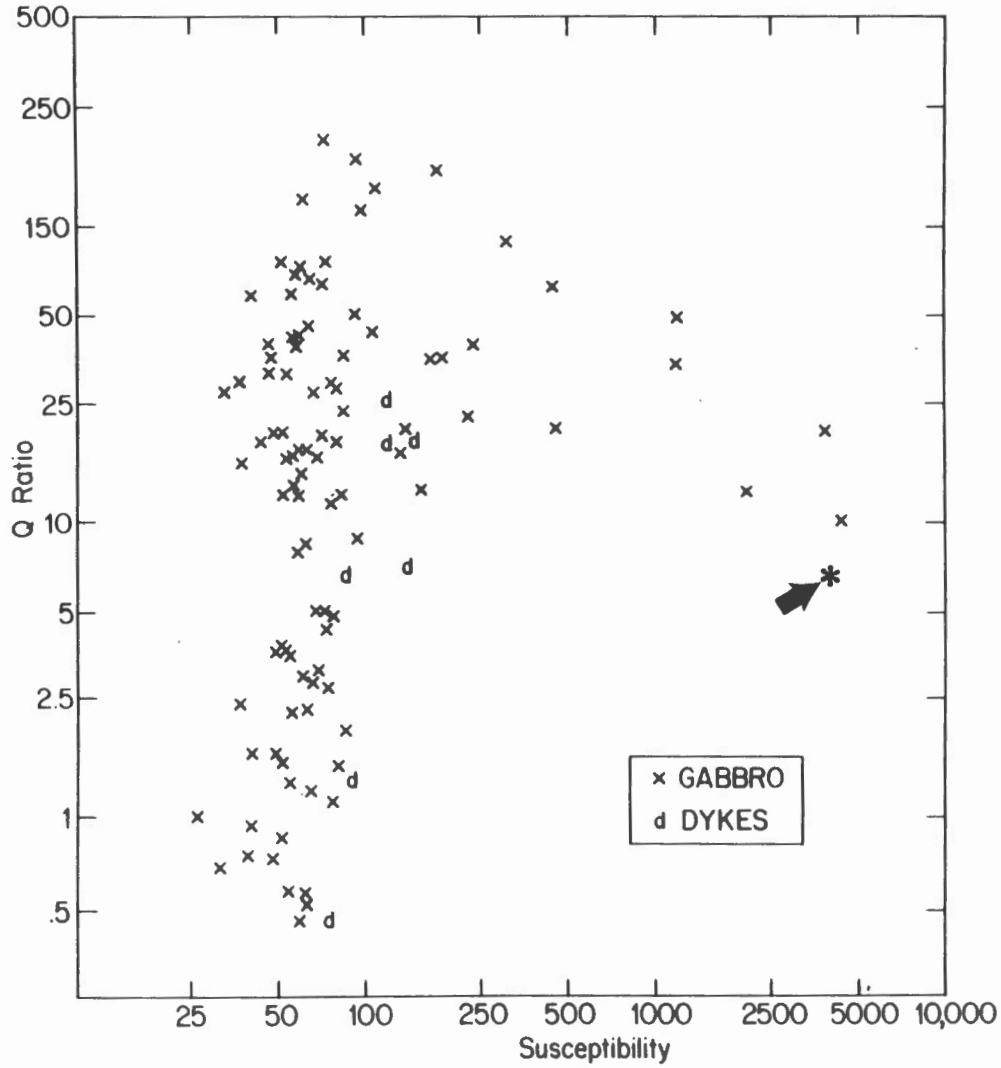
500
250
150
50
25
10
5
2.5
1
.5
Q Ratio
25
50
100
250
500
1000
2500
5000
10,000
Susceptibility
× GABBRO
d DYKES

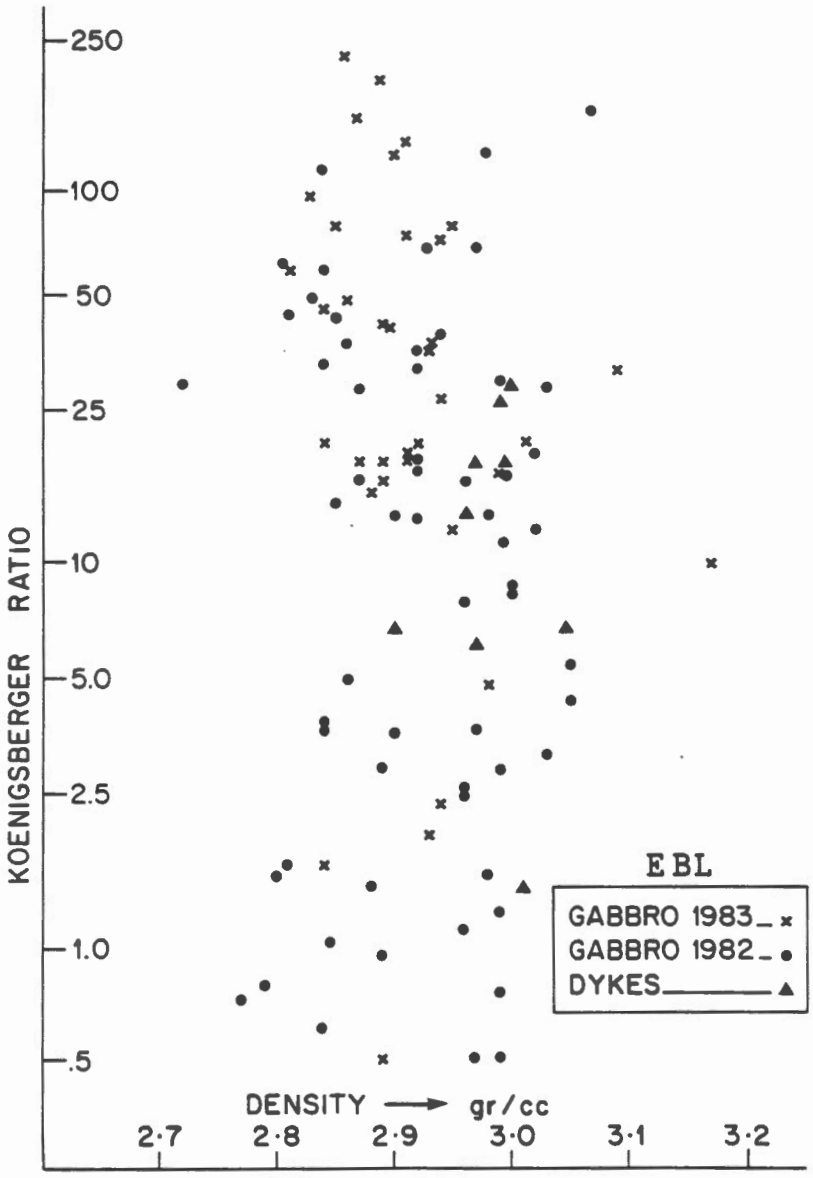
KOENIGSBERGER RATIO
250
100
50
25
10
5.0
2.5
1.0
.5
DENSITY → gr/cc
2·7
2·8
2·9
3·0
3·1
3·2
EBL
GABBRO 1983
GABBRO 1982
DYKES

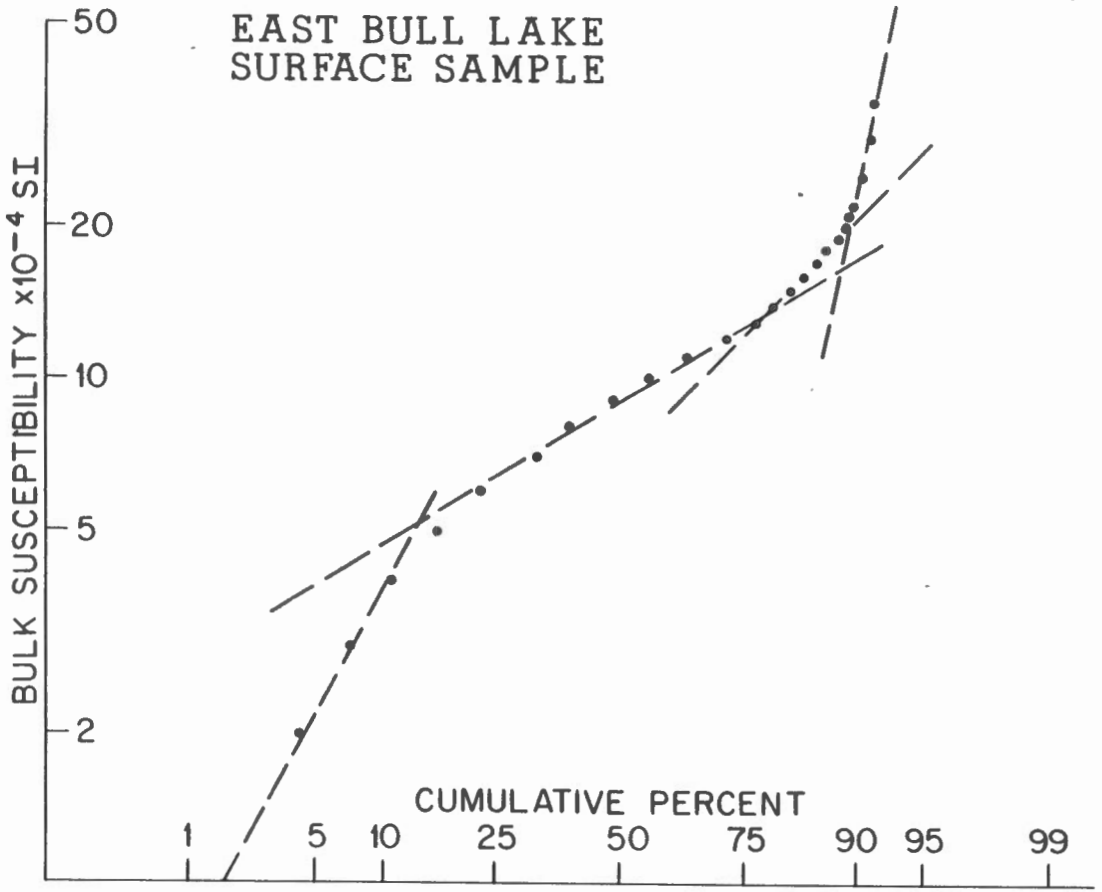
EAST BULL LAKE
SURFACE SAMPLE
BULK SUSCEPTIBILITY x10⁻⁴ SI
50
20
10
5
2
CUMULATIVE PERCENT
1
5
10
25
50
75
90
95
99

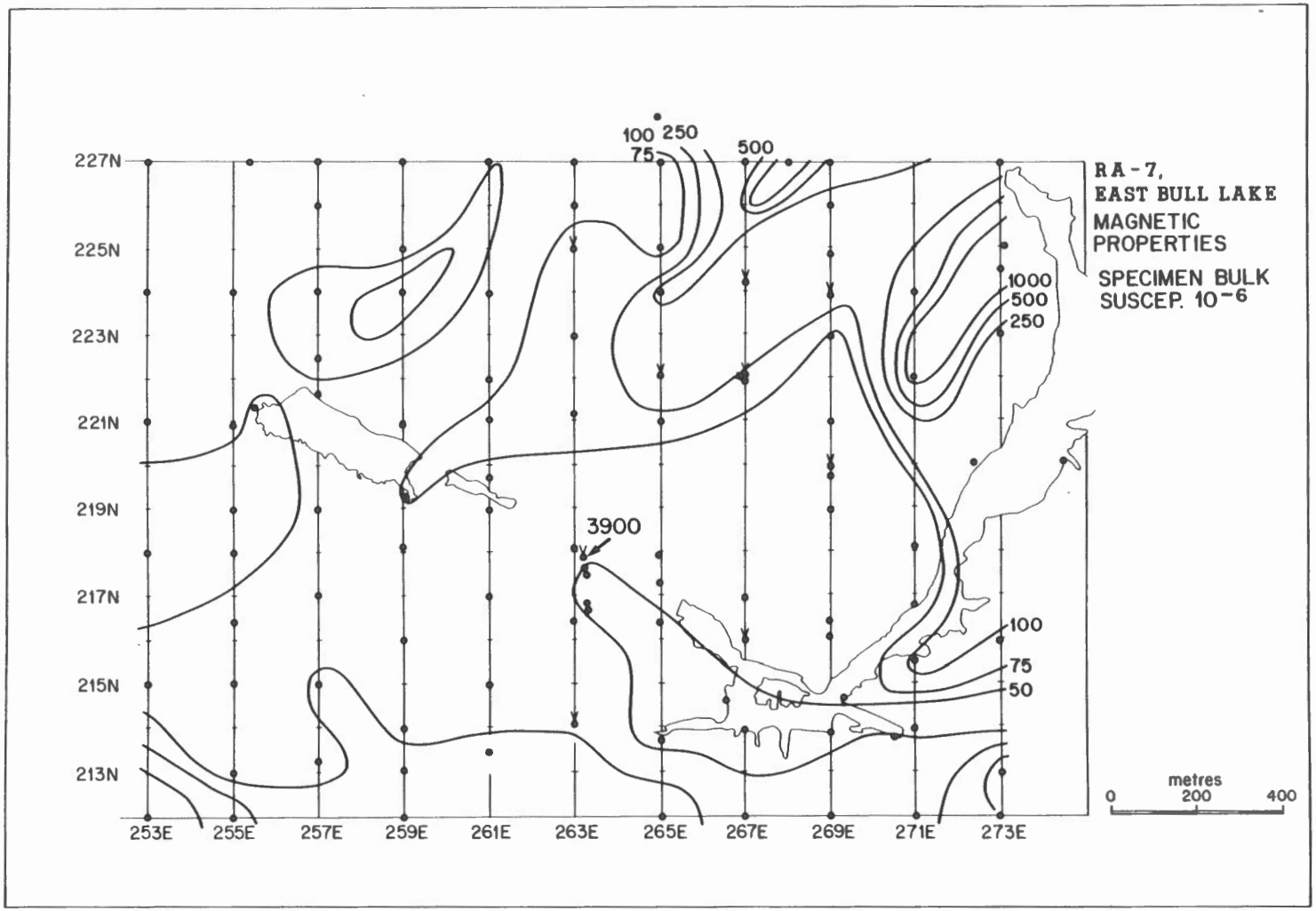
227N
225N
223N
221N
219N
217N
215N
213N
253E
255E
257E
259E
261E
263E
265E
267E
269E
271E
273E
100
250
75
500
1000
500
250
3900
100
75
50
RA-7,
EAST BULL LAKE
MAGNETIC
PROPERTIES
SPECIMEN BULK
SUSCEP. 10⁻⁶
metres
0
200
400

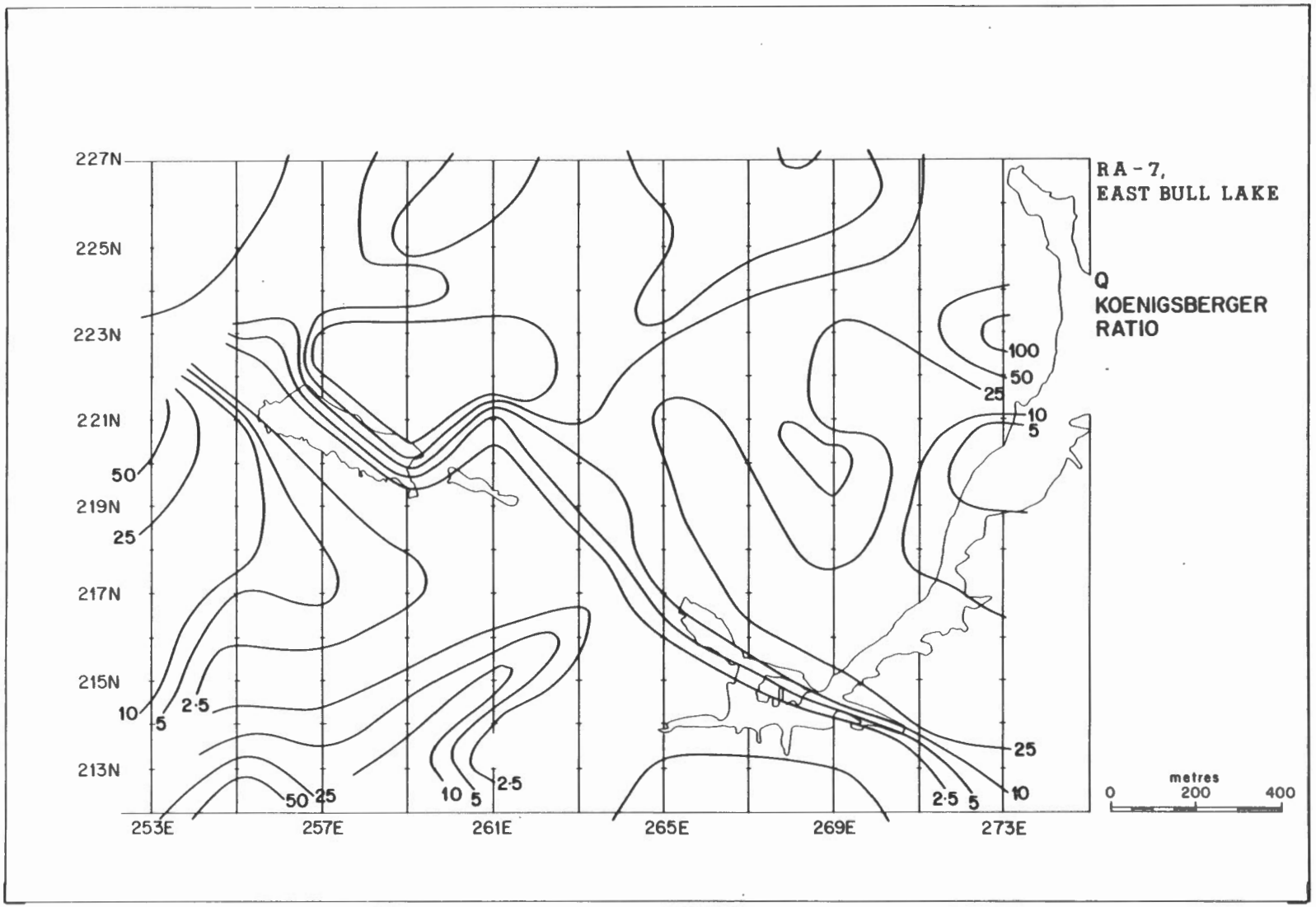
227N
225N
223N
221N
219N
217N
215N
213N
253E
257E
261E
265E
269E
273E
RA - 7,
EAST BULL LAKE
Q
KOENIGSBERGER
RATIO
100
50
25
10
5
2·5
metres
0
200
400

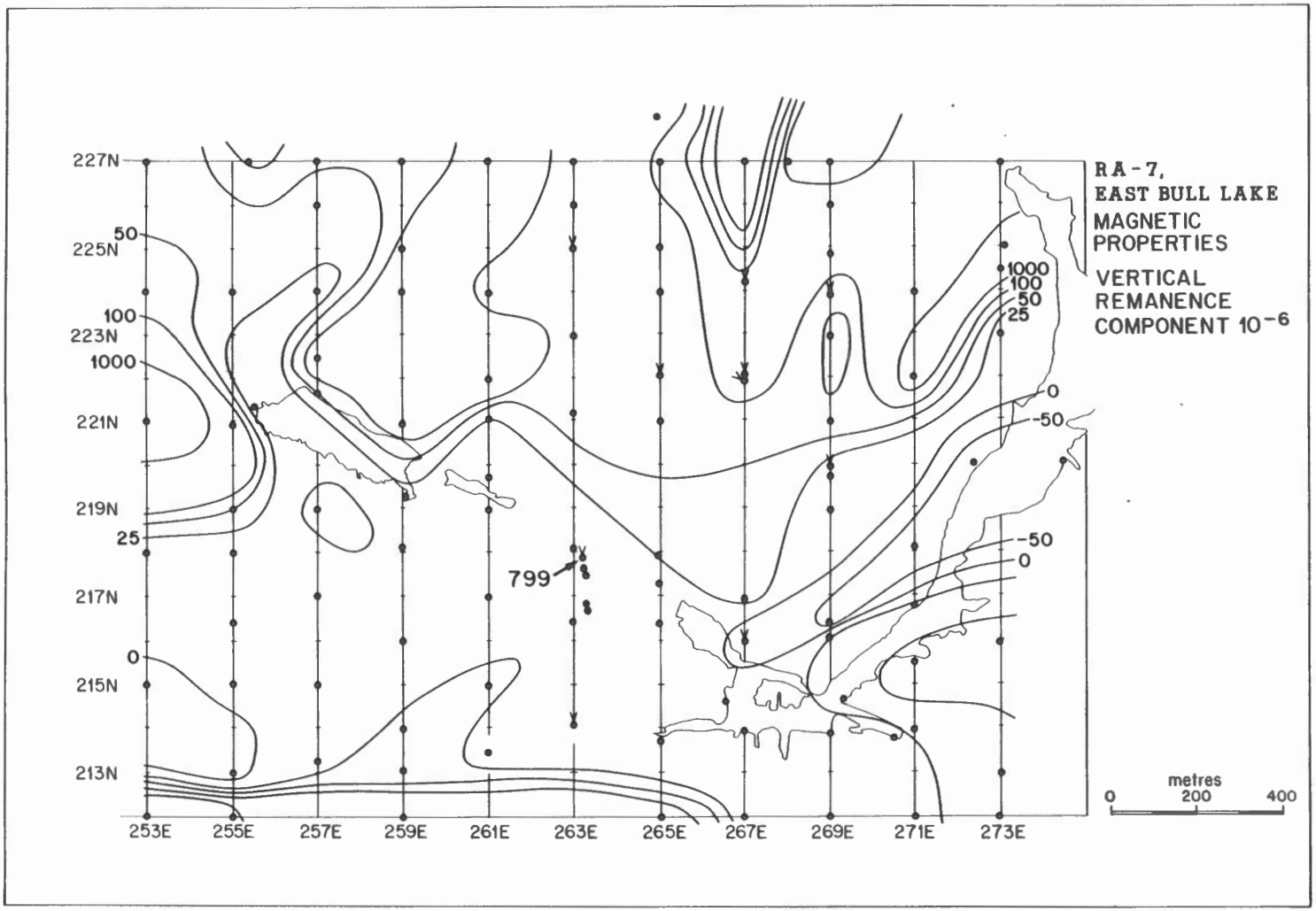
RA-7,
EAST BULL LAKE
MAGNETIC
PROPERTIES
VERTICAL
REMANENCE
COMPONENT 10⁻⁶
227N
225N
223N
221N
219N
217N
215N
213N
50
100
1000
25
0
799
1000
100
50
25
0
-50
-50
0
253E
255E
257E
259E
261E
263E
265E
267E
269E
271E
273E
metres
0
200
400

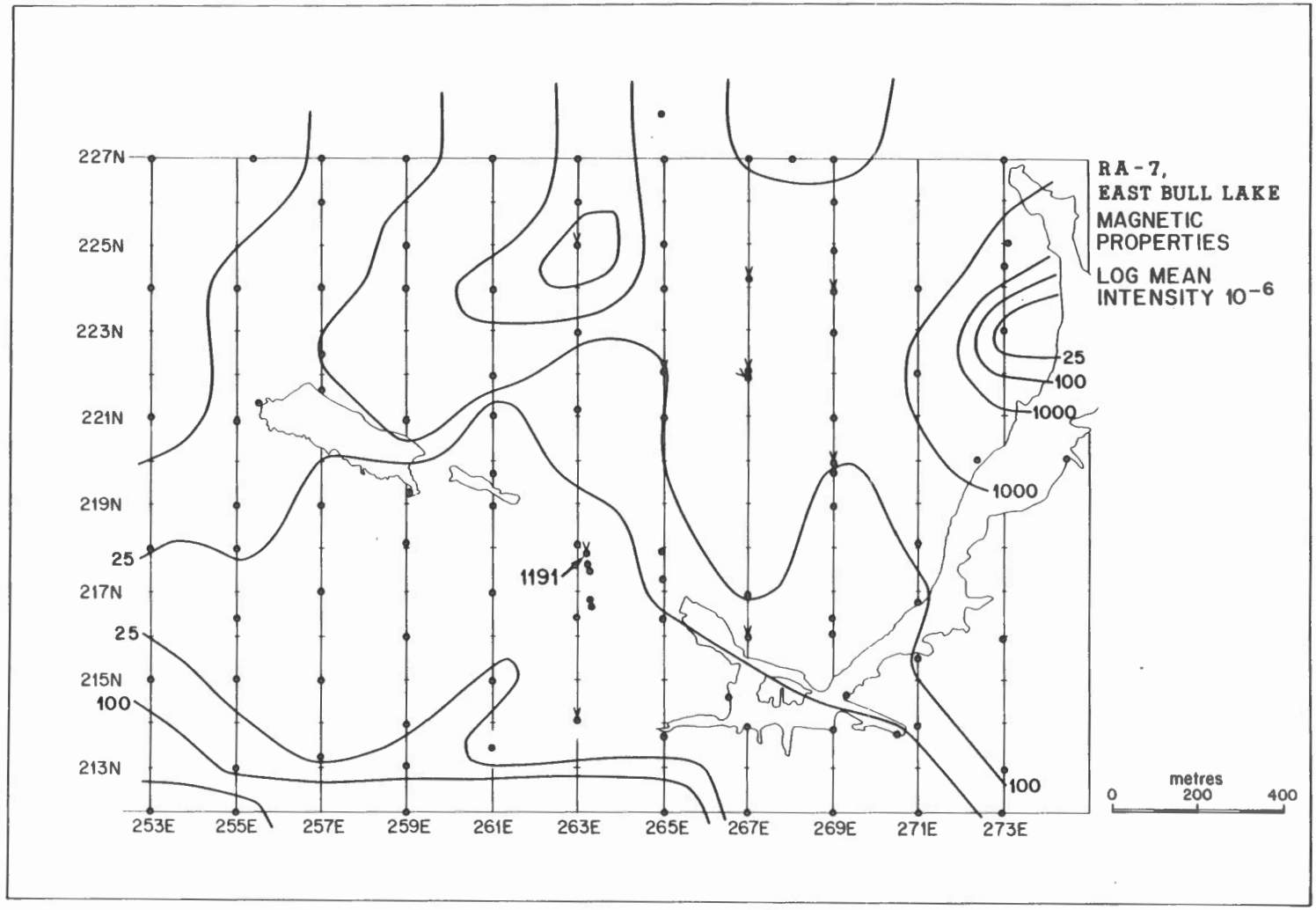
227N
225N
223N
221N
219N
217N
215N
213N
253E
255E
257E
259E
261E
263E
265E
267E
269E
271E
273E
25
25
100
1191
25
1000
1000
100
RA-7,
EAST BULL LAKE
MAGNETIC
PROPERTIES
LOG MEAN
INTENSITY 10-6
metres
0
200
400

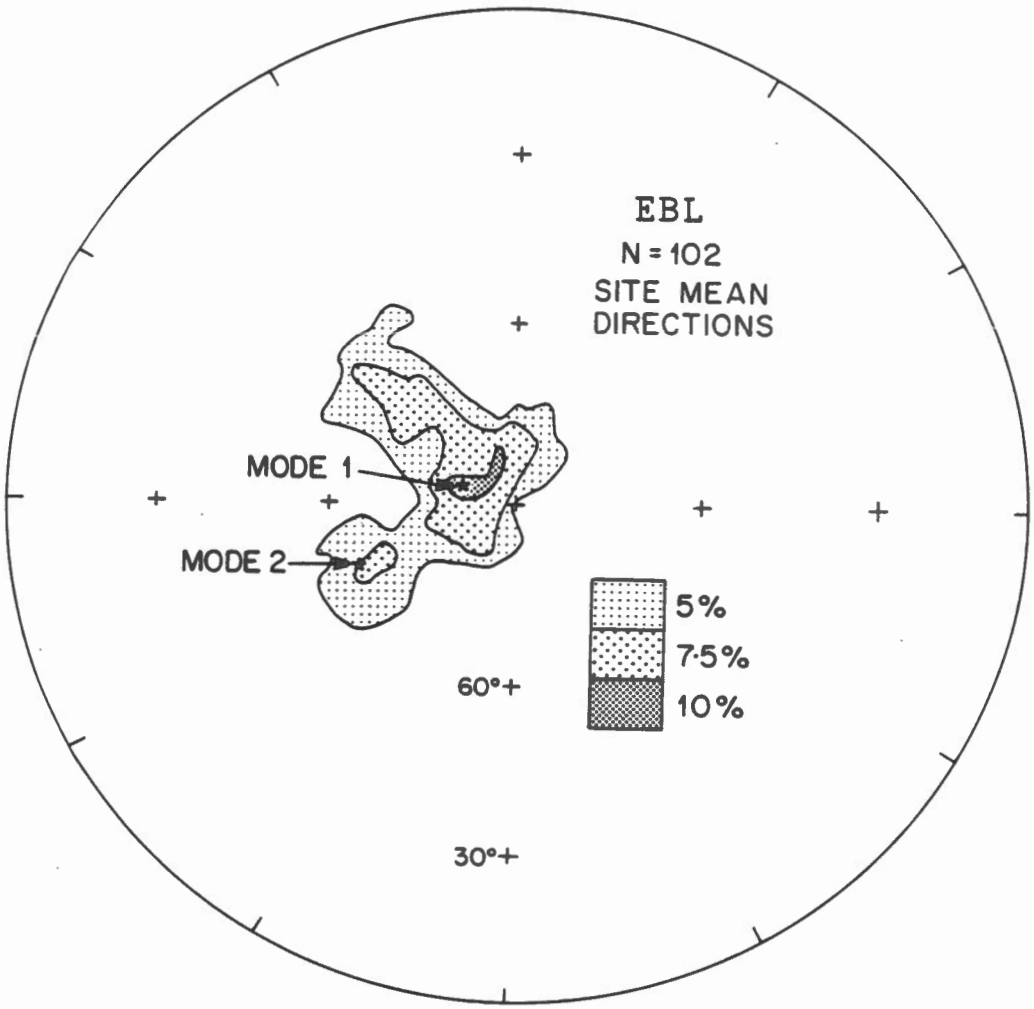
EBL
N = 102
SITE MEAN
DIRECTIONS
MODE 1
MODE 2
5%
7·5%
10%
60°+
30°+

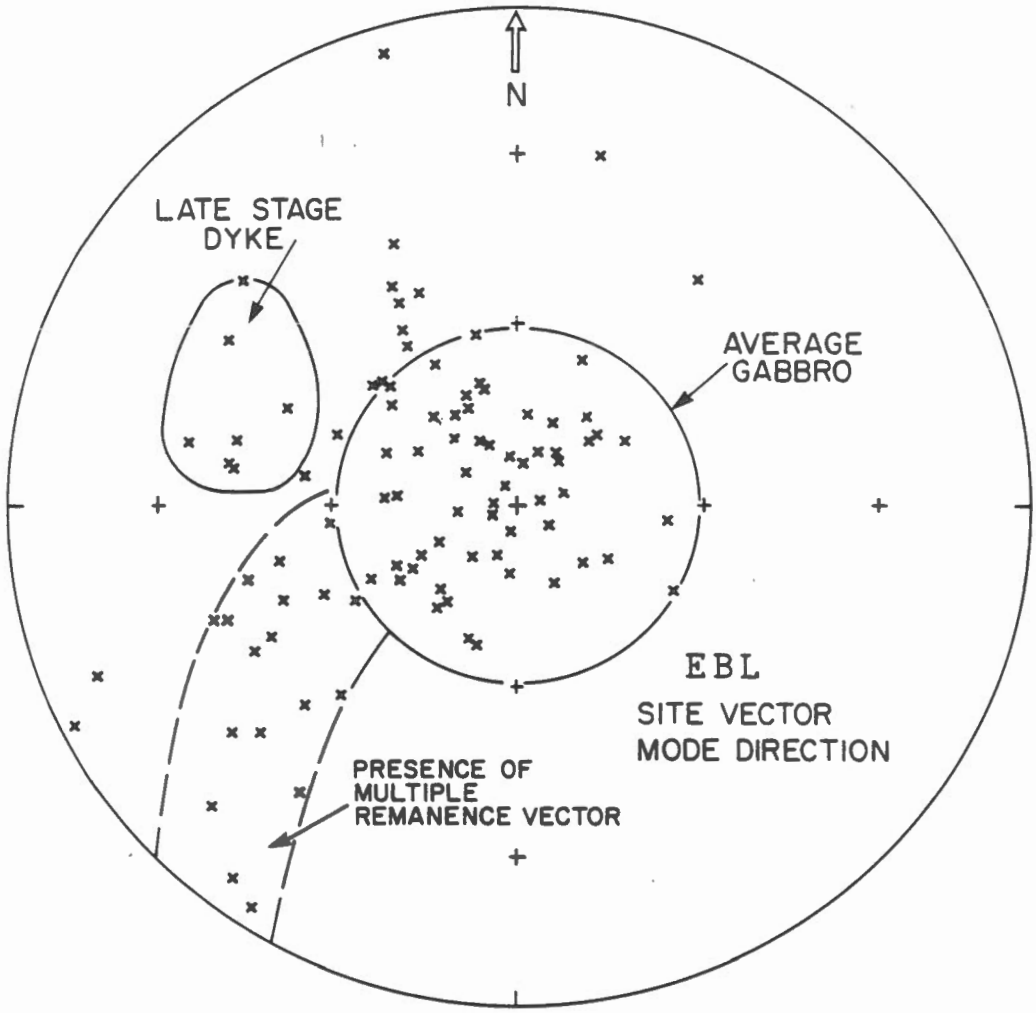
N
LATE STAGE
DYKE
AVERAGE
GABBRO
EBL
SITE VECTOR
MODE DIRECTION
PRESENCE OF
MULTIPLE
REMANENCE VECTOR

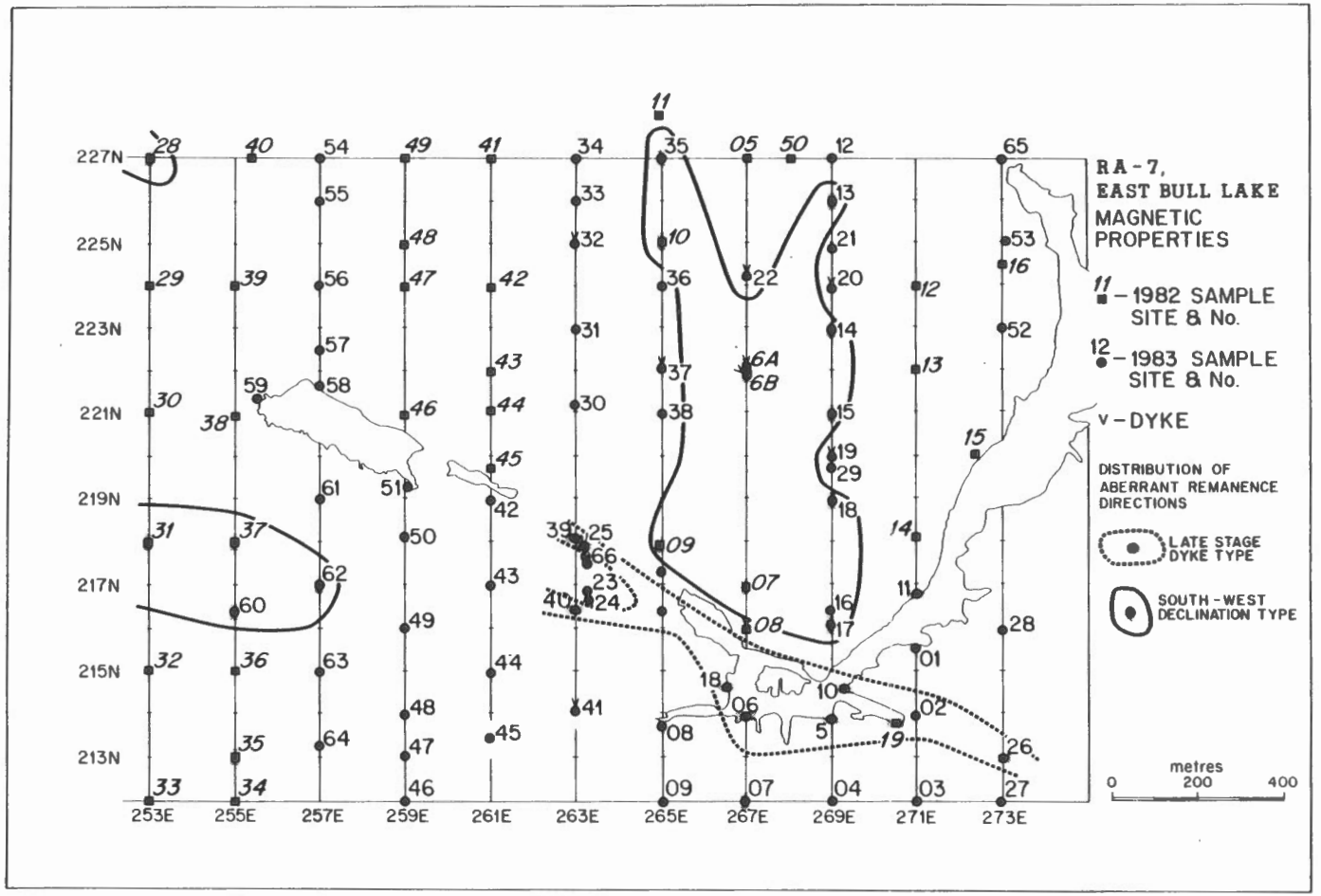
RA-7,
EAST BULL LAKE
MAGNETIC
PROPERTIES
11 – 1982 SAMPLE SITE & No.
12 – 1983 SAMPLE SITE & No.
v – DYKE
DISTRIBUTION OF ABERRANT REMANENCE DIRECTIONS
LATE STAGE DYKE TYPE
SOUTH-WEST DECLINATION TYPE
metres
0 200 400
227N
225N
223N
221N
219N
217N
215N
213N
253E
255E
257E
259E
261E
263E
265E
267E
269E
271E
273E

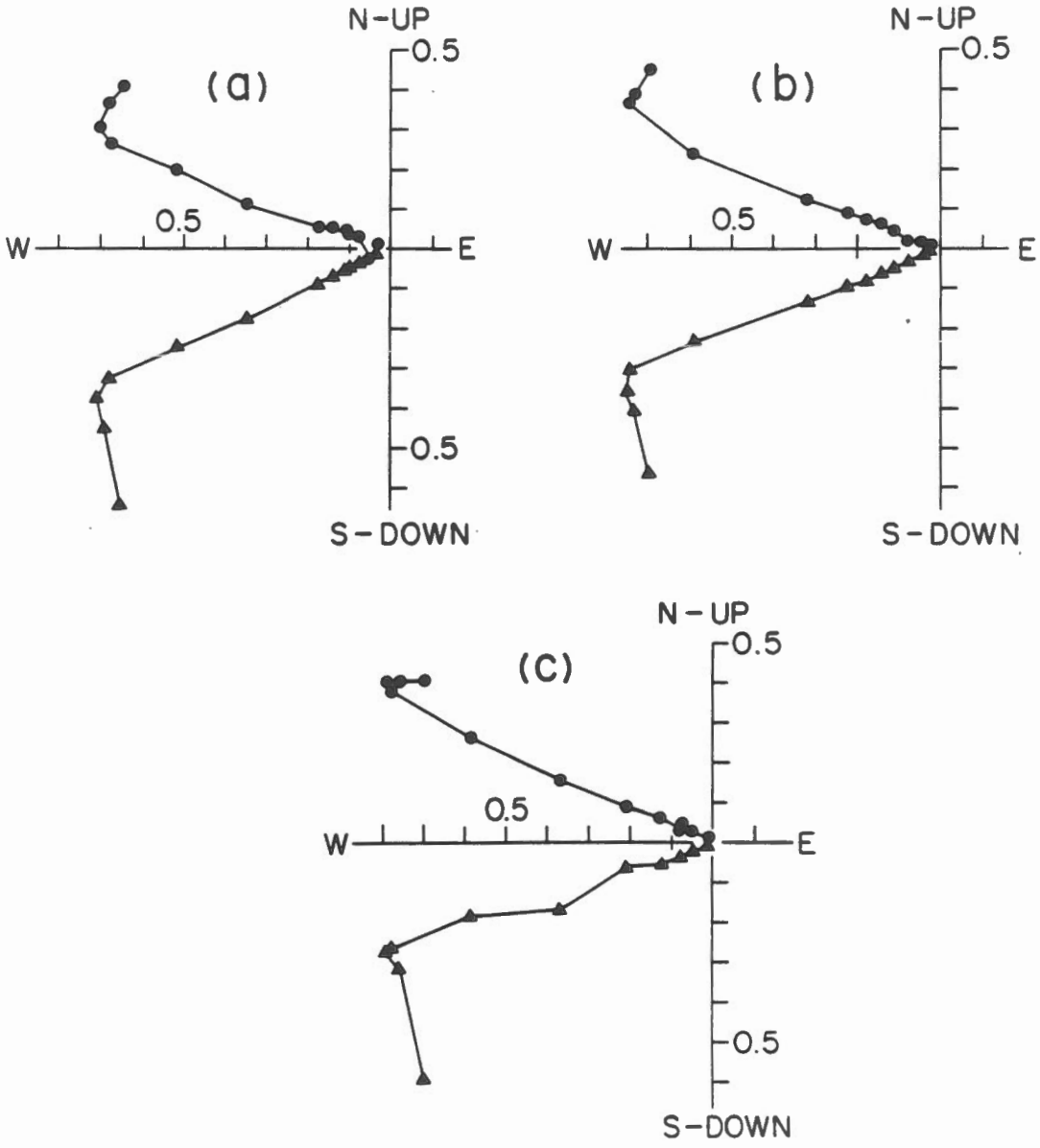
N-UP
0.5
(a)
0.5
W
E
0.5
S-DOWN
N-UP
0.5
(b)
0.5
W
E
S-DOWN
N-UP
0.5
(C)
0.5
W
E
0.5
S-DOWN

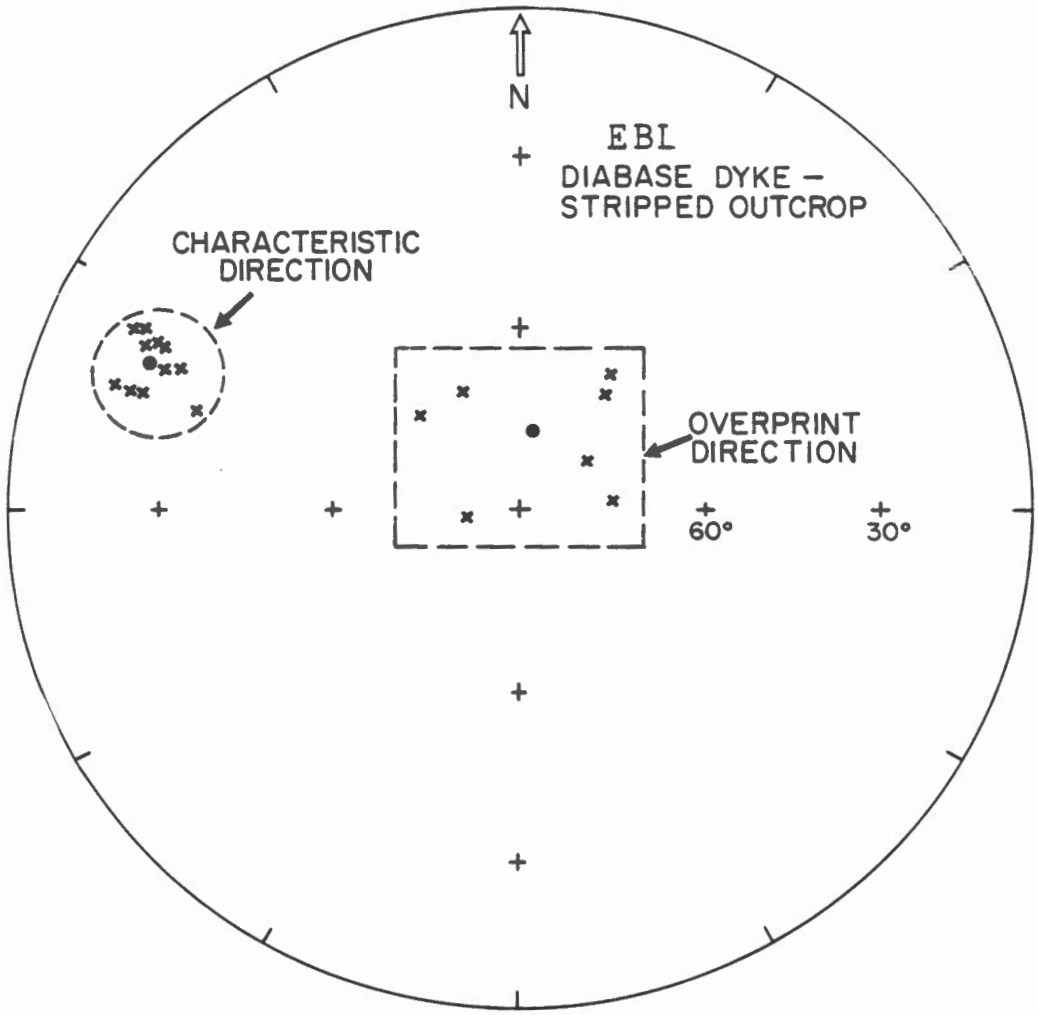
N
EBI
DIABASE DYKE –
STRIPPED OUTCROP
CHARACTERISTIC
DIRECTION
OVERPRINT
DIRECTION
60°
30°

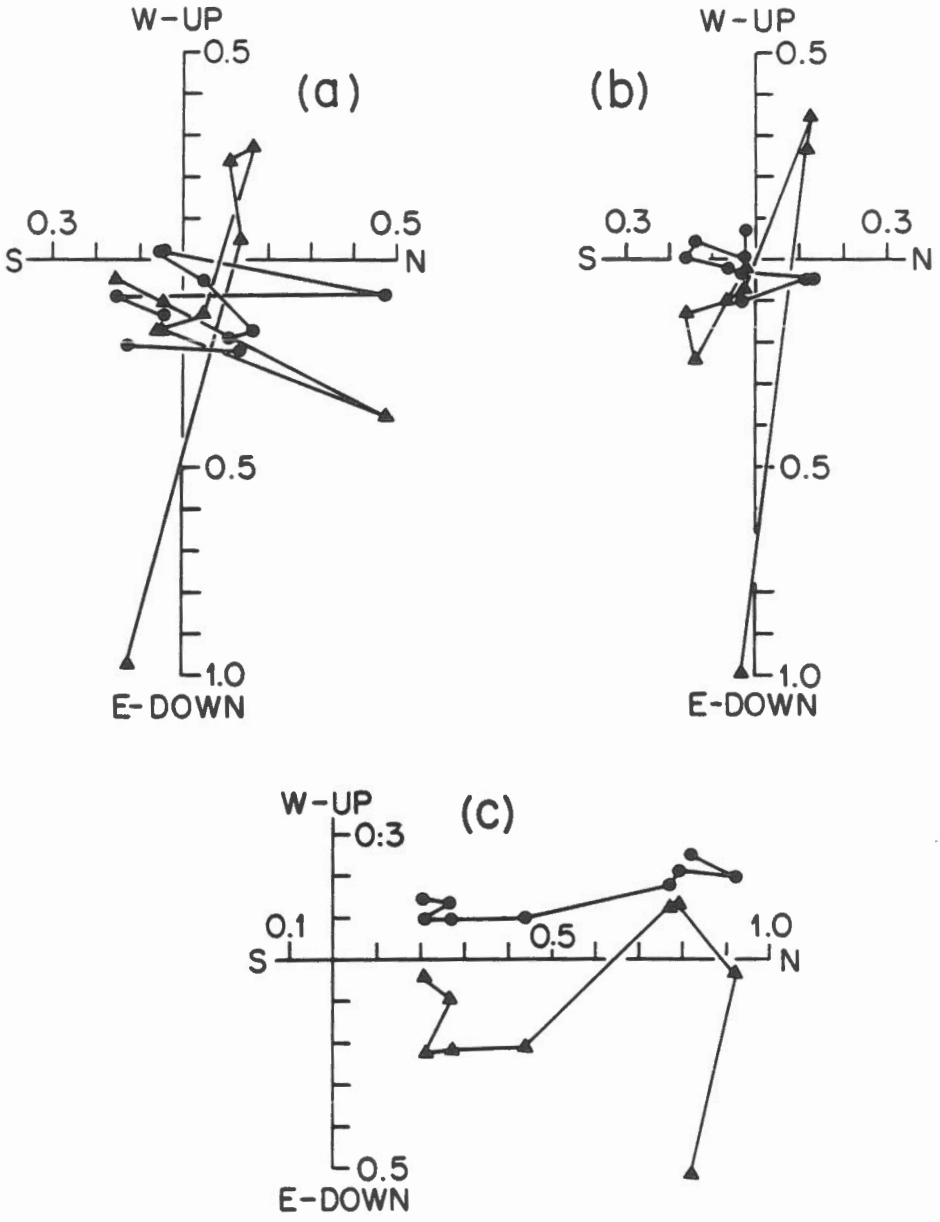
W-UP
0.5
(a)
0.3
0.5
S
N
0.5
1.0
E-DOWN
W-UP
0.5
(b)
0.3
0.3
S
N
0.5
1.0
E-DOWN
W-UP
0:3
(C)
0.1
0.5
1.0
S
N
0.5
E-DOWN

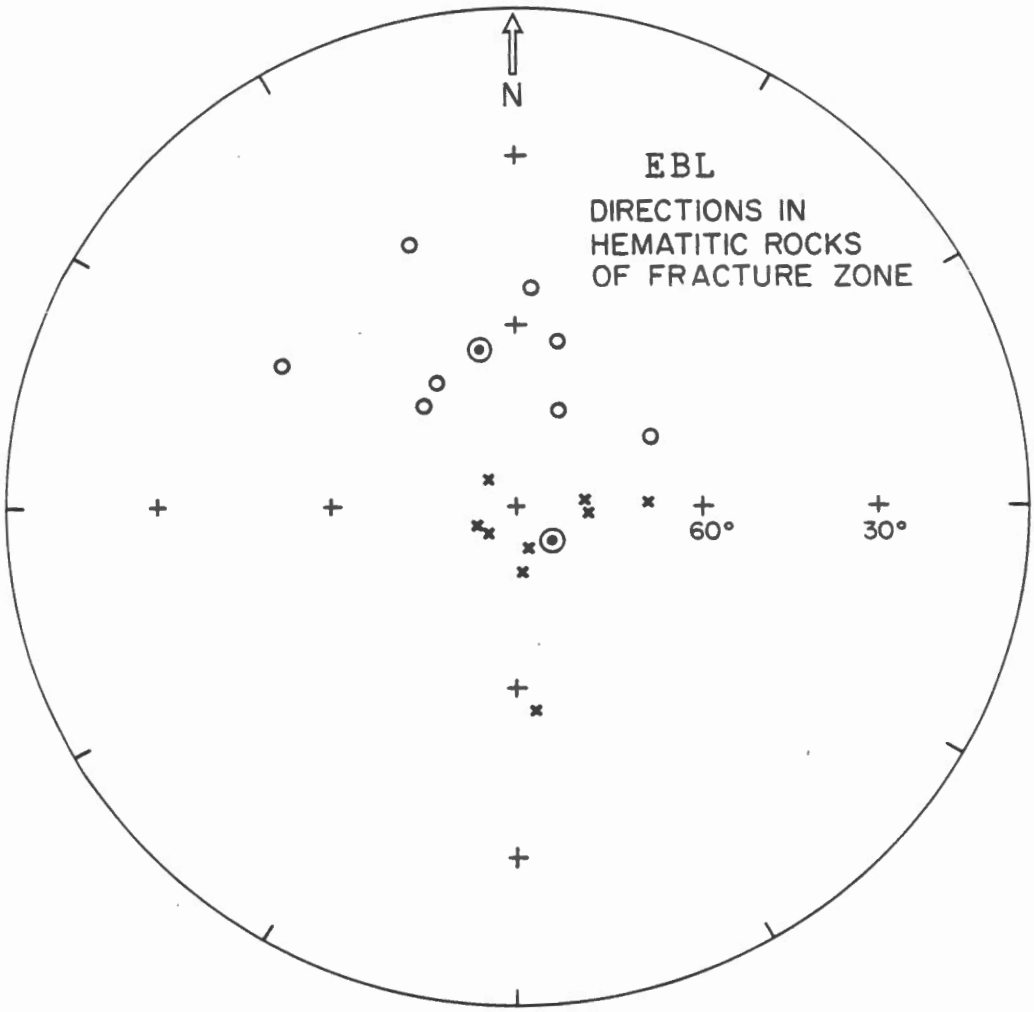
N
EBL
DIRECTIONS IN
HEMATITIC ROCKS
OF FRACTURE ZONE
60°
30°

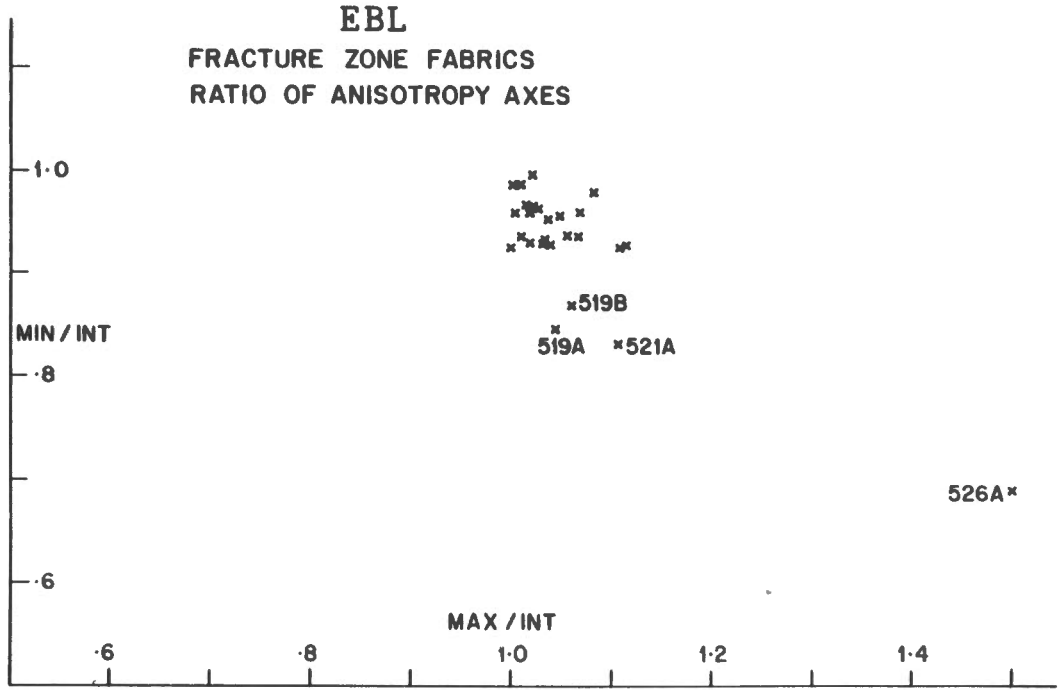
EBL
FRACTURE ZONE FABRICS
RATIO OF ANISOTROPY AXES
1·0
MIN / INT
·8
·6
519B
519A
521A
526A
MAX / INT
·6
·8
1·0
1·2
1·4

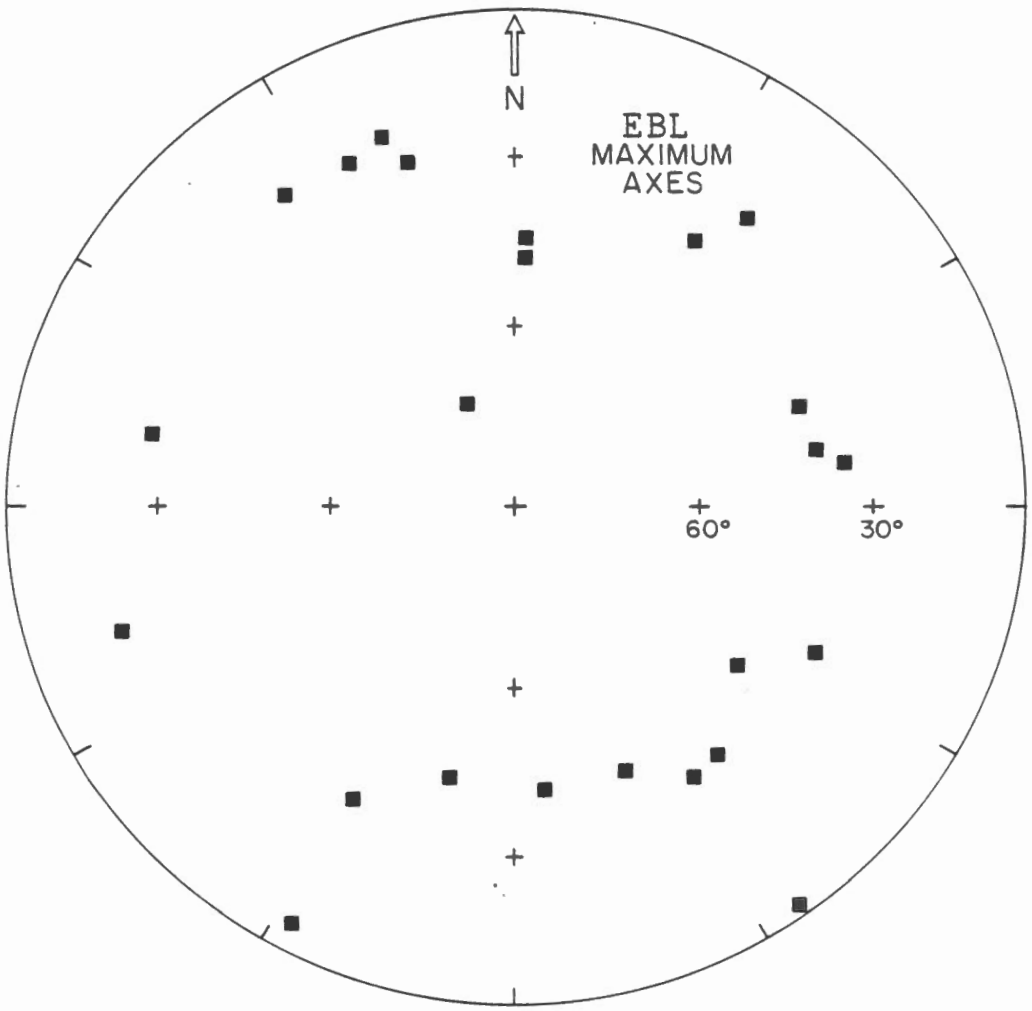
N
EBL
MAXIMUM
AXES
60°
30°

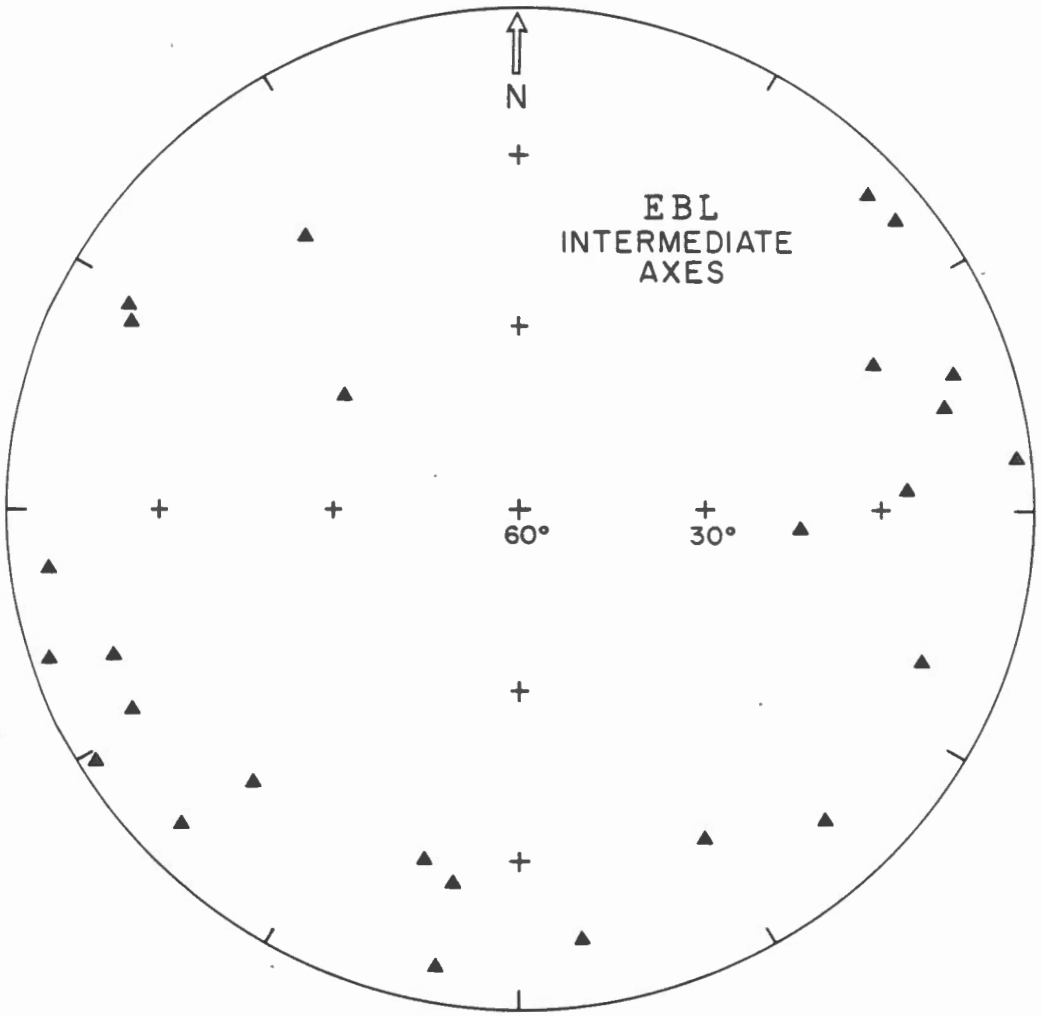
N
EBL
INTERMEDIATE
AXES
60°
30°

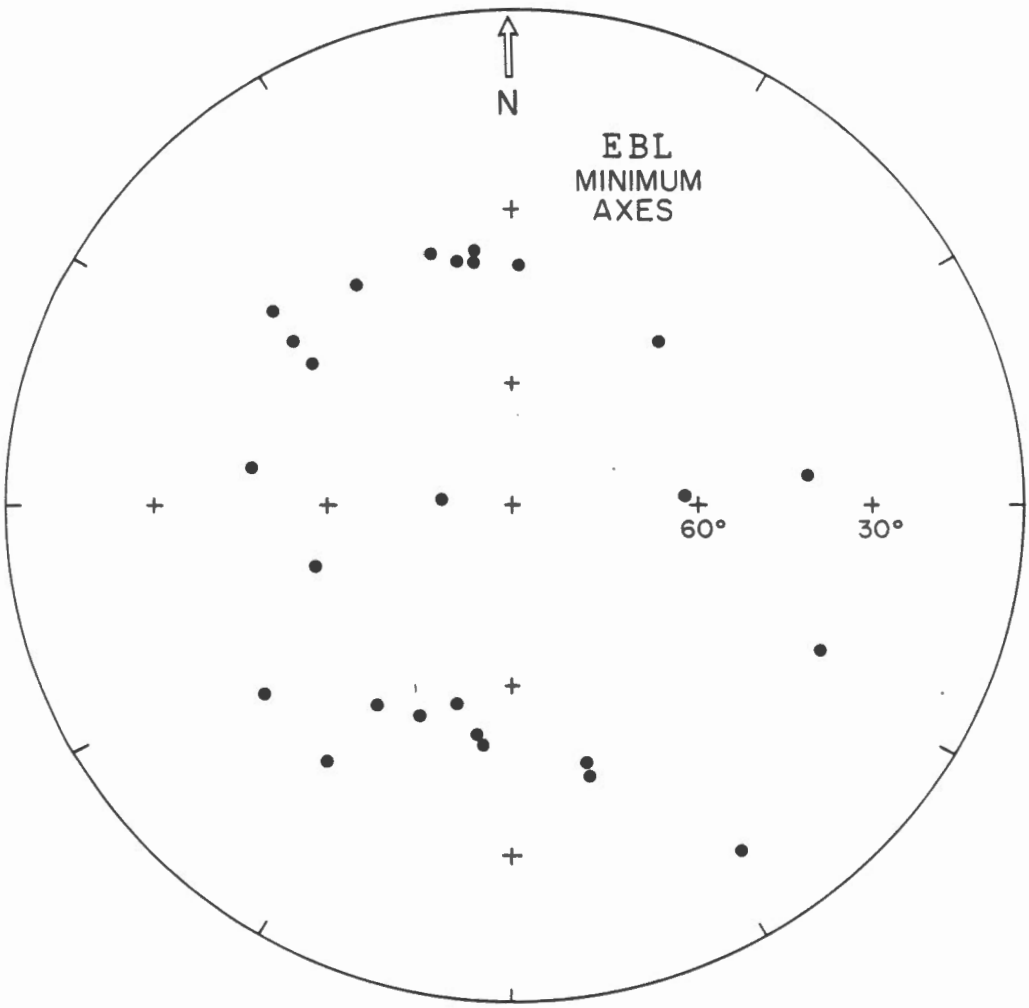
N
EBL
MINIMUM
AXES
60°
30°

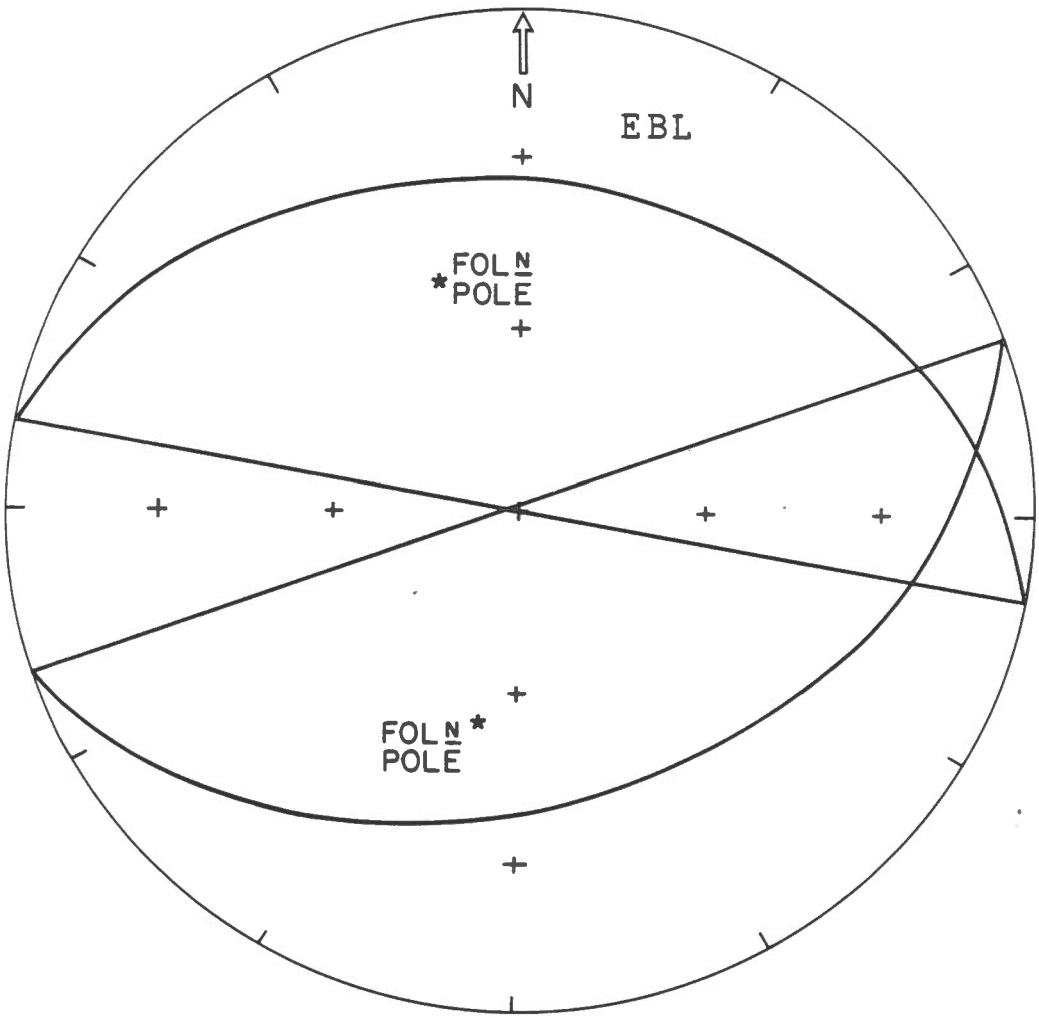
N
EBL
FOL N POLE
FOL N POLE

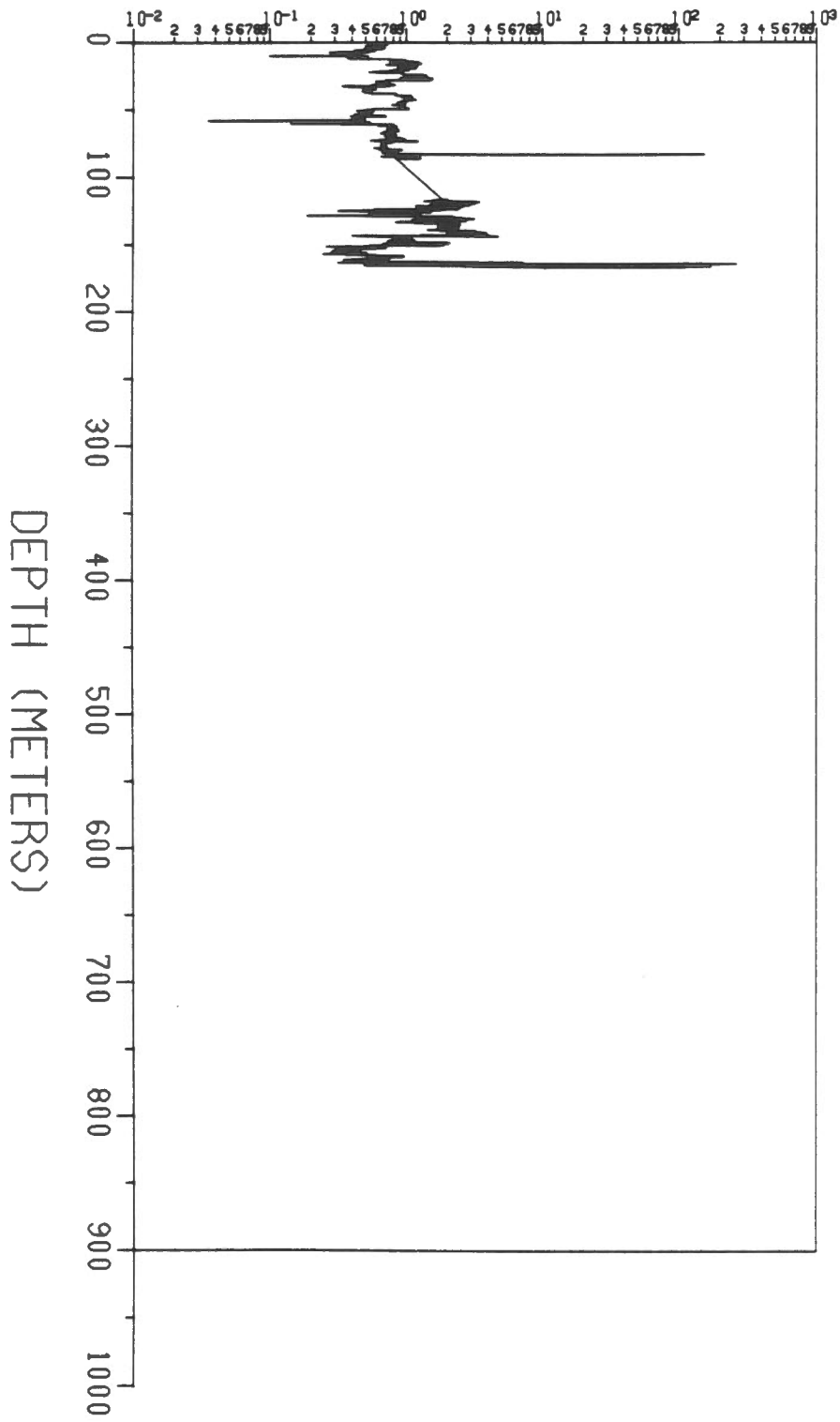
LOG OF MAGNETIC SUSCEPTIBILITY (S.I. UNITS/1000)
10⁻² 2 3 4 5 6 7 8 9 10⁻¹ 2 3 4 5 6 7 8 9 10⁰ 2 3 4 5 6 7 8 9 10¹ 2 3 4 5 6 7 8 9 10² 2 3 4 5 6 7 8 9 10³
0
100
200
300
400
500
600
700
800
900
1000
DEPTH (METERS)
EBL - 1

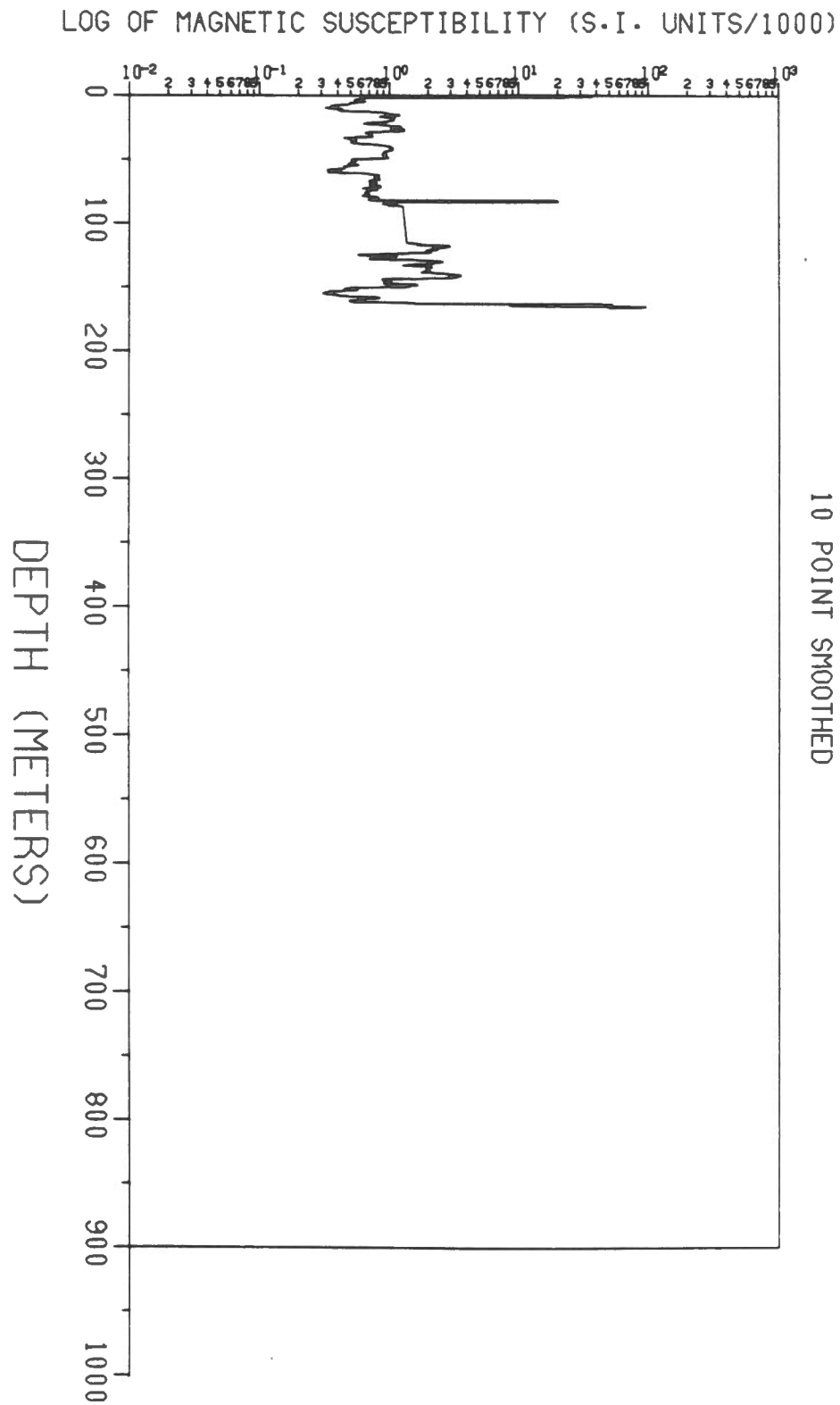
LOG OF MAGNETIC SUSCEPTIBILITY (S.I. UNITS/1000)
10^{-2} 10^{-1} 10^{0} 10^{1} 10^{2} 10^{3}
0
100
200
300
400
500
600
700
800
900
1000
DEPTH (METERS)
EBL - 1
10 POINT SMOOTHED

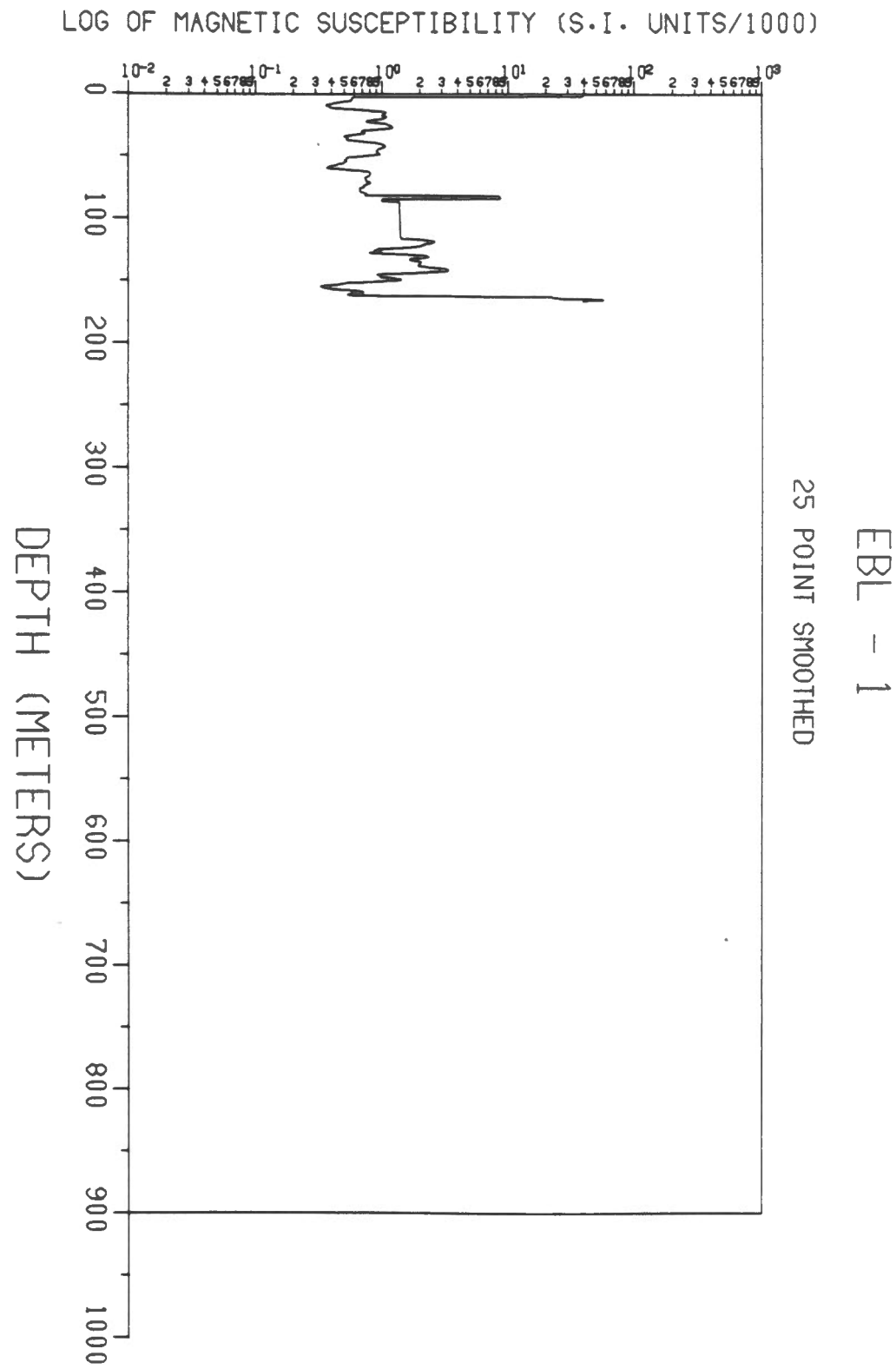
LOG OF MAGNETIC SUSCEPTIBILITY (S.I. UNITS/1000)
10-2
10-1
100
101
102
103
0
100
200
300
400
500
600
700
800
900
1000
DEPTH (METERS)
EBL - 1
25 POINT SMOOTHED

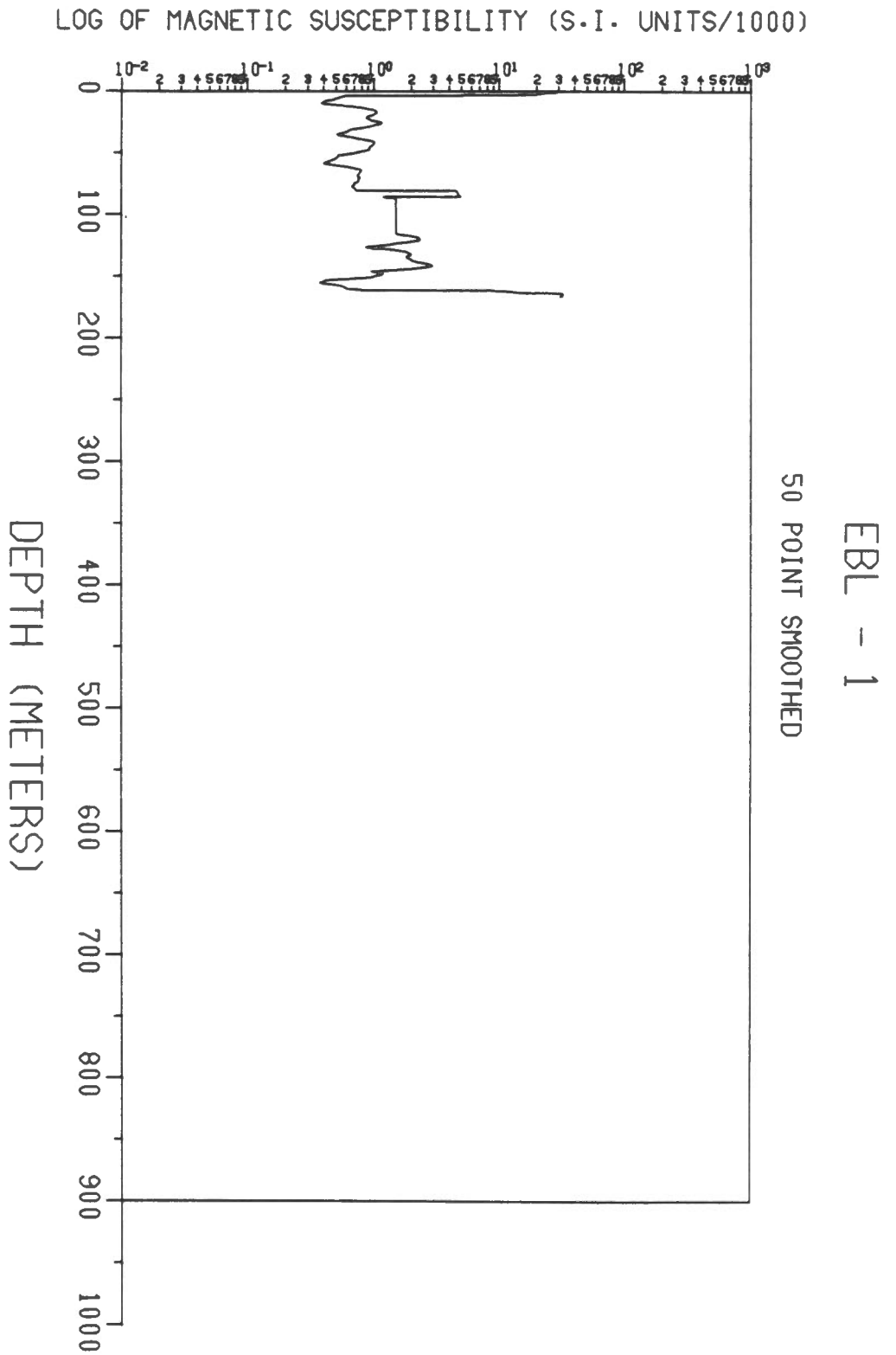
LOG OF MAGNETIC SUSCEPTIBILITY (S.I. UNITS/1000)
10-2
10-1
100
101
102
103
0
100
200
300
400
500
600
700
800
900
1000
DEPTH (METERS)
EBL - 1
50 POINT SMOOTHED

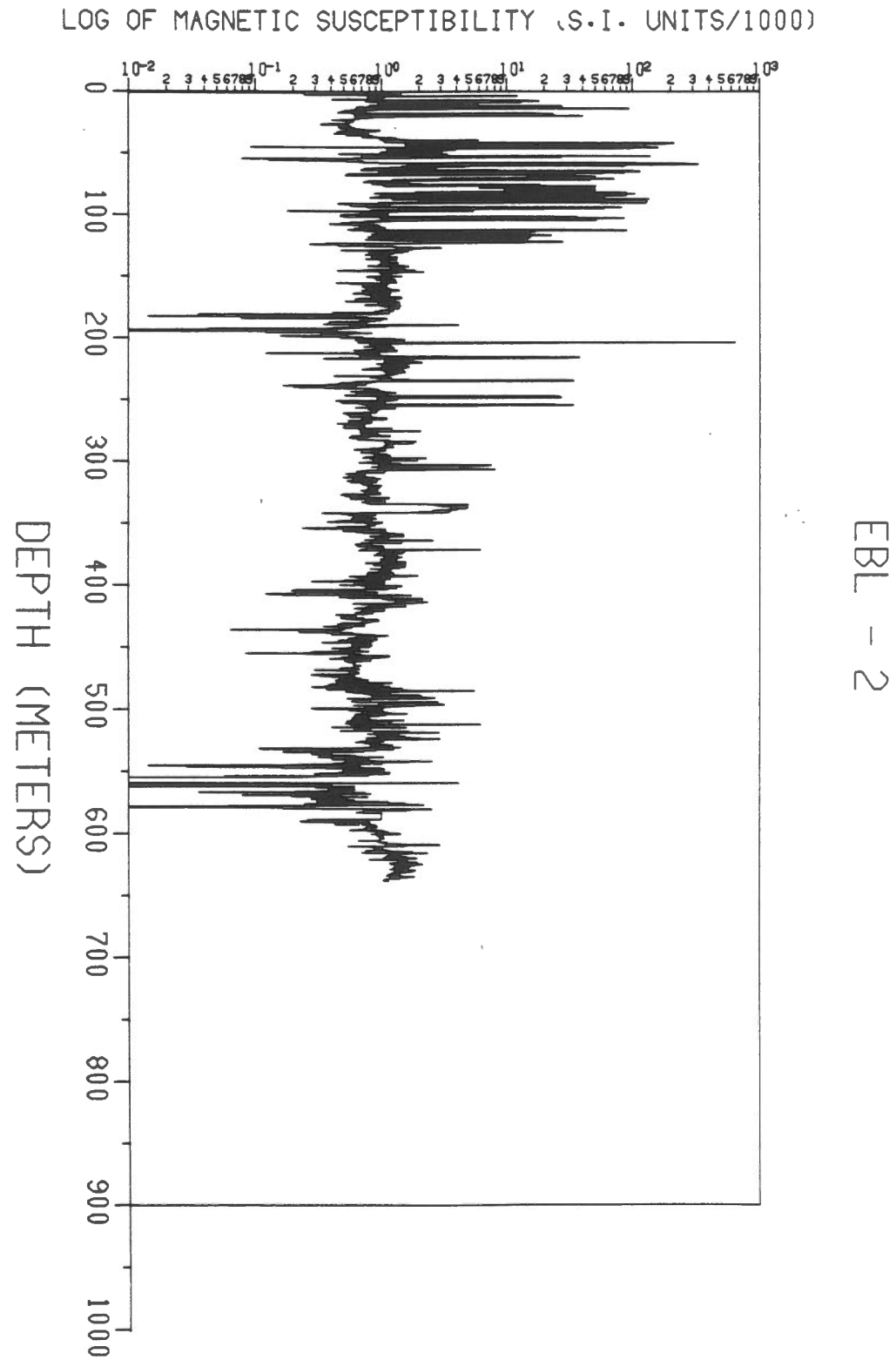
LOG OF MAGNETIC SUSCEPTIBILITY (S.I. UNITS/1000)
10^{-2} 10^{-1} 10^{0} 10^{1} 10^{2} 10^{3}
0
100
200
300
400
500
600
700
800
900
1000
DEPTH (METERS)

EBL - 2

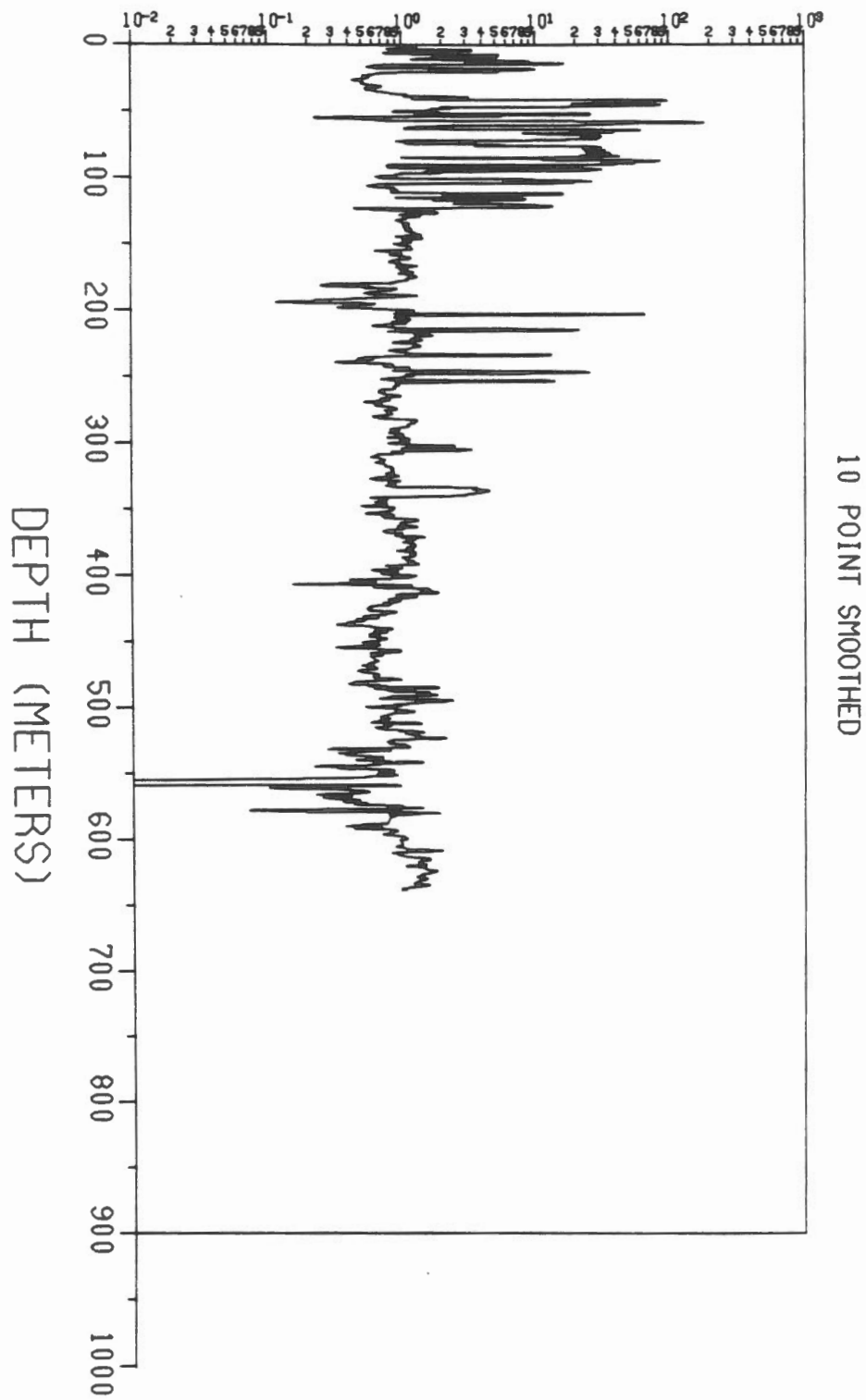
LOG OF MAGNETIC SUSCEPTIBILITY (S.I. UNITS/1000)
10^{-2} 10^{-1} 10^{0} 10^{1} 10^{2} 10^{3}
0
100
200
300
400
500
600
700
800
900
1000
DEPTH (METERS)
10 POINT SMOOTHED
EBL - 2

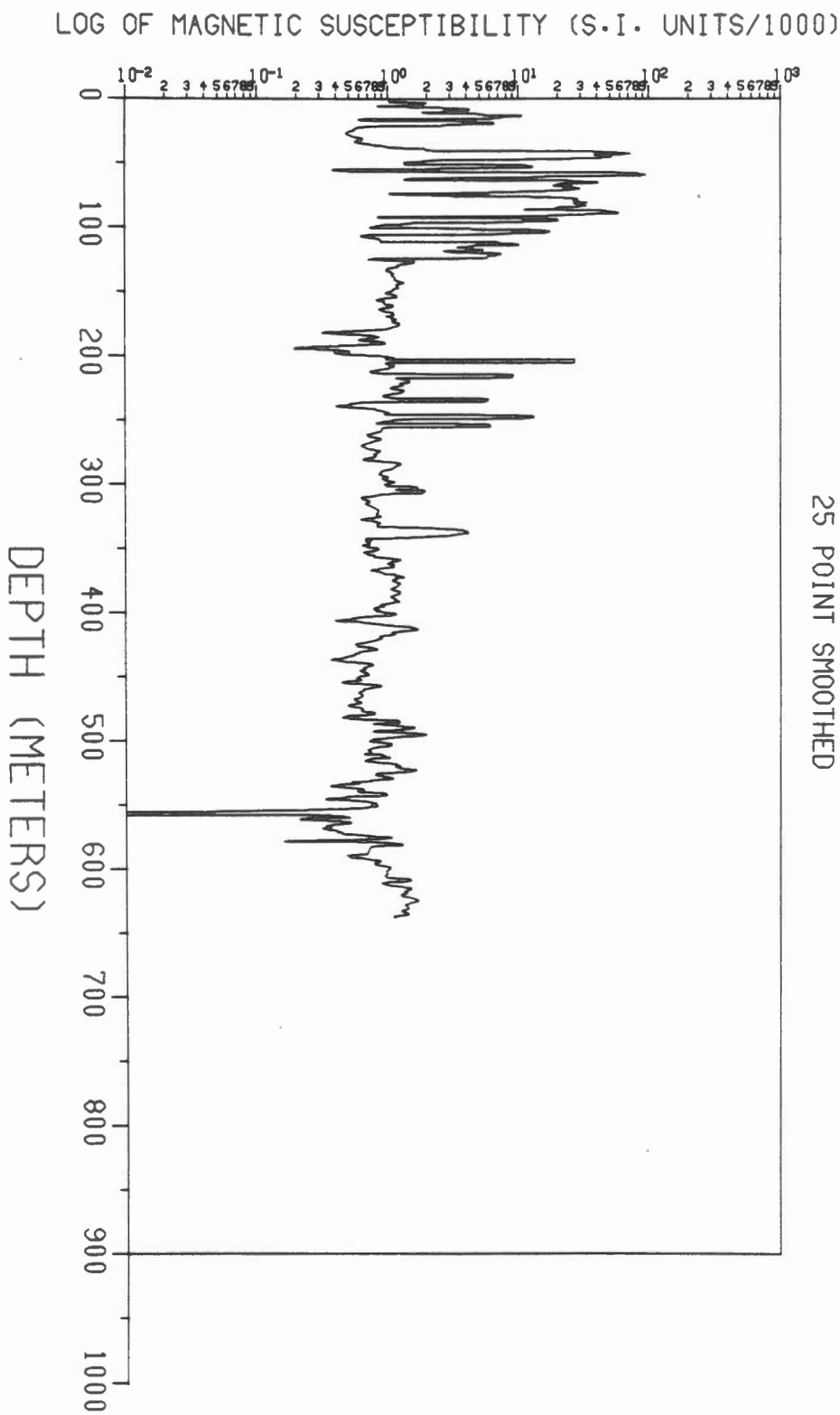
LOG OF MAGNETIC SUSCEPTIBILITY (S.I. UNITS/1000)
10^{-2} 2 3 4 5 6 7 8 9 10^{-1} 2 3 4 5 6 7 8 9 10^{0} 2 3 4 5 6 7 8 9 10^{1} 2 3 4 5 6 7 8 9 10^{2} 2 3 4 5 6 7 8 9 10^{3}
0
100
200
300
400
500
600
700
800
900
1000
DEPTH (METERS)
25 POINT SMOOTHED
EBL - 2

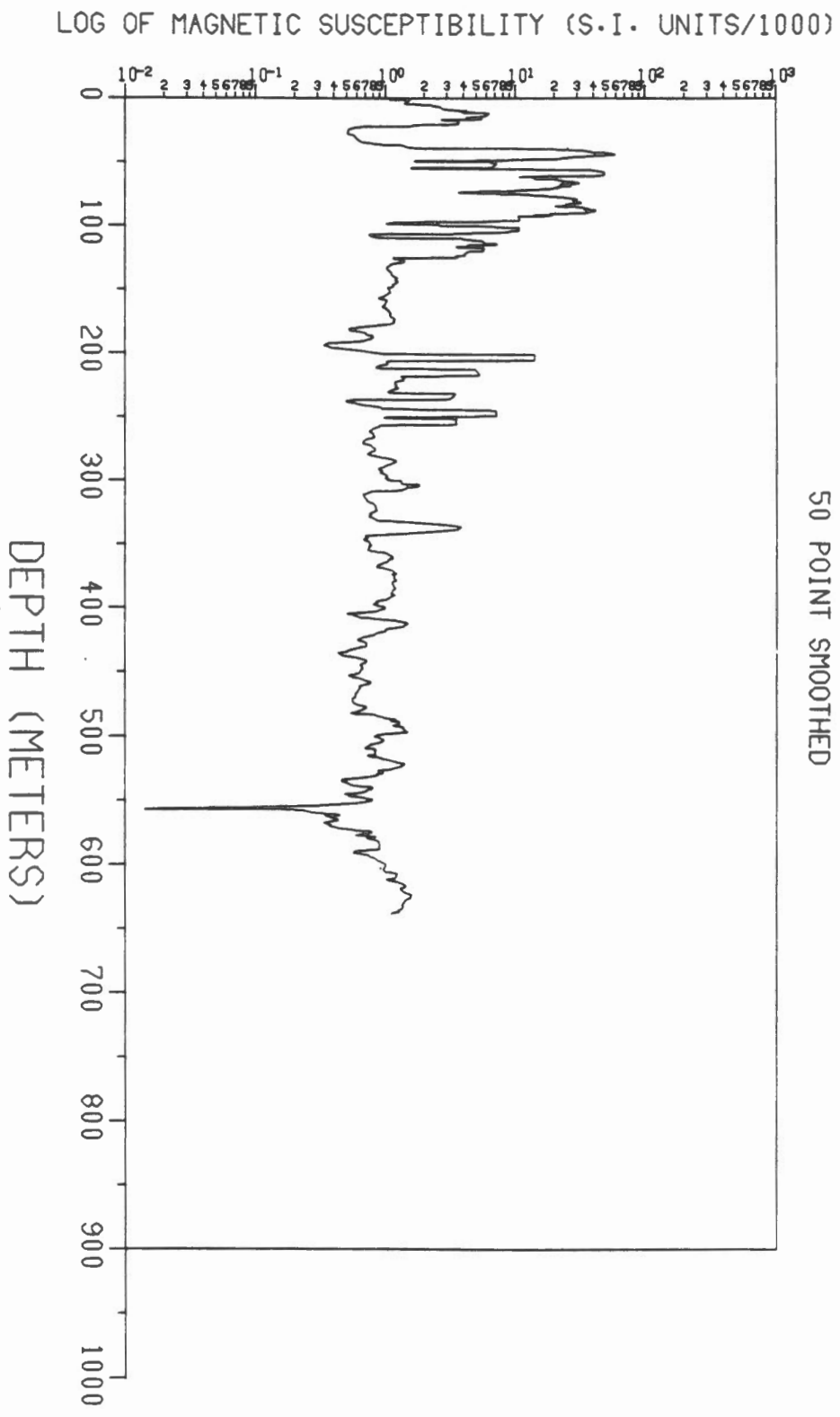
LOG OF MAGNETIC SUSCEPTIBILITY (S.I. UNITS/1000)
10^{-2} 10^{-1} 10^{0} 10^{1} 10^{2} 10^{3}
0
100
200
300
400
500
600
700
800
900
1000
DEPTH (METERS)
EBL - 2
50 POINT SMOOTHED

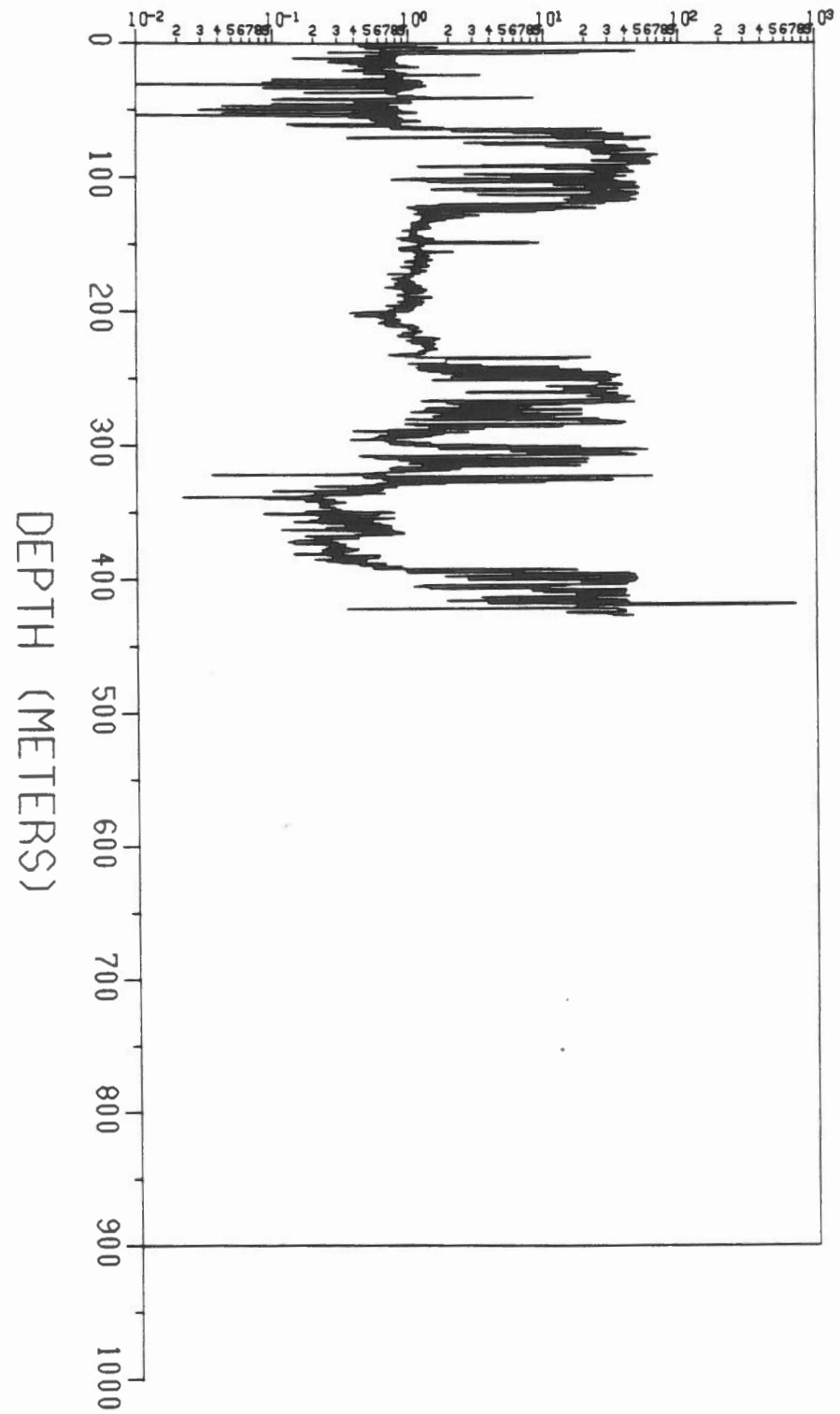
LOG OF MAGNETIC SUSCEPTIBILITY (S.I. UNITS/1000)
10^{-2} 10^{-1} 10^{0} 10^{1} 10^{2} 10^{3}
0
100
200
300
400
500
600
700
800
900
1000
DEPTH (METERS)

EBL - 3

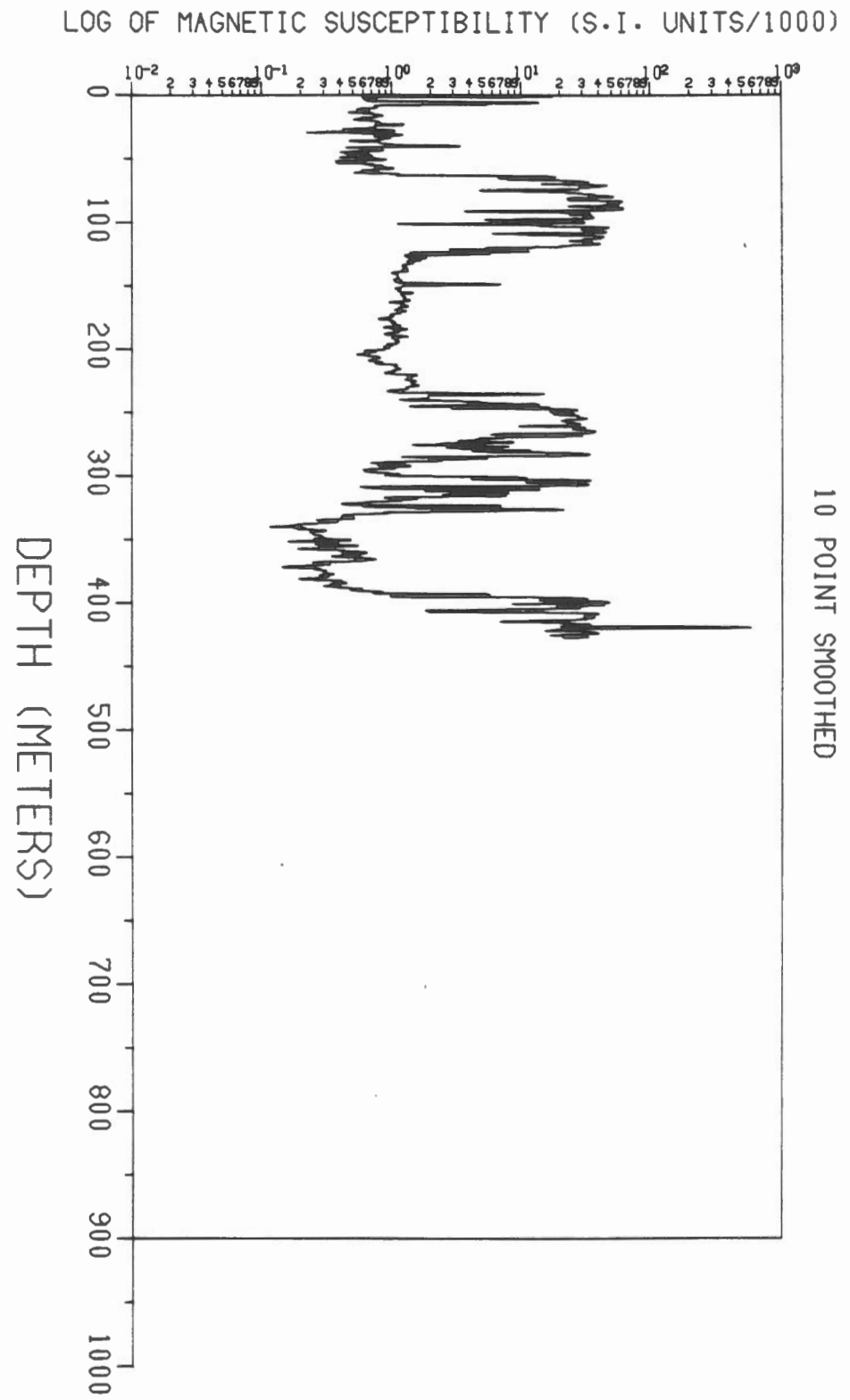
LOG OF MAGNETIC SUSCEPTIBILITY (S.I. UNITS/1000)
10^{-2} 10^{-1} 10^{0} 10^{1} 10^{2} 10^{3}
0
100
200
300
400
500
600
700
800
900
1000
DEPTH (METERS)
EBL - 3
10 POINT SMOOTHED

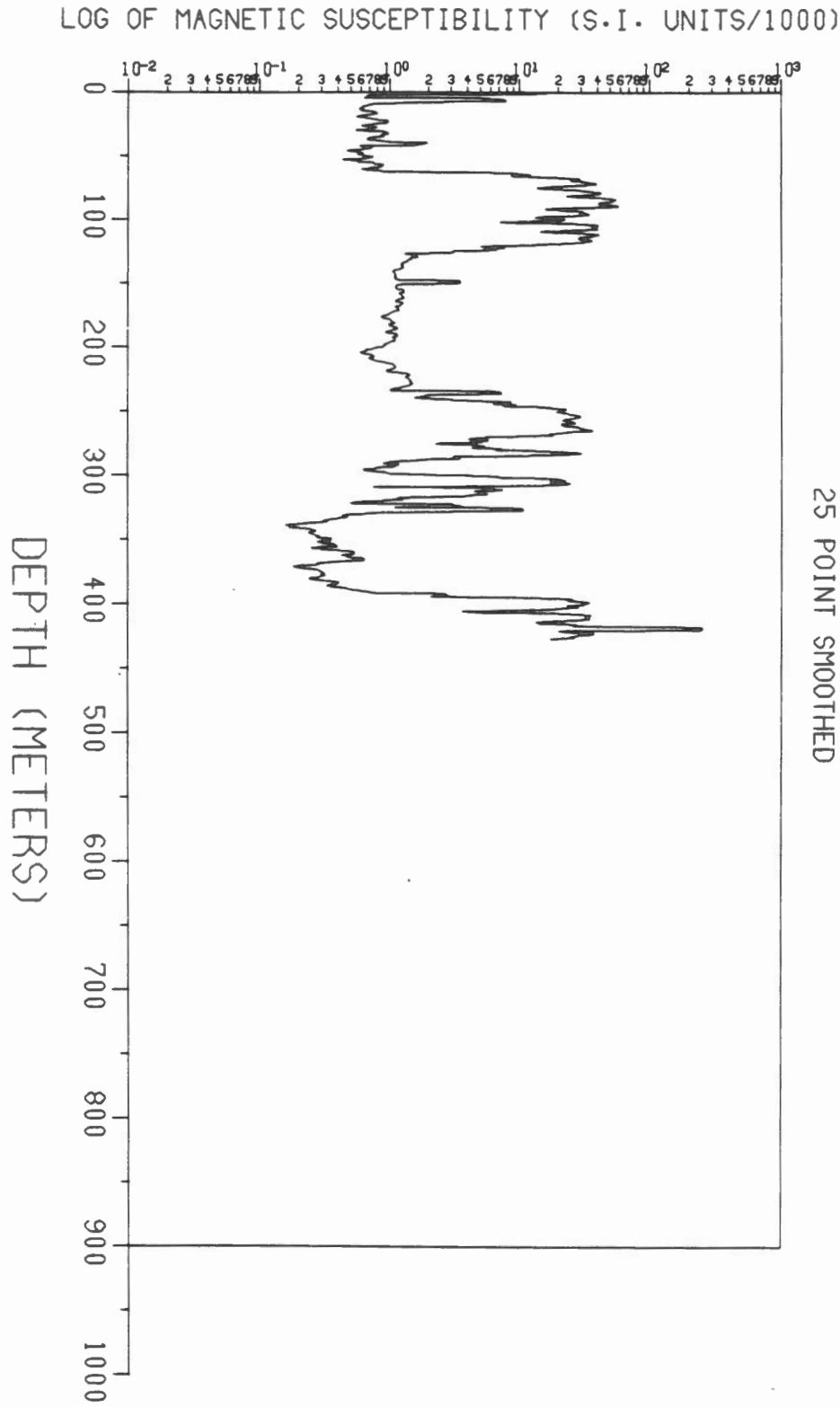
LOG OF MAGNETIC SUSCEPTIBILITY (S.I. UNITS/1000)
10-2 2 3 4 5 6 7 8 9 10-1 2 3 4 5 6 7 8 9 100 2 3 4 5 6 7 8 9 101 2 3 4 5 6 7 8 9 102 2 3 4 5 6 7 8 9 103
0
100
200
300
400
500
600
700
800
900
1000
DEPTH (METERS)
EBL - 3
25 POINT SMOOTHED

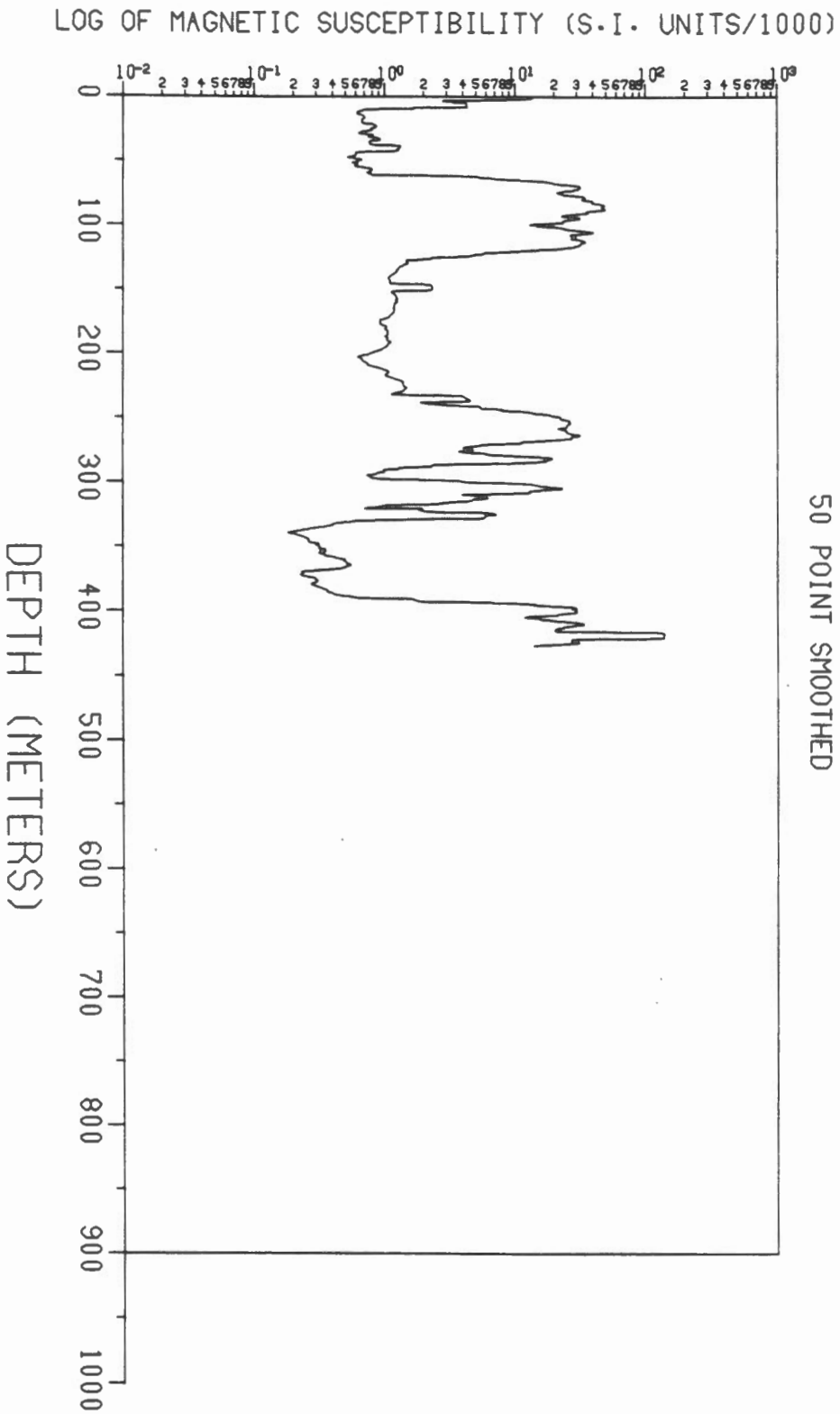
LOG OF MAGNETIC SUSCEPTIBILITY (S.I. UNITS/1000)
10⁻² 2 3 4 5 6 7 8 9 10⁻¹ 2 3 4 5 6 7 8 9 10⁰ 2 3 4 5 6 7 8 9 10¹ 2 3 4 5 6 7 8 9 10² 2 3 4 5 6 7 8 9 10³
0
100
200
300
400
500
600
700
800
900
1000
DEPTH (METERS)
EBL - 3
50 POINT SMOOTHED

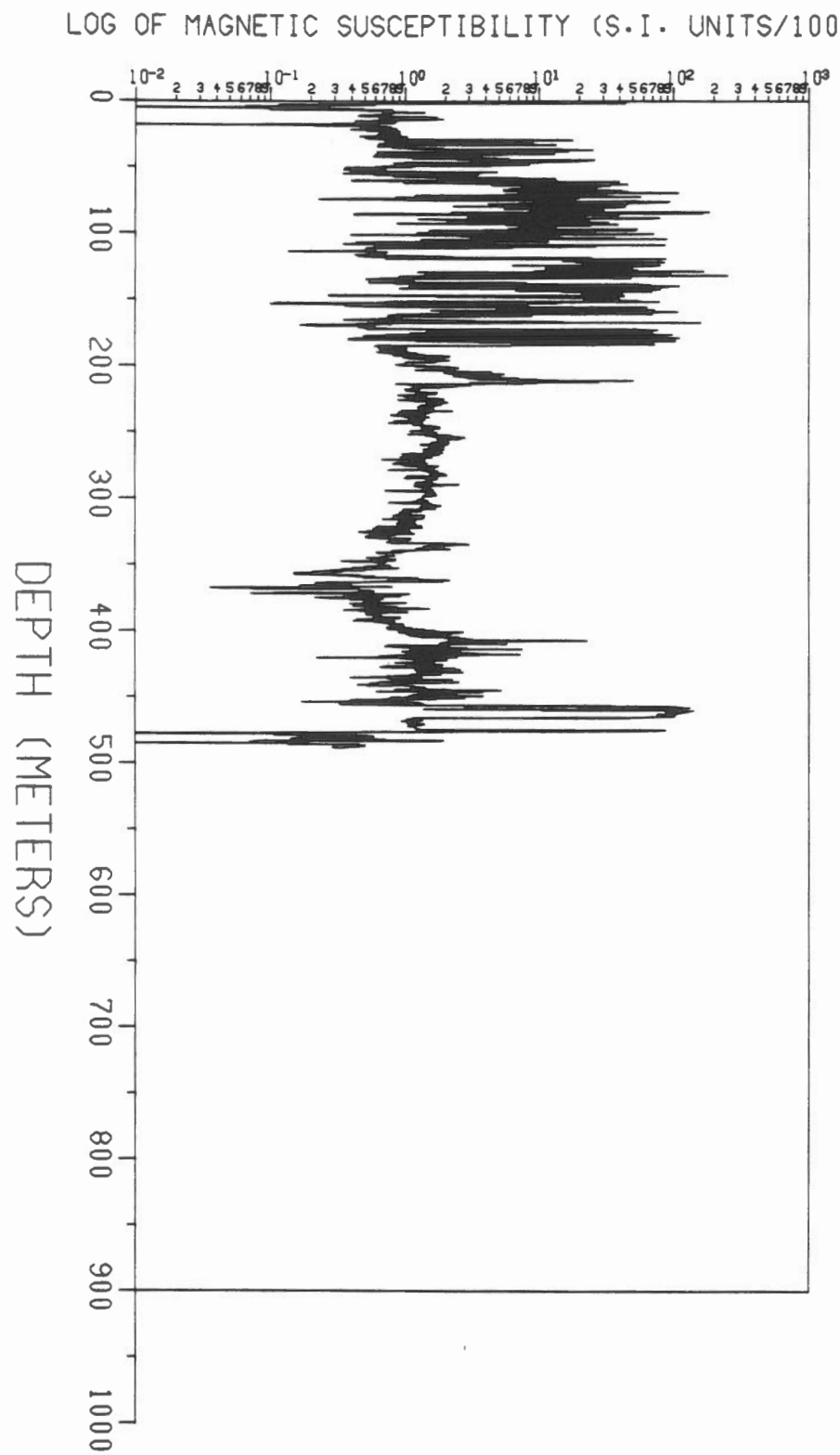
LOG OF MAGNETIC SUSCEPTIBILITY (S.I. UNITS/1000)
10^{-2} 10^{-1} 10^{0} 10^{1} 10^{2} 10^{3}
0
100
200
300
400
500
600
700
800
900
1000
DEPTH (METERS)

EBL - 4

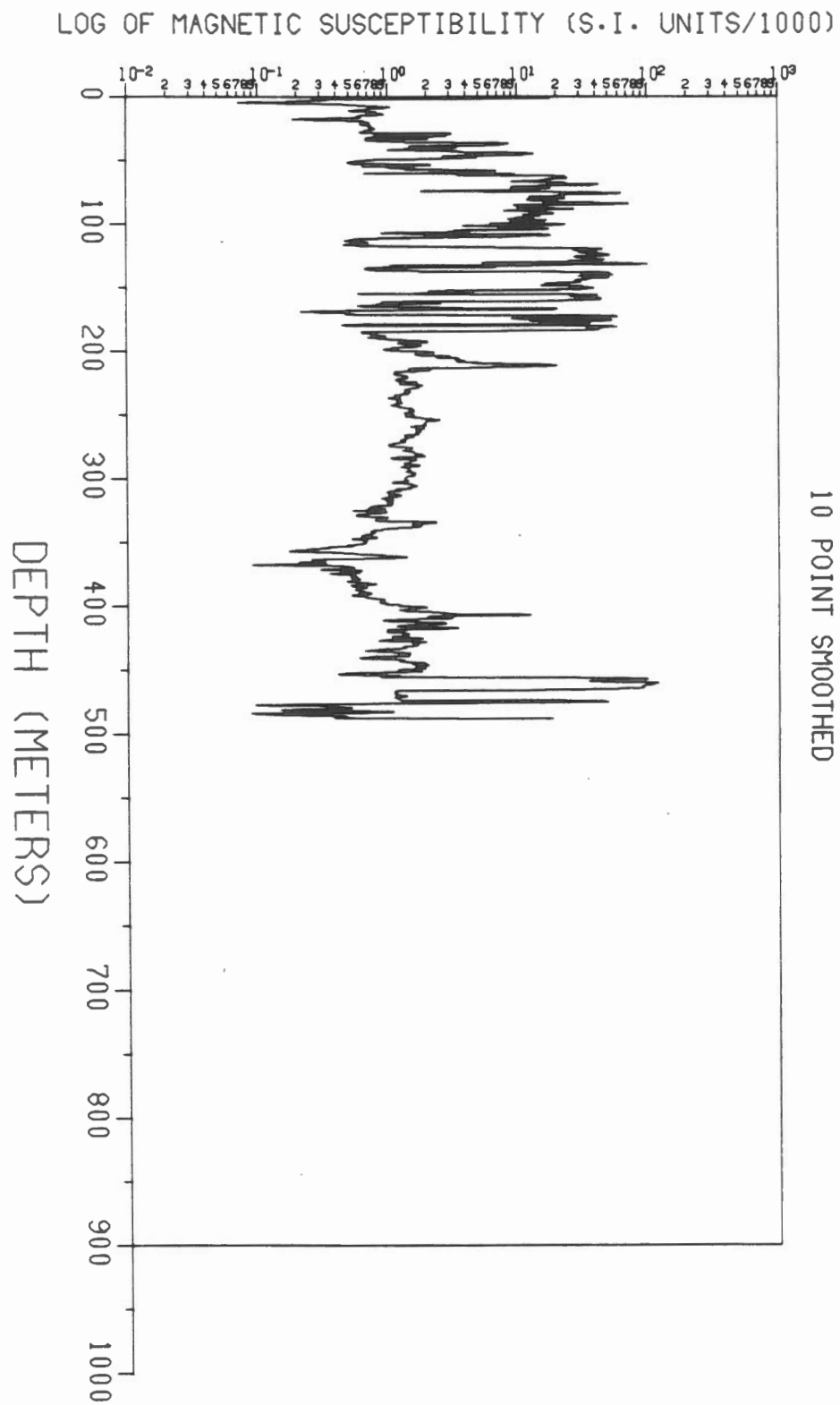

EBL - 4

10 POINT SMOOTHED

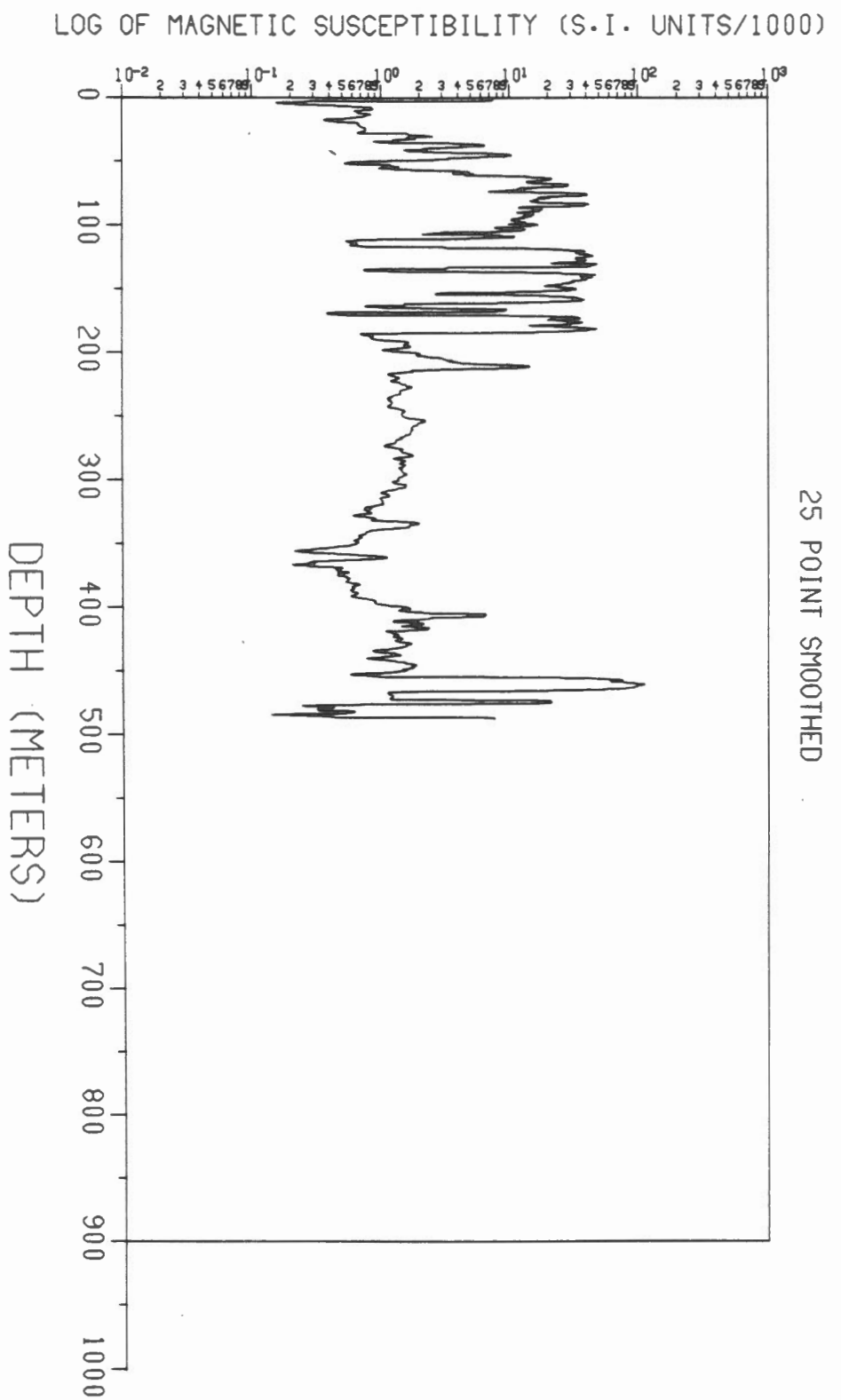
LOG OF MAGNETIC SUSCEPTIBILITY (S.I. UNITS/1000)
10⁻² 2 3 4 5 6 7 8 9 10⁻¹ 2 3 4 5 6 7 8 9 10⁰ 2 3 4 5 6 7 8 9 10¹ 2 3 4 5 6 7 8 9 10² 2 3 4 5 6 7 8 9 10³
0
100
200
300
400
500
600
700
800
900
1000
DEPTH (METERS)
EBL - 4
25 POINT SMOOTHED

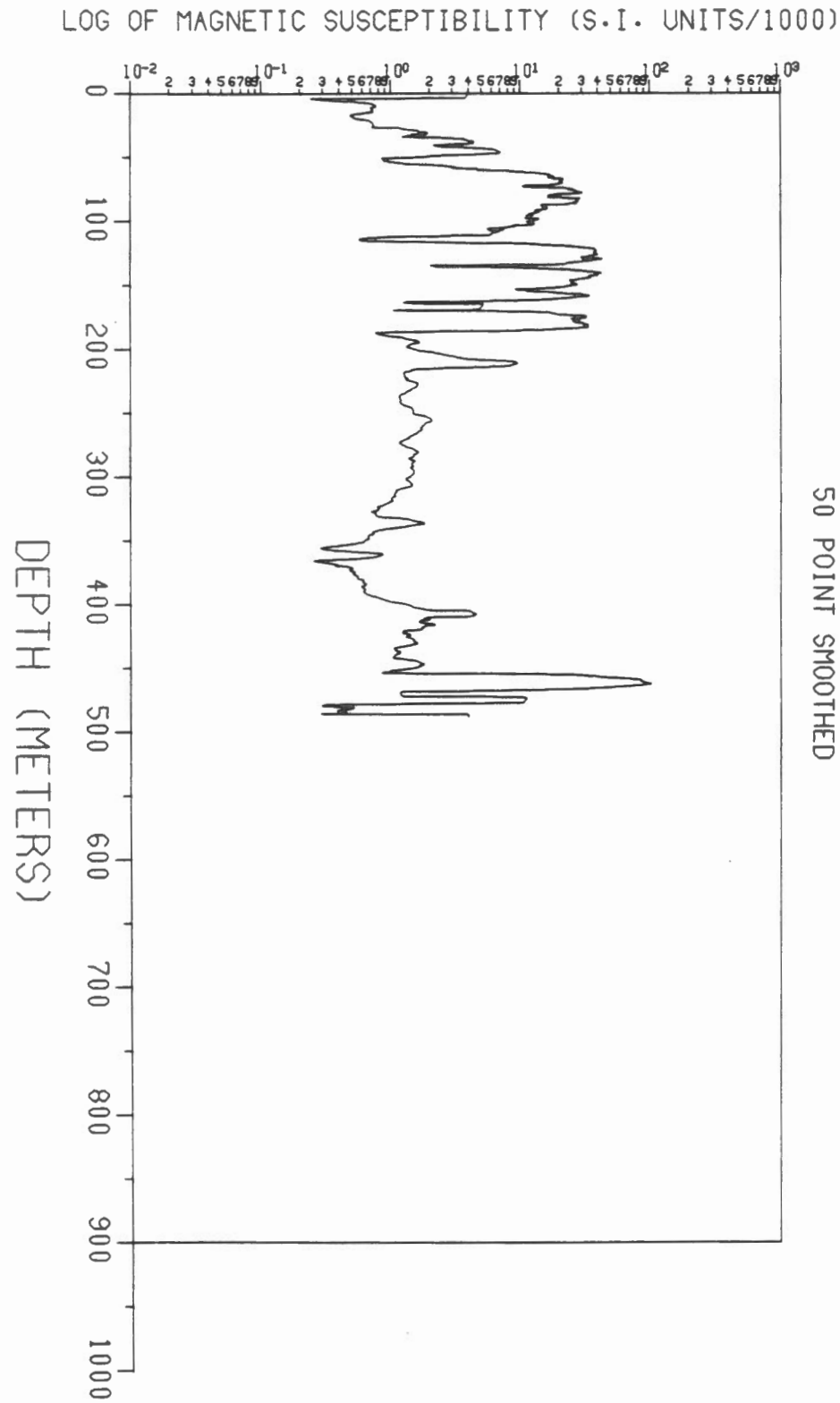
LOG OF MAGNETIC SUSCEPTIBILITY (S.I. UNITS/1000)
10⁻² 2 3 4 5 6 7 8 9 10⁻¹ 2 3 4 5 6 7 8 9 10⁰ 2 3 4 5 6 7 8 9 10¹ 2 3 4 5 6 7 8 9 10² 2 3 4 5 6 7 8 9 10³
0
100
200
300
400
500
600
700
800
900
1000
DEPTH (METERS)
EBL - 4
50 POINT SMOOTHED

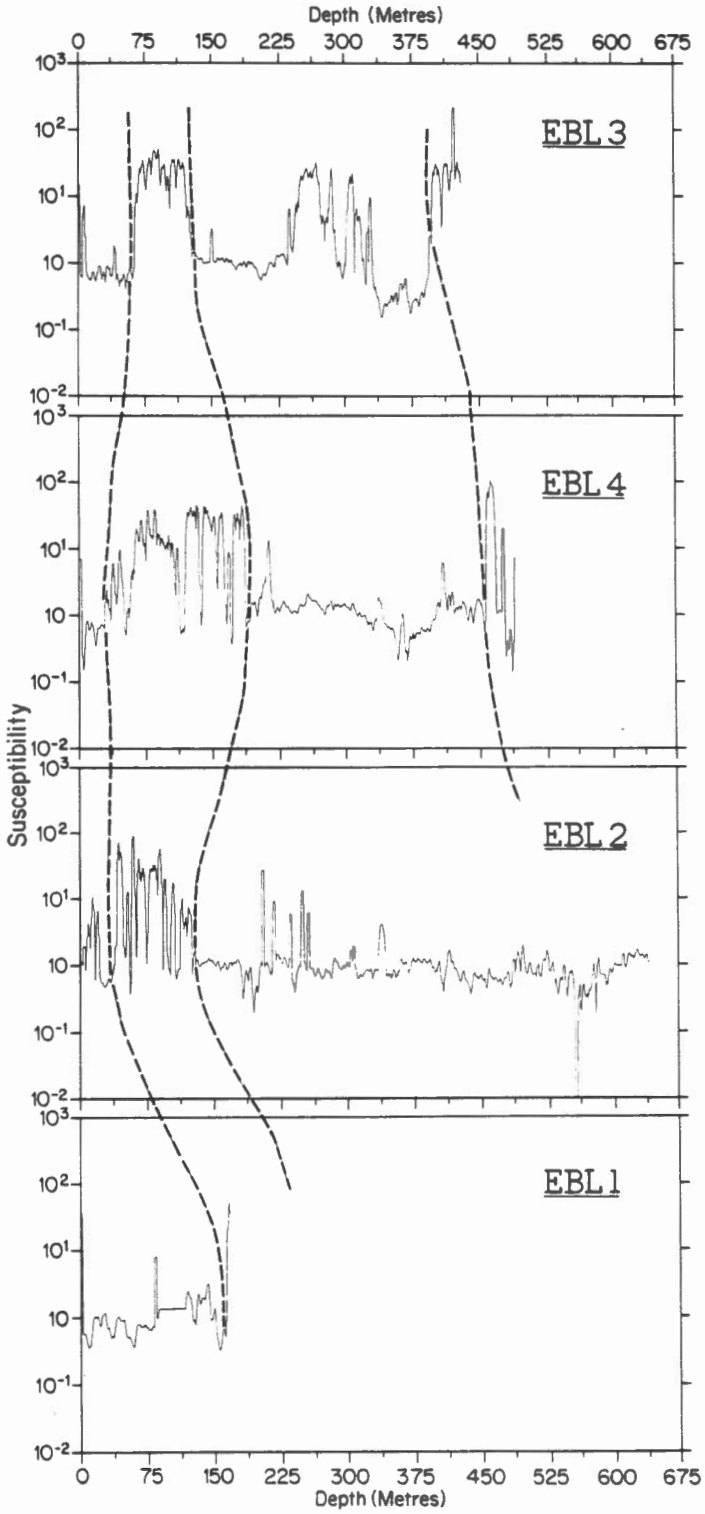
Depth (Metres)
0 75 150 225 300 375 450 525 600 675
EBL 3
EBL 4
EBL 2
EBL 1
Susceptibility
10^3 10^2 10^1 10 10^{-1} 10^{-2}
Depth (Metres)

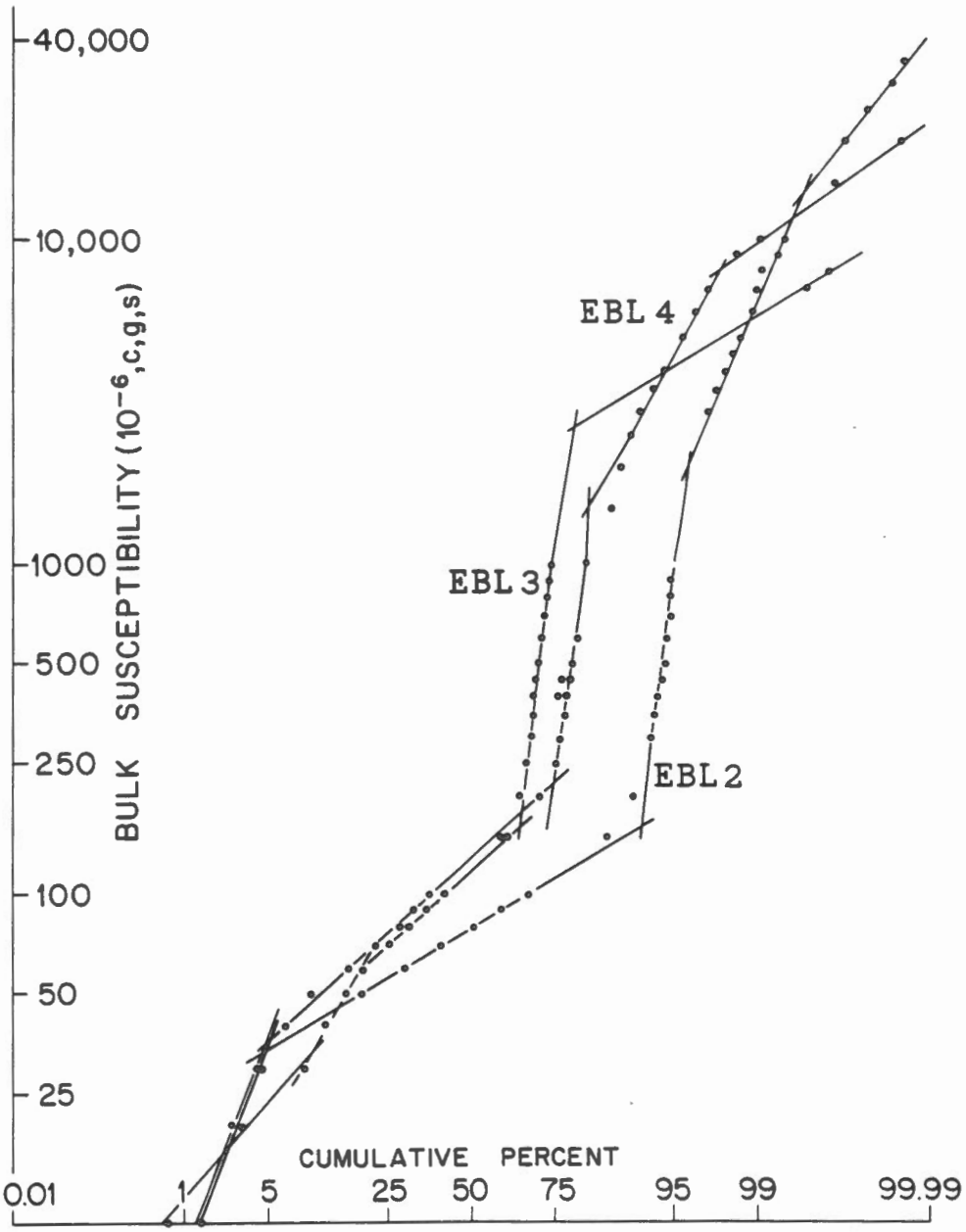
40,000
10,000
1000
500
250
100
50
25
BULK SUSCEPTIBILITY (10^{-6},c,g,s)
EBL 4
EBL 3
EBL 2
CUMULATIVE PERCENT
0.01
1
5
25
50
75
95
99
99.99